ORNL/TM-6867

Meteorological Effects of Thermal Energy Releases (METER) Program Annual Progress Report October 1977 to September 1978

A. A. N. Patrinos
H. W. Hoffman

OAK RIDGE NATIONAL LABORATORY
OPERATED BY UNION CARBIDE CORPORATION · FOR THE DEPARTMENT OF ENERGY

DISCLAIMER

Printed in the United States of America. Available from
National Technical Information Service
U.S. Department of Commerce
5285 Port Royal Road, Springfield, Virginia 22161
Price: Printed Copy $7.25; Microfiche $3.00

ORNL/TM-6867
Dist. Category UC-12

Contract No. W-7405-eng-26

METEOROLOGICAL EFFECTS OF THERMAL ENERGY RELEASES (METER) PROGRAM ANNUAL PROGRESS REPORT OCTOBER 1977 TO SEPTEMBER 1978

Contributions by:

Argonne National Laboratory
Battelle Pacific Northwest Laboratories
Oak Ridge National Laboratory
Pennsylvania State University
Rand Corporation

Compiled by:

A. A. N. Patrinos
H. W. Hoffman

Date Published: June 1979

NOTICE This document contains information of a preliminary nature. It is subject to revision or correction and therefore does not represent a final report.

Prepared by the
OAK RIDGE NATIONAL LABORATORY
Oak Ridge, Tennessee 37830
operated by
UNION CARBIDE CORPORATION
for the
DEPARTMENT OF ENERGY

THIS PAGE

WAS INTENTIONALLY

LEFT BLANK

CONTENTS

PHYSICAL MODELING

PREDICTIVE METHODS

METEOROLOGICAL EFFECTS OF THERMAL ENERGY RELEASES (METER) PROGRAM ANNUAL TECHNICAL PROGRESS REPORT OCTOBER 1977 TO SEPTEMBER 1978

A. A. N. Patrinos H. W. Hoffman

INTRODUCTION

H. W. Hoffman

The METER (Meteorological Effects of Thermal Energy Releases) Program is approaching its fourth anniversary, and from this vantage, it seems appropriate to reexamine the purposes and rationale for the program, to document its accomplishments, and to propose its future.

The program was officially established on July 1, 1976,* under the joint sponsorship of the Division of Nuclear Research and Applications (NRA) and the Division of Biomedical and Environmental Research (BER) of the Energy Research and Development Administration.† Its original name was Atmospheric Effects of Nuclear Energy Centers (AENEC) Program. The initial program structure combined some elements of work already being funded by BER with new studies proposed for funding by NRA; the Oak Ridge National Laboratory (ORNL) was assigned the task of overall technical management. The objective of the program, as stated in the first annual program report, is as follows:

> "It is the objective of this effort to develop and verify methods (analytical or experimental) for predicting the maximum amount of energy that can be dissipated to the atmosphere (through cooling towers or cooling ponds) from proposed nuclear energy centers (NEC's) without affecting (adversely or beneficially) the local and regional environment (weather)."

Four specific tasks were identified:

1. Development and verification of models for predicting the offsite effects of NEC atmospheric waste heat discharges on local and regional meteorology and climatology.

---

*Work in FY 1976 was limited to planning and scoping efforts.

†Now the Department of Energy (DOE).

2. Assessment of the impact of such NEC atmospheric waste heat discharges on the design of nuclear energy centers.

3. Prediction of the effect of NEC atmospheric waste heat discharges on the diffusion and deposition of radioactivity discharged from such centers.

4. Assessment of the public acceptability of predicted off-site effects of NEC atmospheric waste heat discharges.

The program assembled to address these tasks contained 19 defined technical elements[1] plus a general responsibility to focus diverse efforts in this area through a series of workshops bringing together active workers in the university, industrial, and research institute communities.

Since its inception, the METER Program has experienced a continuing process of narrowing of its objectives. Thus, the original wide-ranging scope of mathematical modeling, laboratory and field experimentation, and social assessments gave way to the more pragmatic concern of determining, through well-designed but limited field tests and analog studies, the potential for weather modification. While an awareness of the possibilities for tornado excitation remained, the determination of rainfall changes and drift deposition at selected power plant sites fit better within the program's limited fiscal resources and the current state of meteorology and climatology. At this juncture, METER is organized around a number of field studies: (1) rainfall at the Bowen Electric Generating Station of the Georgia Power Company near Cartersville, Georgia, (2) drift deposition at Pacific Gas and Electric's Pittsburg (California) Power Plant, (3) plume and ambient atmosphere characteristics at the Keystone Plant in Southwestern Pennsylvania, and (4) fog formation around the cooling pond of Commonwealth Edison's Dresden Nuclear Power Station near Morris, Illinois.

What has METER accomplished during these past three years of funded technical activity? A few important, though not inclusive, results are as follows:

- Plume and cloud growth models were refined and extended with respect to both individual plumes and the integrated effects of

discrete energy source concentrations; models were compared with newer data with good success.

- Models were developed and extended to describe plume condensate scavenging, plume bifurcation, and drift deposition.
- Prediction of energy center emission effects through projection from natural analogs (forest fires and volcanoes) was examined; it was found that the limited meteorologic data available in association with these events made extension difficult.
- Physical modeling in water flumes of plume interactions showed terrain effects to be highly significant.
- Field study of the effect of the Bowen Electric Generating Station in Georgia on local rainfall indicated rainfall redistribution rather than enhancement for this 3200-MW(e) coal-fired plant.
- Drift deposition field studies around the Pittsburg Power Plant in California were completed; analysis is under way.
- Fog formation studies in the immediate vicinity of the Dresden Nuclear Power Station in Illinois have led to better predictive capability for fog occurrence.
- Airborne mapping of turbulence fields and air chemistry downwind of the Keystone Power Plant in Pennsylvania was completed.

For details of these accomplishments, the reader is referred to the annual reports thus far issued[1,2] and to the program descriptions and results that follow in the rest of this report.

Where is METER going? In the short term, we see a convergence of field testing at the Plant Bowen site, with most present participants contributing to an enlarged effort. Thus, along with the continuation of the present rainfall study, we envision measurement of near-field velocity and humidity profiles, rainfall and air chemistry, and drift formation and deposition. While model development will not be an active component of this effort, the utilization of these data by modelers will be encouraged. The accumulation of these data over the next several years should provide a valid description of the interaction of the Plant Bowen emissions with the local atmospheric environment and thus enable quantitative estimates to be made of the climatic impact of the plant. Studies

by Argonne National Laboratory examining power plant cooling ponds as a source of fog will shift toward emphasis on improving cooling pond operation — thermal performance, shape, location, etc. — so as to minimize the fogging potential.

As noted above, results to date at Plant Bowen suggest strongly that releases of heat and moisture from a plant of Bowen's size effect minimal changes in the local climate. Thus, the METER Program — while productive — has yet to achieve its primary goal of identifying the maximum amount of energy (heat) and mass (moisture) that can safely be dissipated to the atmosphere without affecting the weather. Field studies at plants of higher energy capacity are not now possible (at least in the United States), since such electric generating stations do not currently exist. The Tennessee Valley Authority's (TVA's) Hartsville Nuclear Station [~5000 MW(e)] is on the horizon, with operation of the first unit scheduled in the 1983–1984 period. Preliminary discussions have been initiated with TVA in regard to a cooperative rainfall modification/enhancement study at Hartsville; schedules and required resources have not yet been identified.

Aside from noting the possibility, METER has not addressed (experimentally or analytically) the question of heat and moisture releases from power plants (energy centers) triggering or intensifying larger-scale events — summer squalls with augmented hail, whirlwinds, tornadoes, etc. Nor are there plans for support of a second stage of model development incorporating new data and understanding. Where then goes METER? Present plans call for completion of the Plant Bowen field study within three years; as noted, studies at Hartsville are a possibility but depend on developing adequate funding by TVA, DOE, and possibly the Environmental Protection Agency (EPA). Support of model development and verification and appropriate laboratory-scale experiments is a desirable, though not optimistic, possibility.

Let's take a different track and, in view of METER's purposes, suggest a "METER future." We begin with the premise that energy production/utilization centers remain a valid option in the United States energy future and that METER is an equally valid means for assessing and predicting the impact of these centers on the atmospheric component of our

environment. It can be anticipated that the growth of energy centers to sizes greater than Plant Bowen or TVA's Hartsville plant will be steady but slow. Thus, we can envision an extended METER Program as a series of extensive (and expensive) field studies of 4- or 5-year duration separated by periods of varying length devoted to integrating the field results and developing improved predictive models. This latter element would necessarily include critical laboratory experiments designed to promote an understanding of the mechanisms involved, to obtain coefficients necessary for engineering utilization of the predictive models, and to develop instrumentation for improved field measurements. During these interregnums, particular attention should be given — as appropriate to the developing scale of energy centers — to the planning of field studies involving more and more severe weather phenomena and to the development of the needed data-acquisition and processing systems. It also seems reasonable to expect that a METER Program of this nature will encourage and accelerate corollary, but independent, research; it is then essential that METER assume the lead in collating this body of knowledge through annual workshops, seminars, etc. In all of this (i.e., field studies plus information consolidation and projection), the twin goals of defining the effect threshold and designing the source to minimize effects should guide the program.

Pie in the sky? Perhaps. If we are to maintain or, hopefully, to increase our standard of living, we must continue to exploit our developing technologies; but we must do so in ways that do not damage the quality of life. To accomplish this, we must have guideposts that maintain our long-range direction while allowing flexibility in the near term. The METER scenario outlined above can fulfill this function.

Admittedly, implementation may be difficult. Today's clime emphasized the near-term demonstration and commercialization of energy technologies. In view of our mounting energy crisis, this is understandable. However, this does not give much opportunity for such apparently less immediate projects as METER. One course for ensuring an active and responsive METER effort over the time period relevant to the study of weather phenomena would be to assign management of the program

to the National Center for Atmospheric Research (NCAR) along with a sustaining budget; incremental funding to support field studies and engineering exploitation of the results could then come from all appropriate federal agencies [DOE (in both its technology development and regulatory aspects), EPA, etc.] under some form of long-term agreement and near-term approval.

The thoughts above will perhaps stimulate responses presenting alternative ideas and approaches. Since we think the goals of METER are important, it would be useful to assemble and discuss such alternative concepts for the longer-range support and implementation of the program.

The sections following document the current status of the several efforts currently comprising the METER Program. The contribution of each author is included in this report without substantive editing.

References

1. A. A. Patrinos and H. W. Hoffman (Compilers), *Atmospheric Effects of Nuclear Energy Centers (AENEC) Program Annual Technical Progress Report for the Period July 1975–September 1976*, ORNL/TM-5778, Oak Ridge National Laboratory (April 1977).

2. A. A. Patrinos and H. W. Hoffman (Compilers), *Meteorological Effects of Thermal Energy Releases (METER) Program Annual Progress Report, October 1976 to September 1977*, ORNL/TM-6248 (August 1978).

FIELD STUDIES

THIS PAGE

WAS INTENTIONALLY

LEFT BLANK

I. STUDIES OF RAINFALL AROUND PLANT BOWEN: IN SEARCH OF EFFECTS

A. A. N. Patrinos

ABSTRACT

The studies of precipitation modification around the Bowen Electric Generating Plant in northwest Georgia are the main activities undertaken by Oak Ridge National Laboratory on behalf of the Meteorological Effects of Thermal Energy Releases Program (METER). Work with the National Weather Service (NWS) data has led to a new method to detect rainfall effects in weather modification experiments. The application of this method, which uses the spatial correlation, has revealed some indication of precipitation modification downwind from Plant Bowen.

Extensive field studies were initiated during FY 1978 with the installation of the METER-ORNL network in northwest Georgia. Composed of 49 recording rain gauges and 4 recording windsets, located on a square 7 × 7 grid and centered at Plant Bowen, it is generating precipitation data of sufficient quality and quantity to determine the extent of the plant's influence on rainfall.

1. INTRODUCTION

The focus of the METER-related activities at Oak Ridge National Laboratory (ORNL) is on studies of rainfall around the Bowen Electric Generating Plant in northwest Georgia. These studies are being performed in response to the speculation that large cooling towers could potentially affect local (and perhaps regional) precipitation patterns by initiating storm activities or enhancing naturally occurring rainfall.[1,2] This speculation is based on several observational studies[3,4] and has been partially substantiated with numerical modeling investigations.[5,6] Much uncertainty surrounds the nature and magnitude of the suspected effect, which is expected to depend strongly on local climatic and topographical features. The problem of natural variability in precipitation further complicates the issue and demands close scrutiny of the available data.[7] From the analytical point of view, the study is

similar to weather modification experiments, such as cloud seeding, and therefore shares the same potential pitfalls which have frustrated experiments of that type in the past.

There are two parts to the METER-ORNL effort: the first part deals with the analysis of National Weather Service (NWS) data and the second with the operation of an ORNL-installed network of recording rain gauges and windsets.[8] The first part was initiated during FY 1977 and prepared the ground for the field study (the second part), which was initiated during FY 1978. It promoted an improved understanding of the climatology of the region and provided the first positive indication of a rainfall modification effect. It should be emphasized, however, that this result is tentative and awaits confirmation from the results of the field study.

The similarity between the Plant Bowen study and weather modification experiments, such as METROMEX,[9] prompted the field study, which involved the installation of the above-mentioned network (labelled the METER-ORNL network). The design and operation of this network followed the techniques and methodology of the METROMEX study[10] both in the field and in the reduction and stratification of the data. It is expected that the field study will provide data of sufficient quality and quantity to determine whether the cooling towers of Plant Bowen affect local rainfall and if so, how much.

2. NORTHWEST GEORGIA AND PLANT BOWEN

A topographical map of northwest Georgia is displayed in Fig. 1. The region under study includes a broad valley which is oriented north-south in the northern study area section and approximately west-east in the middle section. The terrain within the valley consists of gently rolling hills with a minimum elevation of about 600 ft above mean sea level. Beyond the valley, the elevation increases rapidly to the northeast, where the southern tips of the Appalachian Mountains are encountered. Ridge and valley structures, which are generally oriented south-southwest—north-northeast, are present in the northwest portion of the study area. In the southern section the elevation increases gradually with several isolated high points (e.g., Kennesaw Mountain). The general orientation of the hills and valleys within the study area is approximately along the southwest-northeast direction.

The Bowen Electric Generating Plant (Plant Bowen) is situated in the southern part of the valley. It is a 3,160-MW(e) coal-fired power plant utilizing four natural-draft cooling towers. Composed of four units (the first unit was completed in October 1971 and the last in November 1975), it is one of the largest plants in the world, especially among those using cooling towers as the sole cooling method.

There are two additional potential sources of weather modification in the study area, and it is imperative that their possible effects be disassociated from the investigations. The city of Atlanta, located in the southeast section, suggests rainfall modification of the major urban area type.[11] However, detailed statistical analyses based on the NWS data have revealed no significant rainfall modification effects from this source. The second potential source is Allatoona Reservoir, located in the middle eastern area. This man-made, 12,000-acre lake was created in 1950 with the damming of the Etowah River, which flows approximately west-east in the central valley. A lake-induced rainfall effect is possible from this source. This effect, however, can be considered as part of the natural variability background in the following statistical analyses, since the available rainfall data start in 1949.

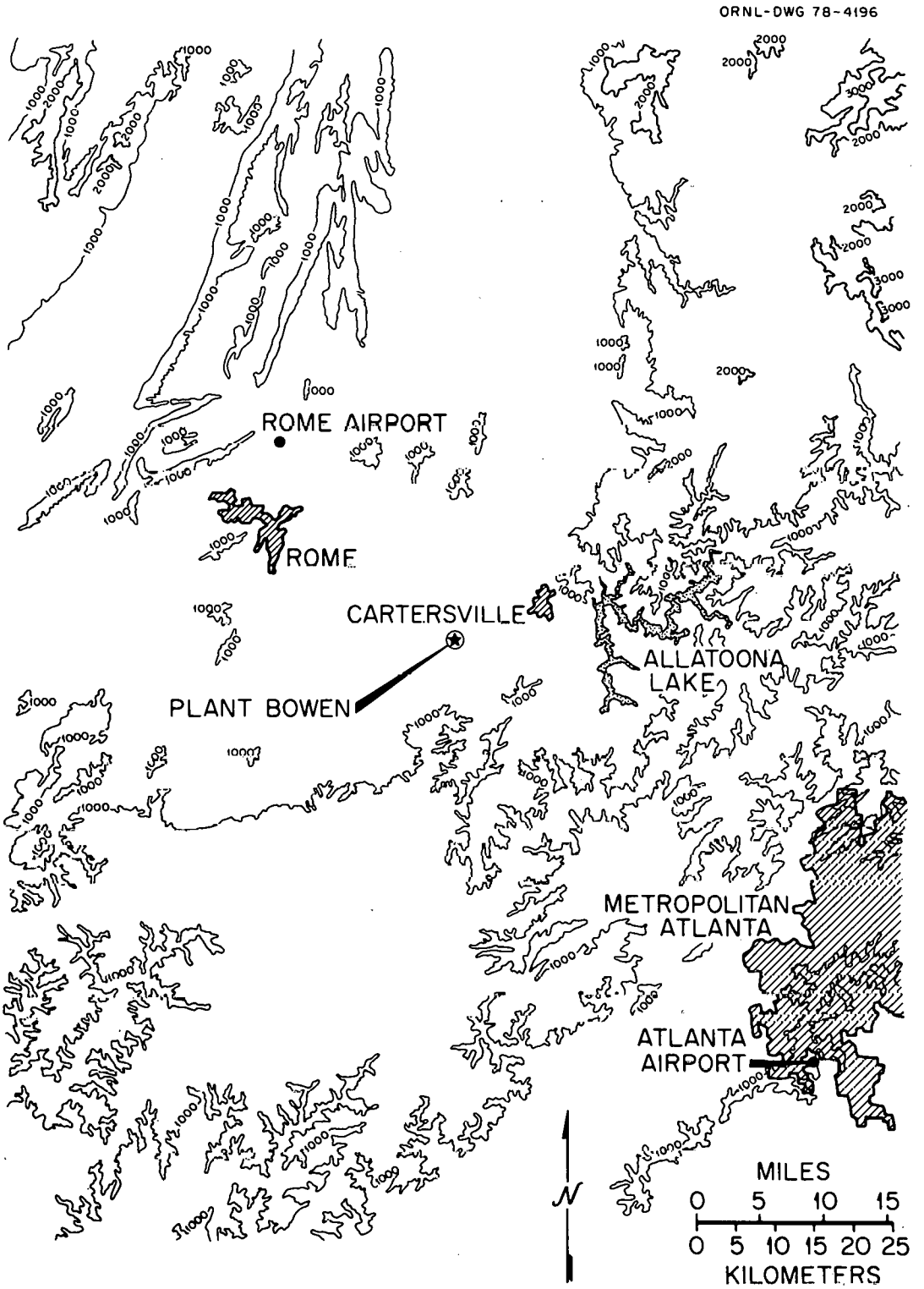

Fig. 1. Topographical map of the general area around Plant Bowen. The minimum elevation in the valley is about 600 ft above mean sea level.

3. STUDIES WITH NATIONAL WEATHER SERVICE DATA

3.1 Precipitation Data

The precipitation data used in this study are obtained by the National Weather Service (NWS) at its regular stations and the stations of the Cooperative Network. Precipitation is measured at daily intervals for most of the stations and on an hourly basis at the remaining stations. The available data cover the period 1949–1977. The NWS 1976 network is shown in Fig. 2. The stations used in this study were chosen after a careful examination of their data revealed the absence of observer or location bias.[12] All analyses were performed with monthly precipitation totals for the above stations. No attempt was made to stratify the data on a daily or storm-event basis, since such stratification represents a laborious task (rainfall measurements at different times during the day, cumulative measurements over several days, etc.).

3.2 Wind Data

Wind direction and speed are important factors to consider in precipitation studies. Upper-air winds, for example, are strongly correlated with storm track movements,[13] which, in turn, appear to control the orientation of isohyetal rainfall patterns[14] and correlation coefficient isopleths.[15] Furthermore, knowledge of low-level and upper-level winds is imperative in studies of inadvertent weather modification from ground-level sources such as urban areas, cooling ponds, etc., since such knowledge permits the application of the control-target technique.[7–9]

Information on surface winds in northwest Georgia was obtained by examining wind data from the Atlanta and Rome airports, while the Athens airport, situated about 90 miles east of Plant Bowen, supplied upper-air wind data. Wind roses were constructed from hourly measurements of surface winds at the Atlanta and Rome airports for the period 1949–1976. Figure 3 displays the wind direction distributions for the Atlanta airport for all conditions other than calm and for winds greater than 15 knots. The prevailing northwesterly component is more evident in the

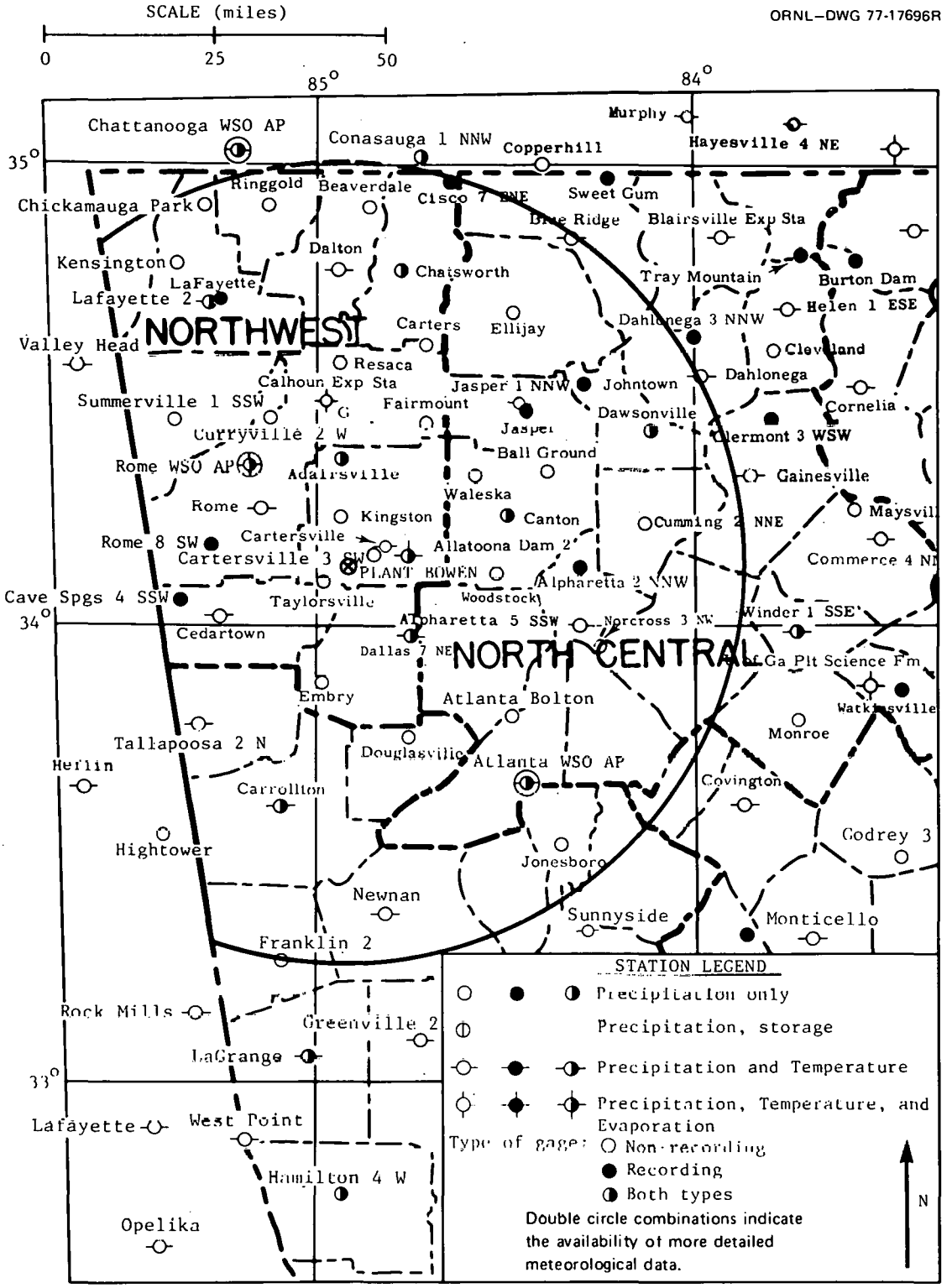

Fig. 2. Map of the National Weather Service (NWS) related stations operating during 1976.

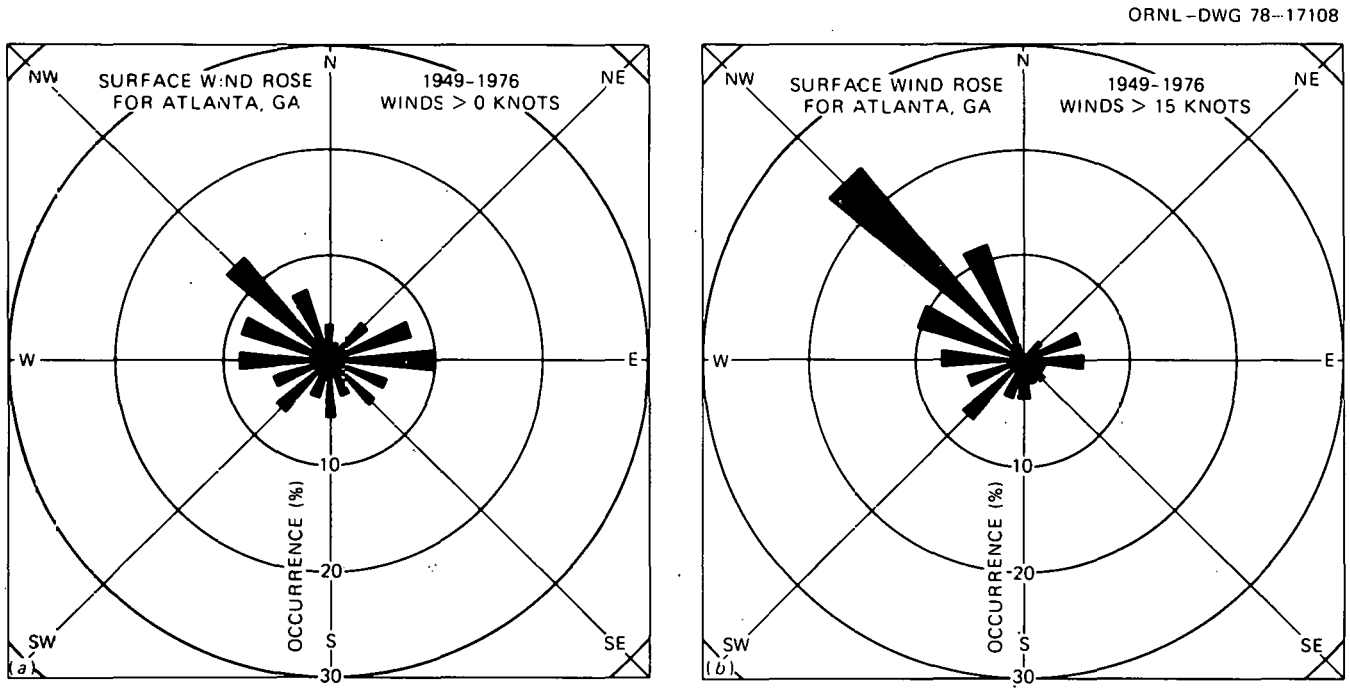

Fig. 3. Wind direction distributions for the Atlanta airport for all conditions other than calm and for winds greater than 15 knots.

latter case. Wind roses for the individual seasons were also constructed. Figure 4 displays the surface wind rose for the Atlanta airport station for the winters of 1950 through 1977. The winter season encompasses the months of December through February. The northwesterly component is strong for the other seasons as well (spring: March through May; summer: June through August; fall: September through November), while

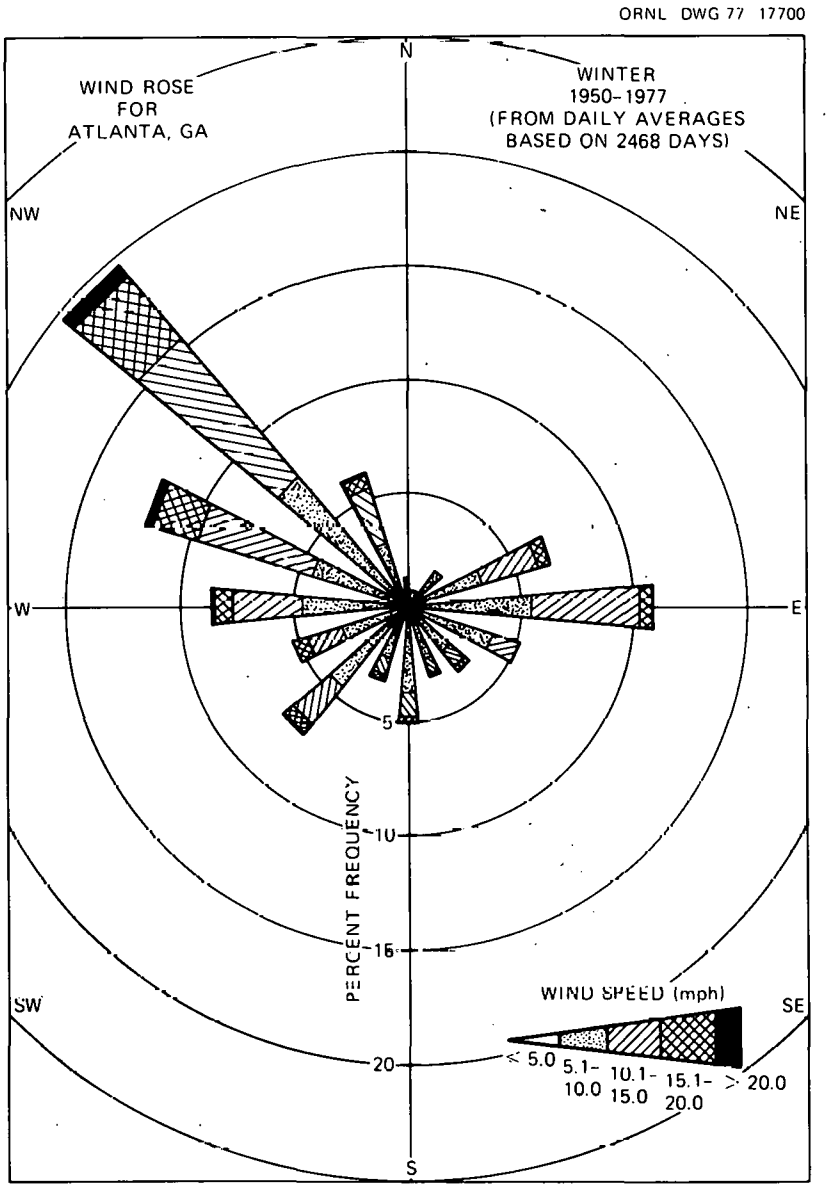

Fig. 4. Surface wind rose for the Atlanta airport station for the winters of 1950 through 1977.

a large easterly component is also present during the summer and fall. Analyses of the Rome airport data confirm the above results to a satisfactory degree,[16] and, consequently, the above wind patterns can be considered fairly representative of prevailing winds in the general study area.

Figure 5 displays the wind roses for the upper-air winds at the Athens airport. Athens, which is the closest station to the study area with upper-air data, is used to approximate upper-air conditions in northwest Georgia. The wind roses were developed for two pressure levels (850 and 500 mb) from the data obtained at 12-hr intervals for the period 1956—1976). The prevailing wind direction is clearly from the west at both levels.

The wind roses shown in Figs. 3 through 5 are useful in obtaining an overall understanding of wind patterns in the study area. However, the wind distribution during storms may vary considerably from the distributions shown in the figures, especially at the surface. For this reason, wind data were analyzed from measurements taken during 114 storm events of 1967. This is part of an ongoing study[5] concentrating on the storm-type stratification of all rainstorm events for the period 1967—1976. The cut-off interval in the determination of separate storm events was 6 hr without precipitation at all of the hourly network stations.[7] The preliminary results, based on the NWS three hourly North American weather maps, indicate a strong southwesterly component of the surface winds for the 1967 storms, which is a shift of 90° from the prevailing northwesterly component in the previous surface wind distributions. These results are presented in Table 1, along with the respective upper-air wind data for the same rainstorms. The upper-air winds also display a shift of prevailing winds from the west to the west-southwest. In a related study, surface winds prior to rainstorms were examined. The data were obtained from observations made at 3-hr intervals at the Atlanta airport station for the period 1967—1976 (contained in the "Local Climatological Data" publications of NOAA). Table 2 presents the results. Strong easterly and east-southeasterly surface winds are present in this case along with a sizable southwesterly component. It is evident that while upper-air winds for the rainfall events, like the overall upper-

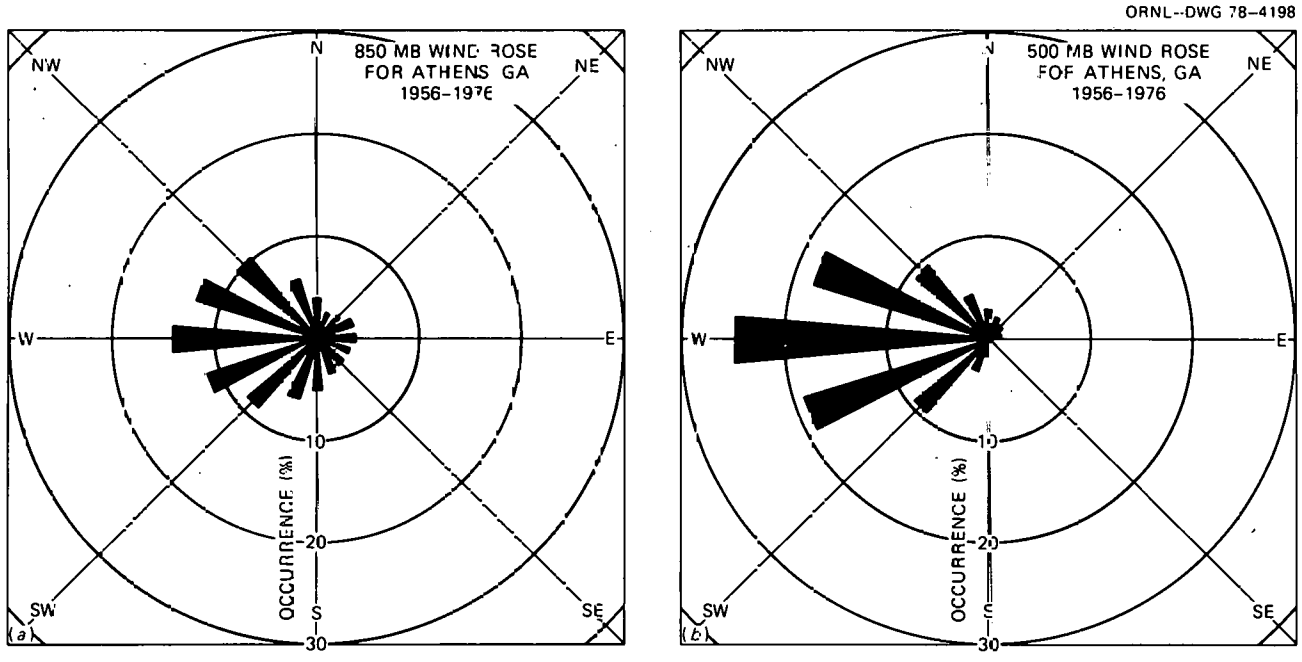

Fig. 5. Wind direction distributions at the 850- and 500-mb pressure levels at the Athens airport for the period 1956–1976.

Table 1. Surface and upper-air wind direction distributions during 1967 storms in northwest Georgia (based on 114 storm events)[a]

Direction	Surface (%)	850-mb level (%)	500-mb level (%)
N	4.4	0.9	3.5
NNE	0.9	0.0	0.0
NE	4.4	0.0	0.9
ENE	0.9	2.7	0.9
E	6.1	2.7	0.9
ESE	1.8	1.8	0.9
SE	9.6	2.7	0.0
SSE	4.4	2.7	0.9
S	8.8	8.0	0.9
SSW	6.1	7.1	2.7
SW	25.4	9.8	13.3
WSW	11.4	27.7	25.7
W	4.4	18.8	27.4
WNW	1.8	8.9	13.3
NW	5.3	3.6	6.2
NNW	4.4	2.7	2.7

[a]The sum of each column approximates 100 percent.

Table 2. Surface wind direction distributions prior to rainstorms for the period 1967–1976 at the Atlanta airport station[a]

Direction	Surface (%)
N	2.4
NNE	1.0
NE	1.1
ENE	4.2
E	13.1
ESE	12.4
SE	8.0
SSE	7.2
S	8.3
SSW	7.0
SW	9.4
WSW	8.4
W	4.8
WNW	4.8
NW	4.2
NNW	3.7

[a]Based on the "Local Climatological Data" publications of NOAA.

air winds, are persistently between west and southwest, the surface winds prior to and during rainstorms may vary widely and, in fact, display a distribution quite different from that of the overall winds. Based on the recent data from the METER-ORNL network, a frequent scenario for the surface winds was easterly prior to rainstorms, swinging southerly and then southwesterly during the rainstorms, and ending as northwesterly. The above findings raise some serious questions about the validity of relying on overall wind statistics for the determination of the control and target areas, especially if surface winds play an important role in this determination. In considering the potential rainfall modification of the cooling tower plumes, it is felt that, due to the elevated nature of the source, surface winds contribute little to the determination of control and target areas.

Support of the results regarding the upper-air winds can be found in studies by Visher[17] and Klein,[18,19] which indicate that the principal storm tracks in northwest Georgia are oriented approximately from the southwest to the northeast during all months of the year (more specifically, the tracks are oriented between southwest and west-southwest). These results are consistent with the conclusions reached by Newton and Katz[13] regarding the motion of some rainstorms in relation to upper-air winds.

3.3 Analysis and Inference

As mentioned in the previous section, the prevailing overall surface winds in northwest Georgia are from the northwest, while much uncertainty surrounds the direction of the prevailing surface winds for the rainfall events. The upper-air winds and the storm tracks are approximately from the west-southwest. In determining the control and target areas, the following situation is hypothesized: the cooling tower plumes initially move in the direction of the surface winds. As they rise and mix with the upper air, they rapidly shift to the direction of the upper-air winds, which is approximately the direction of the prevailing storm tracks (from west-southwest to east-northeast). Figure 6 shows a schematic of the postulated control and target areas for the

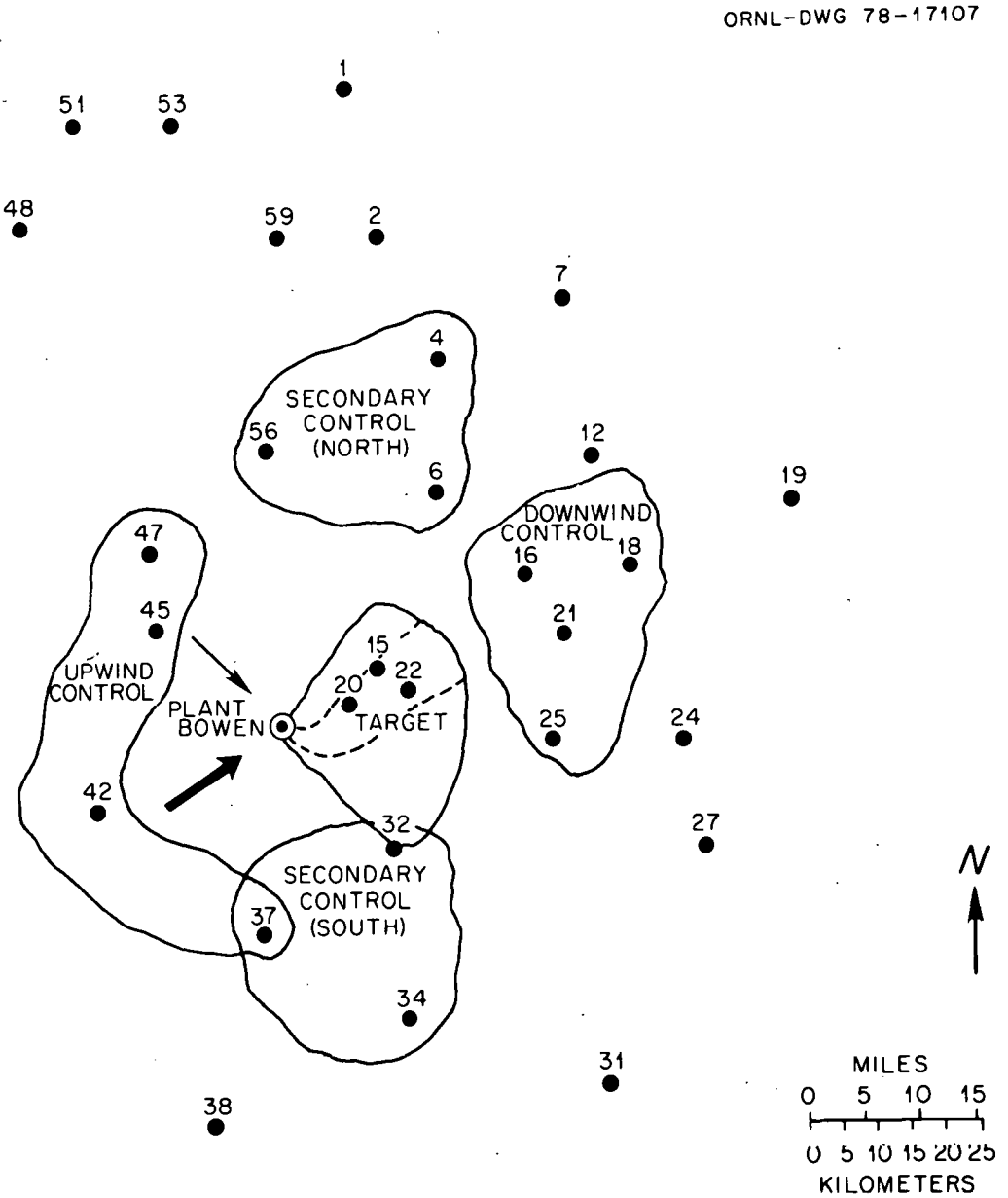

Fig. 6. The postulated control and target areas around Plant Bowen on the basis of prevailing surface and upper-air winds.

case of northwesterly surface winds. It is apparent that these areas would not change appreciably for surface winds of a different direction. Stations 15, 20, and 22 lie in the area where the effect of the cooling tower plumes is expected to maximize (the target area). No noticeable effect is expected beyond a distance of about 30 miles from the power plant. Thus, stations 16, 18, 21, and 25 comprise the downwind control

area. Upwind of the power plant, stations 37, 42, 45, and 47 comprise the upwind control area. Station 37 is also included in a secondary control area (south), along with stations 32 and 34. The secondary control area (north) includes stations 4, 6, and 56. Due to its proximity to the target area, station 32 is also considered a target station. The above-mentioned stations were chosen following field visits to check for adequate exposure of the rain gauges and after double-mass techniques revealed the absence of observer or location bias.[12]

The monthly precipitation data were divided into two periods: before October 1971 (preoperational) and after October 1971 (postoperational). Several statistical and analytical techniques were applied to the data. Two methods developed by Adderley and Twomey[20] are presented here. Figure 7 displays the ratios of the cumulative sums of the mean precipitations in the target area and the various control areas. Small increases in the ratios are evident during the postoperational period. Table 3

Table 3. Medians of the distributions of the ratios of monthly rainfall at target stations to that at control stations (PR = preoperational, PO = postoperational)

Stations	PR	PO	Stations	PR	PO	Stations	PR	PO
15-37	0.94	0.98	20-37	0.92	0.98	22-37	0.93	0.94
15-42	0.93	0.95	20-42	0.94	0.99	22-42	0.94	1.01
15-45	0.93	0.99	20-45	0.91	1.04	22-45	0.92	1.05
15-47	0.93	1.08	20-47	0.96	1.11	22-47	0.93	1.07
15-16	0.90	0.95	20-16	0.90	0.94	22-16	0.90	0.93
15-18	0.88	0.95	20-18	0.89	0.93	22-18	0.90	0.91
15-21	0.89	0.99	20-21	0.89	0.96	22-21	0.91	0.95
15-25	1.00	1.10	20-25	0.99	1.03	22-25	1.00	0.98
15-32	0.95	1.00	20-32	0.96	1.01	22-32	0.99	0.96
15-34	0.92	1.10	20-34	0.92	1.03	22-34	0.95	0.99
15-4	0.90	1.02	20-4	0.92	1.06	22-4	0.89	1.05
15-6	0.98	1.00	20-6	1.02	1.00	22-6	0.97	1.00
15-56	0.88	1.05	20-56	0.92	1.00	22-56	0.89	0.96
15-20	1.00	1.00	20-22	1.00	1.00			
15-22	0.97	1.03						

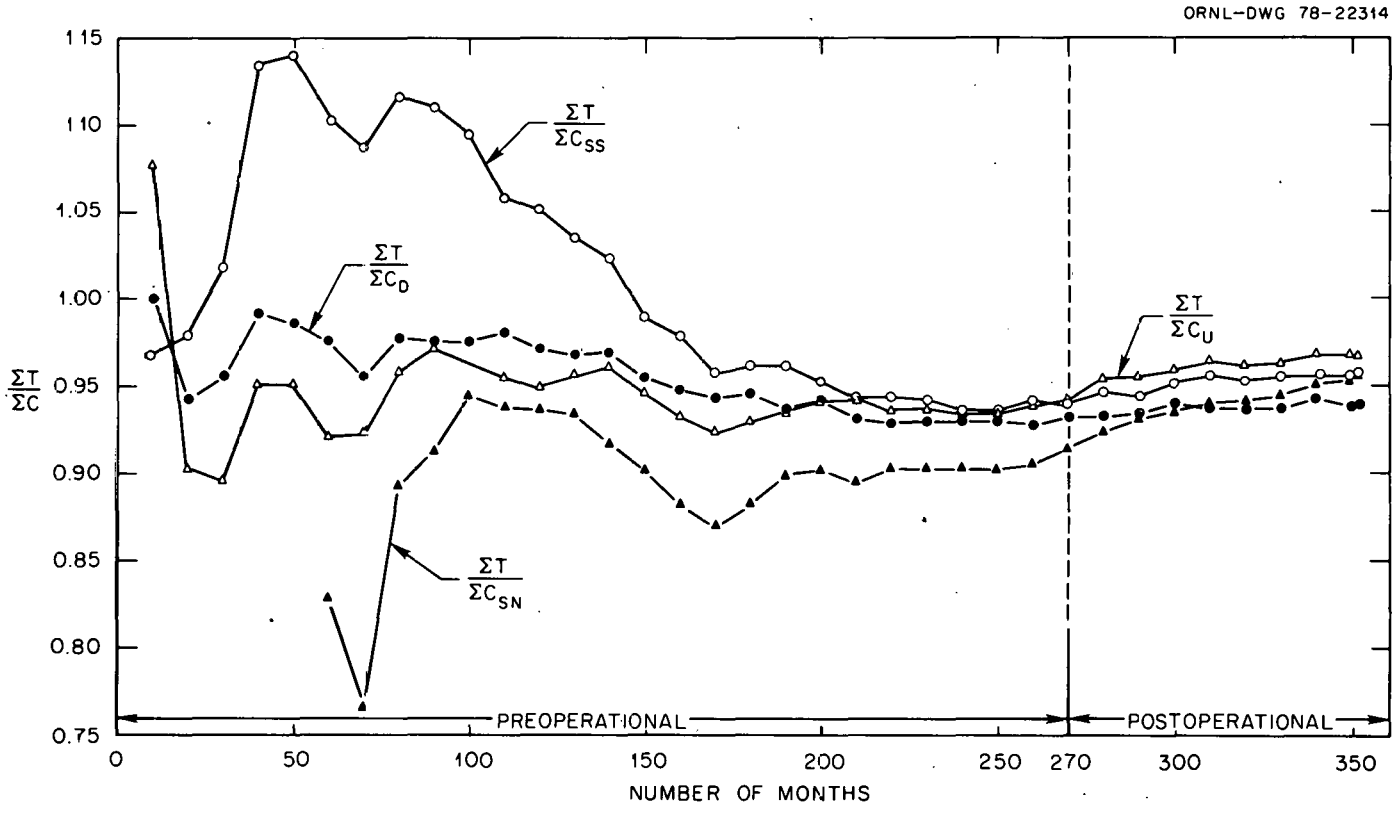

Fig. 7. Ratios of the cumulative sums of the mean precipitations in the target area and the various control areas (T = target, C_U = upwind control, C_D = downwind control, C_{SS} = secondary control — south, C_{SN} = secondary control — north).

contains the medians of the distributions of the ratios of monthly rainfall for combinations of stations in the target and control areas. In several cases, there is a marked increase in the medians during the postoperational period. Both the above techniques demonstrate some evidence of rainfall modification. However, the direct nature of these techniques makes them particularly susceptible to the complications introduced by the natural variability in precipitation. Huff[7] demonstrated how natural variability can affect verification efforts by performing hypothetical seeding experiments on rain gauge network data using basic statistical sampling designs. His studies offered strong evidence that natural variability can lead to fallacious interpretations of rainfall modification experiments unless the experimenter is aware of potential pitfalls and evaluates the data accordingly. The basic concepts of the methodology developed by Huff are incorporated in a statistical technique, using the spatial correlation, which was applied to the data.

Correlation coefficients were computed on the basis of monthly totals.[15,16] In computing the correlation coefficient between two stations, if one or both stations had missing data for some month, that month was dropped from the record. The variation of the correlation coefficient as a function of the record's length (number of months considered) is displayed in Fig. 8 for four typical combinations of stations. It can safely be concluded that the correlation coefficient approaches its steady-state value after approximately 150 months.

The central theme of the analysis proposed at this stage was to compute the spatial correlations for the combinations of stations in the target and control areas before and after the power plant's initial operation (October 1971) and to investigate any substantial differences. This was delayed for two reasons. First, the maximum number of months for the postoperational period is 74 (November 1971 to December 1977); the length of the postoperational record, therefore, is too short for the correlation to reach a steady-state value. Second, a better understanding of the natural variability of the correlation coefficient was imperative before any observed difference in the spatial correlation values could be considered to be significant. The distribution of

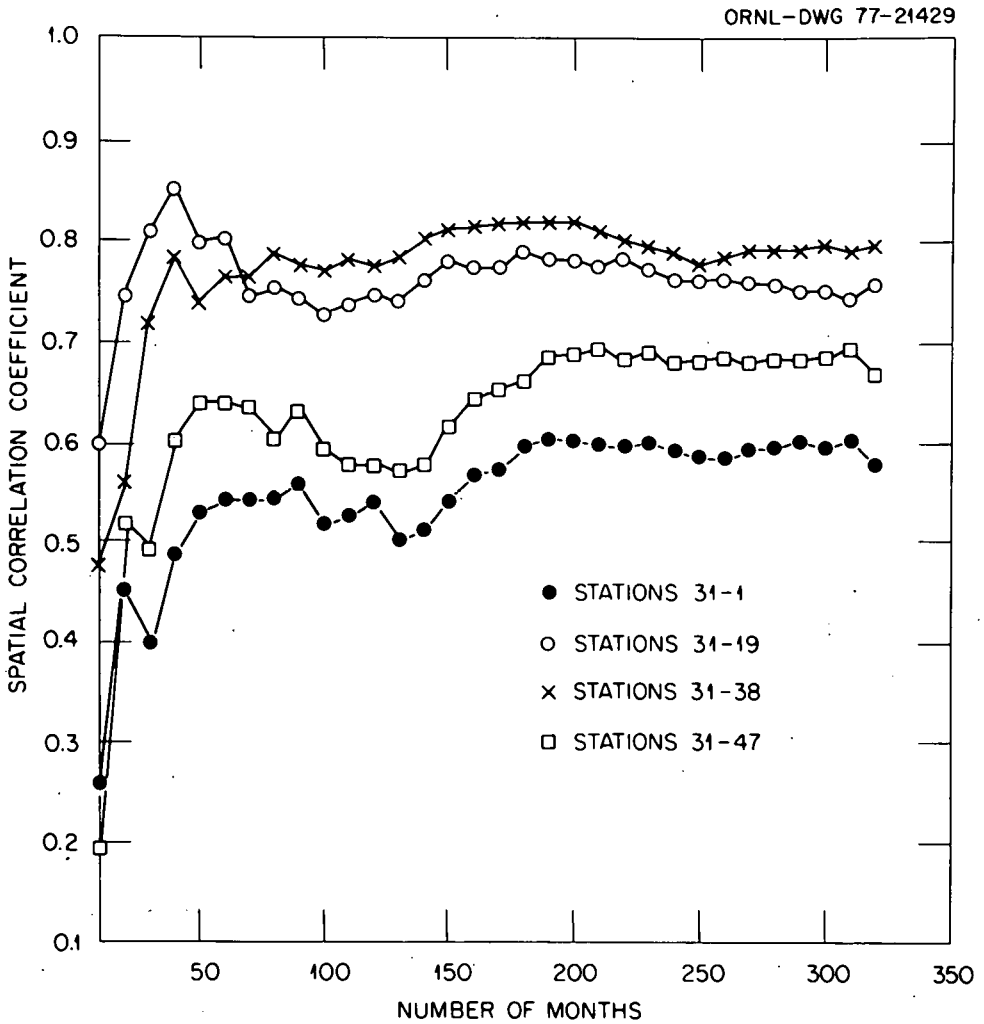

Fig. 8. Spatial correlation coefficients vs number of months considered for the combinations of the Atlanta airport station (31) with the Beaverdale 1E (1), Dawsonville (19), Carrollton (38), and Rome airport (47) stations (see also Fig. 6).

monthly rainfall data is not well known and, as a result, the derivation of the exact distribution of the correlation coefficient is intractable. An attempt was made to determine some distributional properties of the correlation coefficient by empirical distribution functions. A Monte Carlo sampling technique was used. The pairs of monthly rainfall amounts were randomly placed in two sets, each consisting of 150 data pairs, and the correlation coefficients r_A and r_B were computed. This was repeated 300 times for each combination of stations, and the

differences $\Delta r = r_A - r_B$ and the standard forms

$$\Delta r^* = \frac{\Delta r}{\sqrt{\frac{(1 - r_A^2)^2}{\eta_A - 1} + \frac{(1 - r_B^2)^2}{\eta_B - 1}}}$$

were plotted on normal probability graphs. The standardization was performed to obtain a common scale for comparisons.[21] Figure 9 displays the empirical distribution functions of Δr^* for the control and target areas. The graph representing each area is the arithmetic mean of all distribution functions of the combinations of stations in that area. All plots (including the ones for the individual combinations of stations) displayed a linear pattern, indicating the possible acceptance of a normality assumption. The normality of the Δr^* distributions was investigated with an omnibus test of departure from normality,[22] and a 90% acceptance level was found for all cases.

If the null hypothesis of no substantial difference between the correlations of the two samples is considered at the 10% level, the observed acceptance region for Δr^* is approximately between -2.5 and 2.5 (these values correspond to the lower and upper 5% of the distributions). Consequently, the quantity Δr^*, based on the two samples which are suspected to be different (e.g., preoperational and postoperational), is an "indicator" of the effect. If Δr^* is outside the acceptance region of the empirical distribution function for that combination of stations, then at least a suspicion of an effect exists.

As previously mentioned, the length of the postoperational record is insufficient to supply a steady-state value of the correlation coefficient. Nevertheless, the above method was applied for exploratory purposes to investigate the potential effects of the power plant. The two sample sizes were chosen to be 200 and 65 months, respectively. Using similar randomization procedures, the empirical distribution functions of Δr^* were computed for the various combinations of stations. All distribution functions exhibited similar behavior. Figure 10 displays the distribution functions for the combinations of stations in the target area. The apparent normality of the distribution functions for the

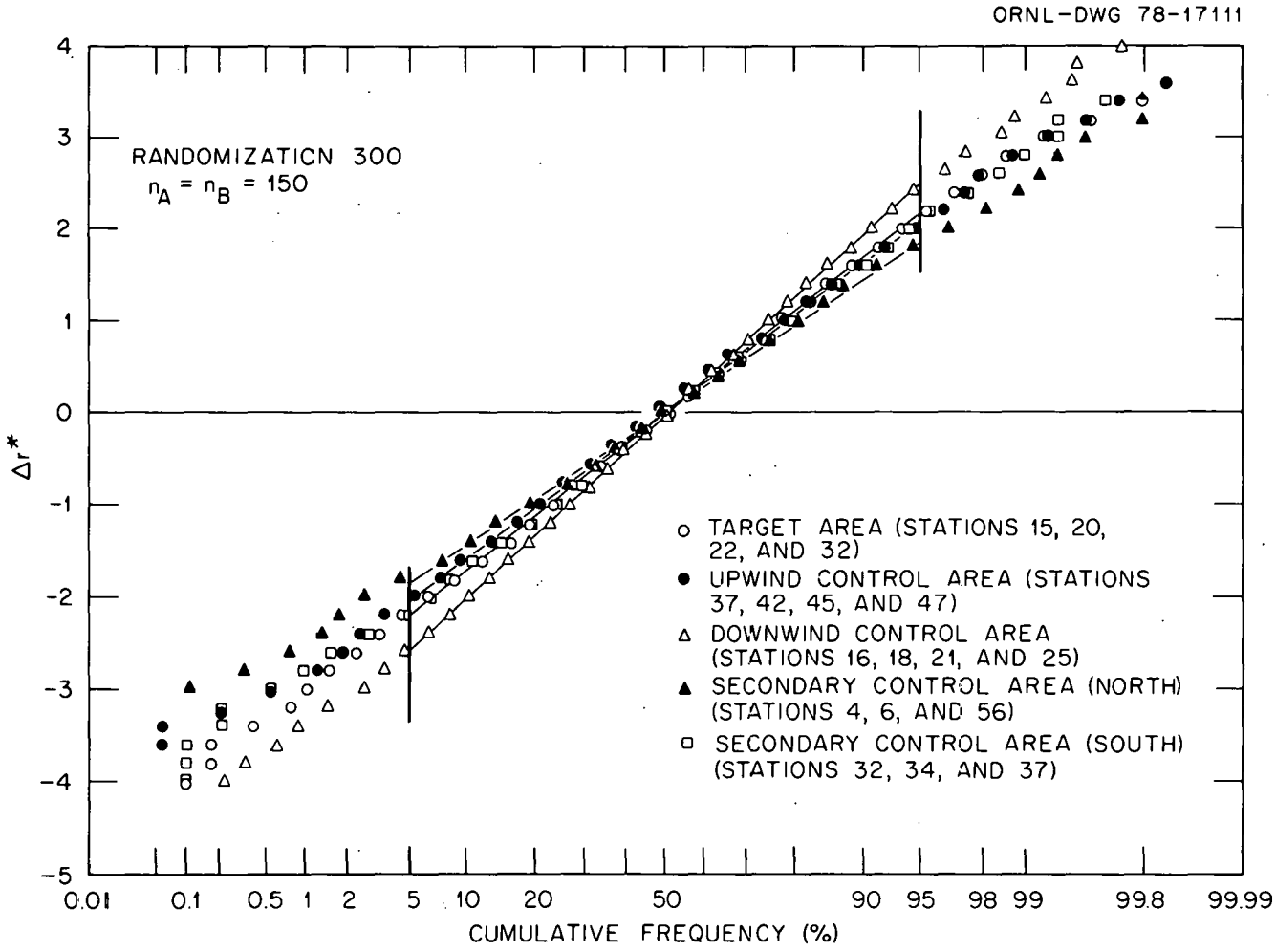

Fig. 9. Empirical distribution functions of Δr^* for the control and target areas ($N_A = N_B = 150$).

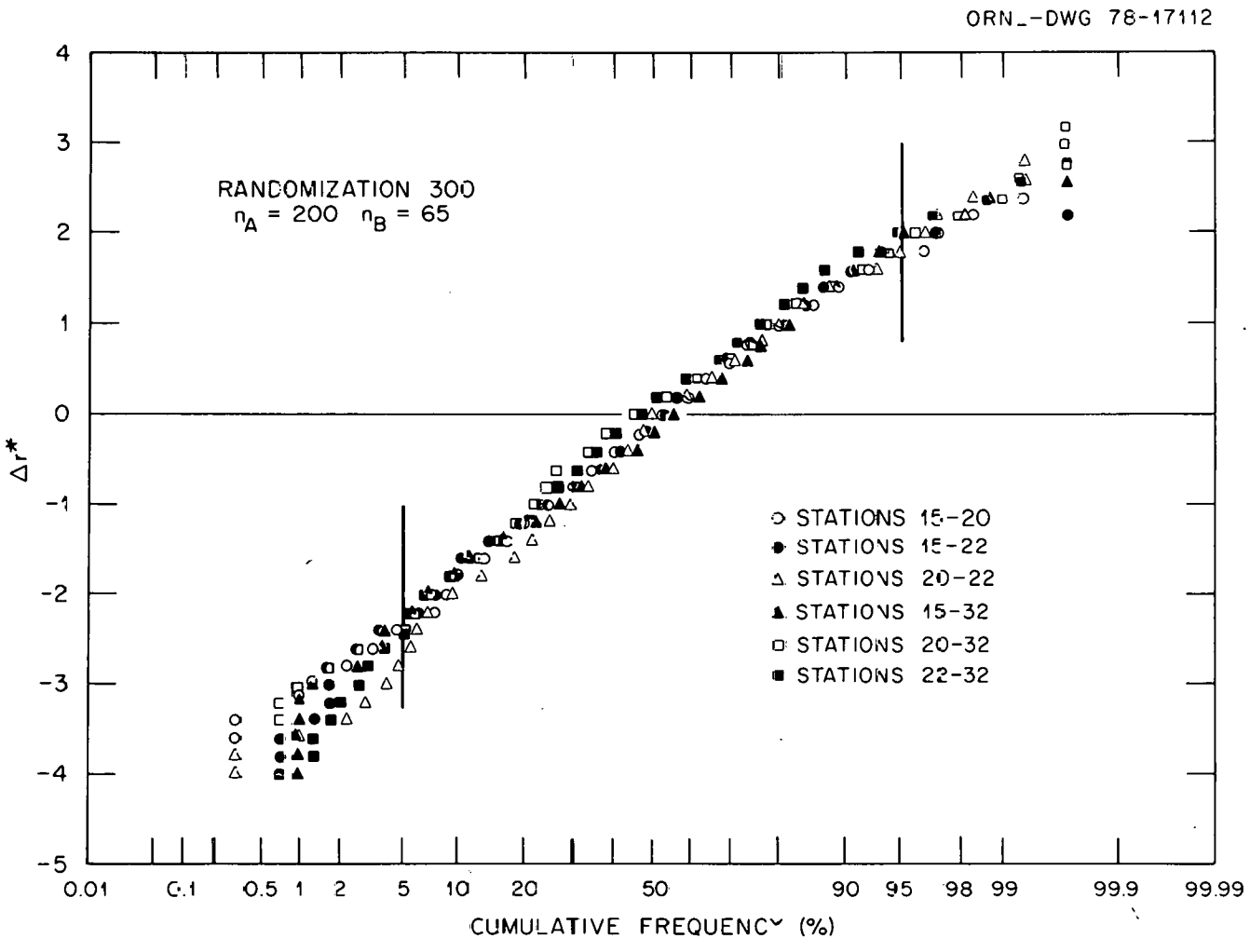

Fig. 10. Empirical distribution functions of Δr^* for the combinations of stations in the target area (N_A = 200, N_B = 65).

150-150 month case breaks down in the 200-65 month case because of the skewness of the distribution functions. As a result, the observed acceptance region for the 10% level is approximately between −2.5 and +2.0 due to the bend of the functions for large positive values of Δr^*.

Finally, the Δr^* based on a 200-month preoperational sample and the 65-month postoperational sample was computed for all combinations of stations and compared with the empirical distribution functions. The results are summarized in Table 4. For all combinations of stations in the control areas, the computed Δr^* is insignificant at the 10% level.

Table 4. Comparisons of the computed correlation differences with the respective empirical distribution functions

Area	Stations	r_A	r_B	Δr^*	Distribution level (%)
Upwind control	37-42	0.812	0.793	0.379	61
	37-45	0.759	0.765	−0.102	49
	37-47	0.763	0.791	−0.511	35
	42-45	0.860	0.864	−0.123	46
	42-47	0.827	0.822	0.114	55
	45-47	0.905	0.900	0.149	57
Downwind control	16-18	0.904	0.916	−0.482	45
	16-21	0.893	0.916	−0.933	31
	16-25	0.874	0.859	0.410	60
	18-21	0.899	0.917	−0.756	39
	18-25	0.869	0.852	0.458	66
	21-25	0.910	0.898	0.458	66
Secondary control (south)	32-34	0.835	0.872	−1.007	23
	32-37	0.870	0.900	−1.026	25
	34-37	0.866	0.849	0.458	65
Secondary control (north)	4-6	0.866	0.867	−0.028	52
	4-56	0.853	0.865	−0.331	40
	6-56	0.864	0.818	1.013	83.5
Target	15-20	0.911	0.842	1.803	96
	15-22	0.911	0.816	2.199	99.7
	15-32	0.695	0.786	−1.508	14
	20-22	0.931	0.889	1.520	93.5
	20-32	0.792	0.873	−2.020	7
	20-32	0.750	0.859	−2.413	5

In fact, the associated levels are close to 50%, indicating the absence of an effect. For the stations in the target area, however, some of the computed Δr^*'s indicate significant effects at the 10% level. For the combination 15-20, the computed Δr^* represents the 96% point of the distribution; for 15-22, 99.7%; and for 20-22, somewhat lower at 93%. At the lower end the Δr^* for the combination 20-32 represents the 5% point of the distribution, while for the combinations 20-32 and 15-32, the Δr^*'s correspond to the 7% and 14% points of their respective distributions. The large positive values of Δr^* (or Δr) for the stations in the target area (15, 20, and 22) imply a significant decrease of the correlations for those stations during the postoperational period. This suggests a plausible explanation of the nature of the suspected effect. Specifically, the cooling tower plumes might enhance rainfall or initiate scattered rainshowers directly downwind of the plant at the expense of other localities within the target area which are not along the path of the plumes at that time; thus, the correlation between stations in the target area would be expected to decrease substantially without, necessarily, a major increase in the average rainfall in the area. An underlying assumption is that this enhanced and depressed rainfall at stations within the target area would still be evident in monthly rainfall amounts without being completely smoothed out. The particular stations with increased or decreased rainfall might vary from month to month. The application of the method presented above to combinations of stations in a cross target-control framework (e.g., 15-6, 20-45, 22-21, etc.) revealed no significant levels for the respective Δr^*'s. It is hypothesized that the rainfall modification at the target station is insufficient to alone affect the correlation between that station and the control station.

The behavior of station 32, when considered in the target area, raises some interesting questions, since the large negative values of the correlation coefficient imply an increase of the spatial correlation during the postoperational period. Two explanations of this result are offered: the first deals with the plot of the correlation coefficient vs the record length (Fig. 8). For some combinations of stations, the plot overshoots the final steady state value at approximately 50 months.

It is possible, therefore, that the observed high negative values of Δr^* are due to this overshooting of the correlation coefficient plots. The second explanation is based on the history of station 32. This station (Dallas 7NE) has been frequently relocated during the period 1949–1977. In fact, during 1967, it was moved almost 6 miles to the north from its previous location. Double-mass techniques provided sufficient evidence to consider all records as belonging to one continuous station representing the present general area. Nevertheless, it is possible that the computed higher correlations during the postoperational months are due to the increased proximity of station 32 to stations 15, 20, and 22.

An mentioned in the Introduction, the above results should be considered tentative because of the short postoperational record and our reluctance to conclude the existence of an effect solely on the basis of the NWS data — particularly since the nature of the suspected effect is more qualitative than quantitative. It is expected that the data from the METER-ORNL network will succeed in confirming or rejecting the above findings.

4. THE METER-ORNL FIELD STUDY

4.1 Scope

The need to confirm or reject the preliminary findings of the studies with the NWS data was an important incentive to the birth of the METER-ORNL field study. The realization that the study of the potential effects of the cooling tower plumes on rainfall was akin in several ways to the studies of urban effects on rainfall, such as METROMEX,[9,10] had a considerable bearing on the development of the field study. The similarities included, among others, the need to monitor precipitation on a storm-event basis, the requirement of storm stratification, and the need for a high-density rain gauge network. These similarities suggested that approaches similar to those used in the studies of urban effects on rainfall could be used in the design and operation of the field study. There are, however, important differences between the two potential sources of weather modification which should be highlighted. Foremost is the fact that the cooling tower plumes are, in a practical sense, a highly concentrated and elevated source of heat and moisture, while the urban island is usually considered a diffuse low-level areal source. Other differences include the generation of mechanical turbulence in the case of the urban source (which is unimportant in the case of cooling towers), the change in the radiative properties of the surface in the urban source, etc. Whether these differences are sufficient to produce effects of an entirely different nature remains to be seen; nevertheless, circumstances such as the "thermal mountain," which is suspected to enhance rainfall, through orographic lifting, upwind of large cities,[23] would be highly unlikely in the case of Plant Bowen. Such circumstances would be expected in the case of power parks with an order-in-magnitude increase in power output.

It is important to note that the amounts of heat [$\sim$5,000 MW(t)] and moisture ($\sim$40,000 gal min^{-1}) discharged by the cooling towers at Plant Bowen are small compared with even a moderately sized thunderstorm.[2] However, the elevated and concentrated nature of the cooling tower plumes contributes to the likelihood of a triggering effect in a latently unstable atmosphere. Such speculations regarding the nature of the effect

necessitated the establishment of the METER-ORNL precipitation network, described below.

4.2 Design and Operation

The METER-ORNL precipitation network was designed to match the requirements of the field study, in accordance with Changnon.[10] The expected life of the network was set at five years, and consideration was given to the possibility of relocations and modifications on an annual basis.

The primary instruments of the network are the rain gauges. A few windsets were also installed for monitoring surface winds. The Georgia Power Company's 115-ft meteorological tower located 2.8 miles northeast of Plant Bowen provides supplemental wind information. Upper-air winds are determined from NWS North American maps that are printed from rawinsonde measurements taken every 12 hr. A knowledge of the speed and direction of the surface and upper-air winds permits the tracking of the cooling tower plumes, which in turn permits the determination of the control and target areas for the various rainfall events.[8]

The prior experience of others[10] played a key role in the determination of the size and shape of the precipitation network. Past research by Huff[24] indicated that a rain gauge spacing of 4 miles, or one rain gauge per 16 sq miles, would detect 99% of all storms during the summer for a network size of approximately 800 sq miles. Although the study applied to the midwestern region of the United States, climatic conditions in northwest Georgia would not be expected to differ appreciably from conditions in the Midwest during the summer. The detection percentage would be even greater during other seasons of the year or for detection of storms with a network mean precipitation above a given value (e.g., network mean >0.5 in.). With a density of one rain gauge per 16 sq miles, the 40 rain gauges of the METER-ORNL network would cover a 784-sq-mile area, which agrees with the network size mentioned above. Therefore, this density was chosen, since it permitted the largest possible network size having the capability of detecting 99% of all summer storms.

A square shape was selected for the METER-ORNL precipitation network. Based on experience with previous networks,[24] it was felt that a square would best depict both synoptic and local effects in an unbiased manner. A circular study area probably has an intrinsic tendency to deemphasize synoptic trends in favor of local anomalies, especially in contour plots of precipitation. Therefore, it was decided that the network would consist of a 7 × 7 square matrix measuring 24 miles on a side. The center of the network was positioned about 2 miles east of the power plant, because it was felt that the target area for the vast majority of storms would be in the eastern half rather than the western half of the network.[17] Figure 11 displays the location of the METER-ORNL precipitation network with respect to Plant Bowen, the cities of Atlanta and Rome, and the stations of the NWS and the Cooperative Network. A topographic map with the network superimposed on it is presented in Fig. 12. The rain gauges are of the recording weighing-bucket type, while the windsets continuously record wind speed and direction at the 20-ft level. The network was installed in February 1978 (Ref. 8).

The network is serviced weekly by an ORNL staff member who maintains the instruments at a high level of operation and attends to the multitude of major and minor problems that arise in every field study. The continuous interfacing with Plant Bowen management provides information on the plant's thermal output and the data from the plant's meteorological station.

Data processing and analysis

The vast amount of data continuously being recorded in this field study are reduced from analog charts to a form that allows for analysis on a storm-event basis. A storm is defined as precipitation which occurs at one or more rain gauge stations within the network and which is separated from other storms by an interval of at least 2 hr without precipitation throughout the network. The data reduction is performed through a digital tablet (Tektronix 4956) coupled to a minicomputer (Tektronix 4051) which interfaces with the PDP-10 and IBM 360/91 computers. The primary input to this data processing circuit is the rainfall data. Additional data which are utilized are the various types of

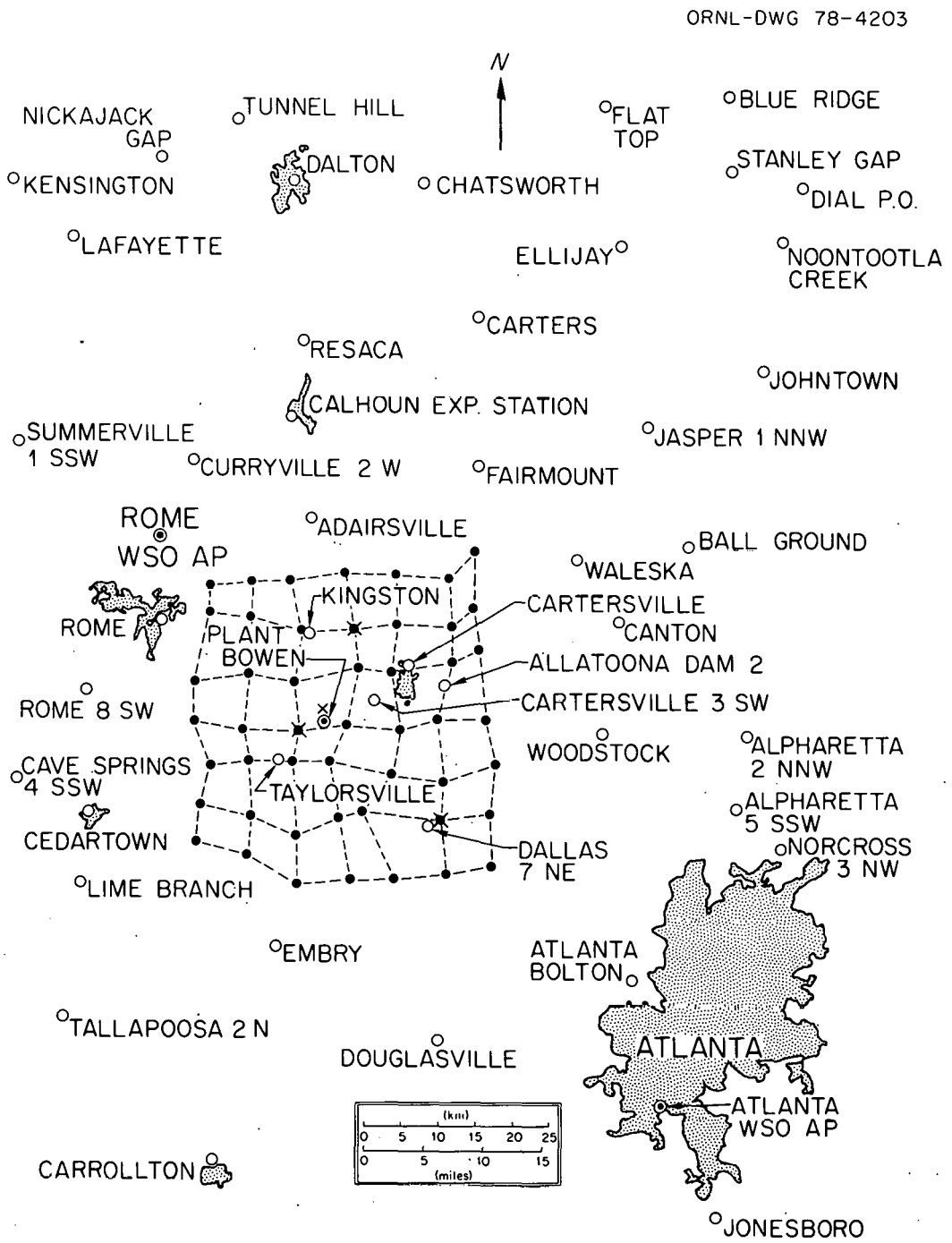

Fig. 11. The METER-ORNL precipitation network in relation to Plant Bowen, larger towns and cities, and the stations of the NWS and Cooperative Network. The entirely darkened circles represent METER-ORNL rain gauge sites, and the crosses indicate METER-ORNL windset sites.

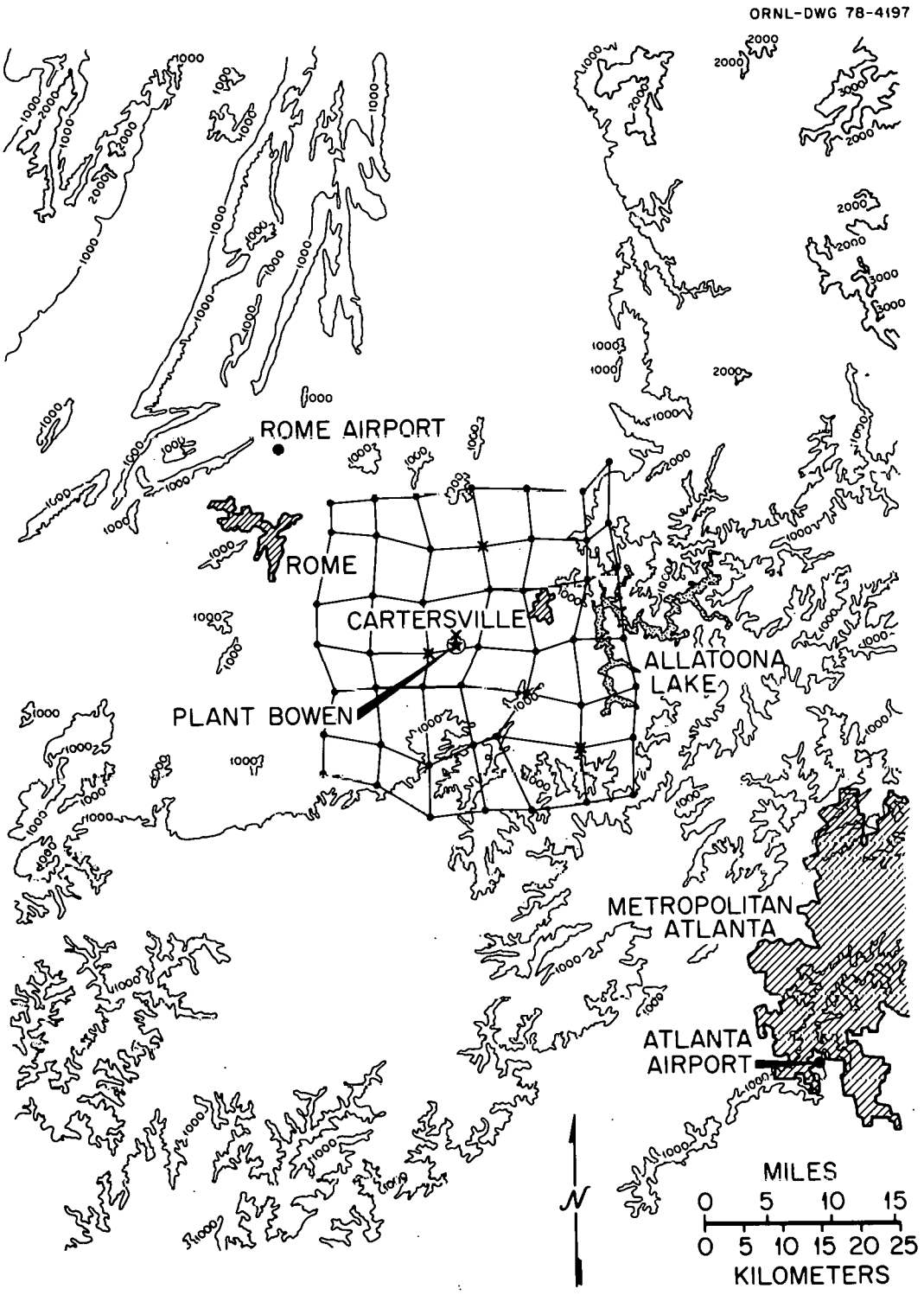

Fig. 12. The METER-ORNL precipitation network superimposed on the topographic map of Fig. 1. The symbols for the rain gauge and windset sites are the same as for Fig. 11.

wind data (METER-ORNL surface windsets, Plant Bowen meteorological station, NWS rawinsondes), storm type descriptions, power plant output, etc. The aggregate of all data relating to one storm is termed the storm "profile" and forms the unit in the final data set which will be used to explore the potential of rainfall modification by the cooling towers of Plant Bowen.

The storm type is identified using a classification developed by the Illinois State Water Survey.[25] The NWS surface maps during the time of the storm are examined to classify the storm. Knowledge of both surface and upper-air winds permits the tracking of the cooling tower plumes during the storm and establishes the area where the effect is expected to maximize (the target area). The fluctuations of the power plant's thermal output supplies an additional parameter in this multiparameter problem. A positive correlation between the magnitude of a potential effect and the plant's output of electricity is plausible.

Figures 13 and 14 display two typical storm profiles during March 1978. The contours of precipitation are generated with a computer program, and all other pertinent information is printed alongside each plot.

Analysis of storm No. 9 (Fig. 13) reveals the contours to be basically aligned in the southwest-northeast direction. The upper-air winds, which approximate the storm track, were from the southwest. These two statements indicate that the storm traveled from the southwest to the northeast. The areas of greatest precipitation within the network occurred southwest and northwest of Plant Bowen. Examination of the rain gauge charts indicates that the precipitation high northwest of the plant was caused by a convective entity which passed through the network 90 min before a convective cell associated with the precipitation high southwest of the plant crossed into the network. The two cells are included together as one storm, however, since the cutoff period required for separate storms is 2 hr. No plant-induced effect is evident for this storm; indeed, the areas of greatest precipitation are outside the target area, which is northeast of the plant.

For storm No. 10 (Fig. 14), the storm track is again from southwest to northeast. The principal region of high precipitation lies in the east-to-northeast portion of the network. This precipitation anomaly is

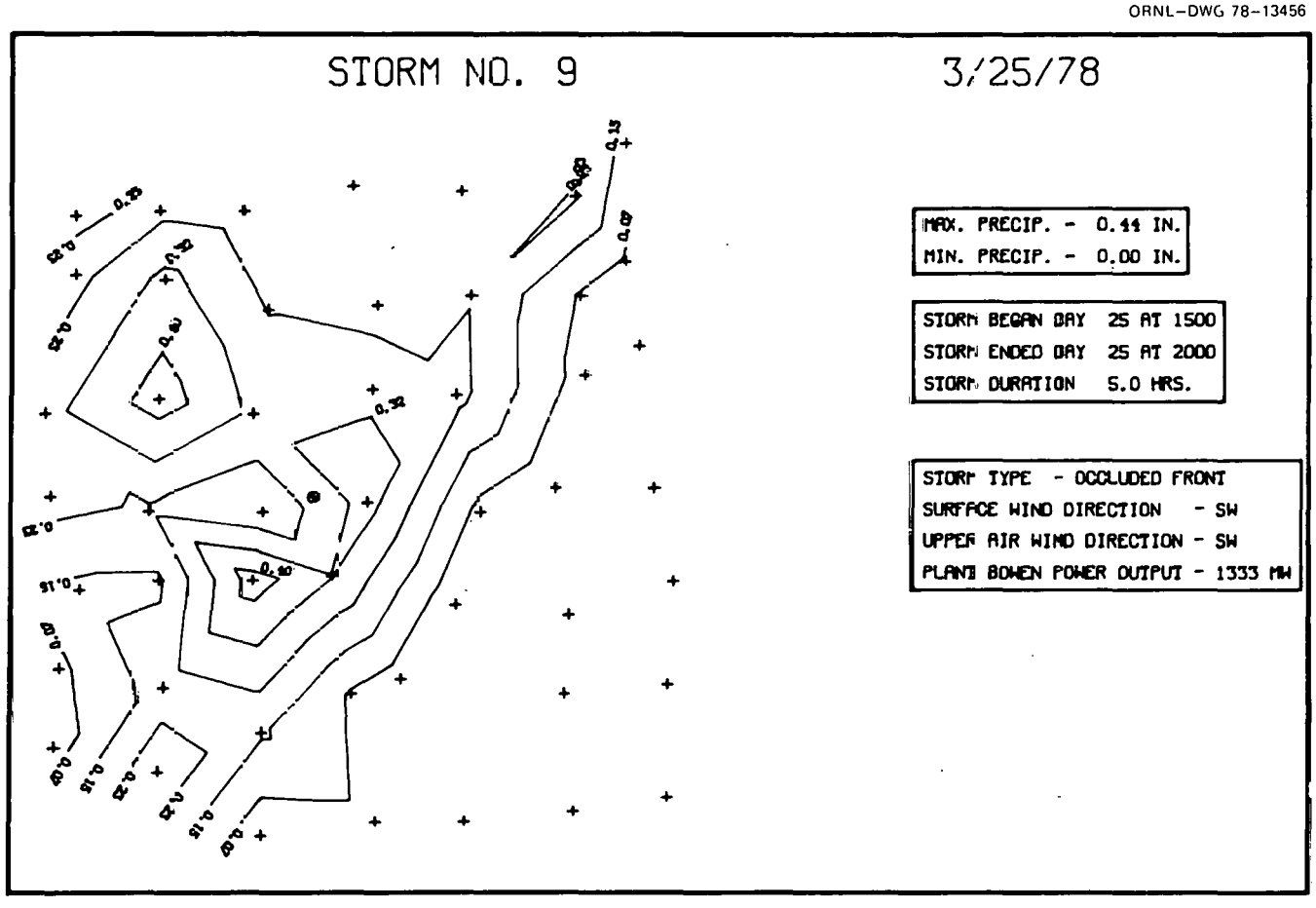

Fig. 13. Storm profile No. 9. The contours of rainfall are in inches.

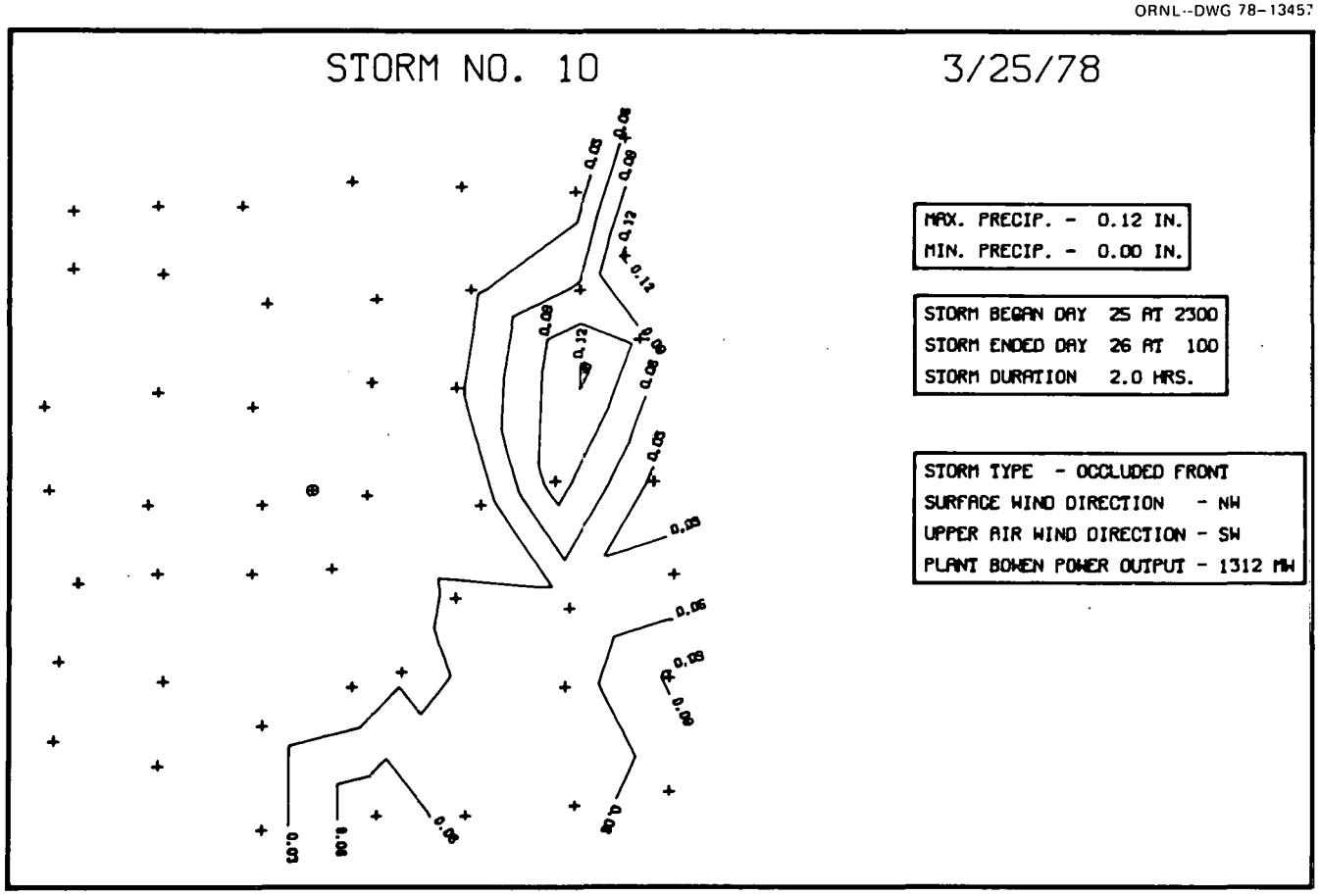

Fig. 14. Storm profile No. 10. The contours of rainfall are in inches.

noteworthy, since it coincides with the target area derived from northwest surface winds and southwest upper-air winds.

The above two examples highlight the type of analysis currently under way with the METER-ORNL network data. Many more storms must be analyzed before an effect can be claimed or refuted by statistical means. As the number of analyzed storms increases, further techniques will be employed involving the stratification of storms by type and power plant output. These techniques include multiple regression,[26] factor analysis,[27] double ratio analysis,[28] etc.

5. CONCLUSIONS

The detailed climatological and field studies described herein have concentrated on the investigation of potential rainfall modification from Plant Bowen's cooling towers. Work with National Weather Service data has focused on the determination of the natural variability of rainfall in northwest Georgia. A statistical method, employing the spatial correlation, has been applied to these data and has yielded a positive indication of an effect in the general downwind area of the power plant. The results indicate that the possible effect is not necessarily an increase in the areal rainfall but rather an increase in the variability of rainfall in the target area. This conclusion is considered tentative because of the short postoperational record and the insufficiencies of NWS data.

The METER-ORNL field study, initiated in February 1978, is tackling the above problems in a rigorous and concise manner. Employing a network of 49 recording rain gauges and 4 recording windsets along with other meteorological information, it is generating data of sufficient quality to substantiate the effect described above. Rainfall is being investigated on a storm-event basis, the power plant thermal output is being monitored, and detailed statistical techniques are being developed for use in this weather modification experiment. It is expected that over the expected life of the field study (five years) a sufficient data base will be created to provide the necessary qualitative and quantitative estimates of the power plant's effect on rainfall.

ACKNOWLEDGMENTS

This contribution to the METER annual report represents work performed by the author and the following members of the Engineering Technology Division of the Oak Ridge National Laboratory: N. C. J. Chen, L. Jung, R. L. Miller, and R. E. Saylor.

The field study around the Bowen Electric Generating Plant is being performed with the full cooperation of the Georgia Power Company.

REFERENCES

1. S. R. Hanna and F. A. Gifford, "Meteorological Effects of Energy Dissipation at Large Power Parks," *Bull. Amer. Meteor. Soc.* 56, 1069–1076 (1975).

2. F. A. Huff, "Potential Augmentation of Precipitation from Cooling Tower Effluents," *Bull. Amer. Meteor. Soc.* 53, 639–644 (1972).

3. M. L. Kramer et al., "Snowfall Observations from Natural-Draft Cooling Tower Plumes," *Science* 193, 1239–1241 (1976).

4. W. M. Culkowski, "An Anomalous Snow at Oak Ridge, Tennessee," *Mon. Wea. Rev.* 90(5), 194–196 (1961).

5. A. A. Patrinos and H. W. Hoffman, *Meteorological Effects of Thermal Energy Releases (METER) Annual Progress Report, October 1976–September 1977,* ORNL/TM-6248 (1978).

6. A. A. Patrinos and H. W. Hoffman, *Atmospheric Effects of Nuclear Energy Centers (AENEC) Program Annual Technical Progress Report for Period July 1976–September 1976,* ORNL/TM-5788 (1977).

7. F. A. Huff, "Evaluation of Precipitation Records in Weather Modification Experiments," *Advances in Geophysics* 15, 59–135 (1971).

8. R. L. Miller, R. E. Saylor, and A. A. N. Patrinos, *The METER-ORNL Precipitation Network: From Design to Data Analysis,* ORNL/TM-6523 (1978).

9. F. A. Huff and S. A. Changnon, Jr., "Climatological Assessment of Urban Effects on Precipitation at St. Louis," *J. Appl. Meteor.* 11, 823–842 (1972).

10. S. A. Changnon, Jr., "Operations of Mesoscale Networks, Illustrated by METROMEX," *Bull. Amer. Meteor. Soc.* 56, 971–977 (1975).

11. F. A. Huff and S. A. Changnon, Jr., "Precipitation Modification by Major Urban Areas," *Bull. Amer. Meteor. Soc.* 54, 1220–1232 (1973).

12. M. A. Kohler, "On the Use of Double-Mass Analysis for Testing the Consistency of Meteorological Records and for Making Required Adjustments," *Bull. Amer. Meteor. Soc.* 30, 188–189 (1949).

13. C. W. Newton and S. Katz, "Movement of Large Convective Rainstorms in Relation to Winds Aloft," *Bull. Amer. Meteor. Soc.* 39, 129–136 (1958).

14. E. M. Hansen, "Isohyetal Orientation for Heavy Rains in the Eastern United States," in *Second Conference on Hydrometeorology, Toronto, Canada, October 25–27, 1977,* American Meteorological Society, Boston, 1977.

15. F. A. Huff and W. L. Shipp, "Spatial Correlations of Storm, Monthly, and Seasonal Precipitation," *J. Appl. Meteor.* 8, 542–550 (1969).

16. A. A. N. Patrinos, N. C. J. Chen, and R. L. Miller, *Spatial Correlations of Precipitation in Northwest Georgia,* ORNL/TM-6544 (1978).

17. S. S. Visher, *Climatic Atlas of the United States,* pp. 163–166, Harvard University Press, Cambridge, Mass., 1954.

18. W. H. Klein, "Prevailing Tracks of Lows and Highs (Parts 1–4)," *Weatherwise* 9, Nos. 3–6 (1956).

19. W. H. Klein, "Prevailing Tracks of Lows and Highs (Parts 5, 6)," *Weatherwise* 10, Nos. 2–3 (1957).

20. E. E. Adderley and S. Twomey, "An Experiment on Artificial Stimulation of Precipitation in the Snowy Mountains Region of Australia," *Tellus* 10, 275–280 (1958).

21. F. N. David, *Tables of the Correlation Coefficient,* Cambridge University Press, New York, 1954.

22. K. Bowman and L. R. Shenton, "The Development of Techniques for the Evaluation of Sampling Moments," *Int. Stat. Rev.* 43(3), 317–334 (1975).

23. B. B. Hicks, Argonne National Laboratory, personnal communication (1978).

24. F. A. Huff, "Precipitation Detection by Fixed Sampling Densities," *J. Appl. Meteor.* 8, 834–837 (1969).

25. J. L. Vogel, "Synoptic Weather Relations," pp. 85–112 in *Summary of METROMEX, Volume 1: Weather Anomalies and Impacts,* Illinois State Water Survey, Bul-62 (1977).

26. J. Neter and W. Wasserman, *Applied Linear Statistical Models,* Irwin, Homewood, Ill., 1974.

27. D. G. Morrison, *Multivariate Statistical Methods,* McGraw-Hill, New York, 1976.

28. K. R. Gabriel and P. Feder, "On the Distribution of Statistics Suitable for Evaluating Rainfall Stimulation Experiments," *Technometrics* 11(1), 149–160 (1969).

II. COMPREHENSIVE STUDY OF DRIFT FROM MECHANICAL DRAFT COOLING TOWERS

N. S. Laulainen*

ABSTRACT

A comprehensive experiment to study drift from mechanical draft cooling towers was conducted during June 1978 at the PG&E Pittsburg Power Plant. The data from this study are to be used for drift deposition model validation. Results show the effects of tower geometry and orientation with respect to the wind and to single or two tower operation. The effect of relative humidity on droplet evaporation as a function of downwind distance can also be seen.

1. INTRODUCTION

A comprehensive experiment to study emissions, transport and downwind deposition of drift from a mechanical draft cooling tower was conducted at the PG&E oil-fired Pittsburg Power Plant at Pittsburg, CA during the two week period June 12-26, 1978. The purpose of the study was to develop a data base which can be used for validation of drift deposition models.

The key aspects of the study were to measure the characteristics of the drift droplets emitted from the tower, the ambient meteorological conditions responsible for the transport and dispersion of the drift, and the downwind deposition patterns and near-surface air concentrations of the drift. The source characteristics, including updraft air temperature and velocity profiles, and the meteorological data provide inputs to the models. The measured deposition patterns serve as comparisons to model outputs.

Source characterization measurements were performed by Environmental Systems Corporation (ESC, Knoxville, TN) under Electric Power Research Institute (EPRI) sponsorship. Meteorological and surface deposition measurements were carried out by Pacific Northwest Laboratory (PNL). In addition, other limited comparison tests were also performed by other organizations. Calfran Industries (Springfield, MA) also under EPRI sponsorship, measured drift droplet size distributions using a photographic

* Atmospheric Sciences Department, Battelle Pacific Northwest Laboratory, Richland, WA.

technique; these measurements were to be compared to the ESC derived size distributions and drift emission rates. Xonics (Van Nuys, CA) provided some limited remote wind profile measurements with a Doppler acoustic radar system for comparison to the PNL tethered-balloon system used during the experiment.

The site is located on the shore of Suisun Bay near the confluence of the Sacramento and San Joaquin Rivers. The plant consists of seven oil-fired units. Units 1-6 employ once through cooling, while Unit 7 (rated at 720 MWe net) is cooled by two 13-cell Marley rectangular mechanical draft cooling towers located on the center berm in a cooling canal west of the plant. The cooling towers are approximately 0.5 km from Unit 7. The two cooling tower units are identified as Tower 7-1 and Tower 7-2; Tower 7-2 is about 350 m west of Tower 7-1, measured from center to center. Individual cells are numbered 1-13 from west to east.

The cooling towers have a guaranteed drift rate of 0.004% and a nominal circulating water flow rate of 23.5 m^3/s. During a maintenance outage in December 1977, Marley and the general construction office at the PG&E Pittsburg Plant sealed leaks around the cooling tower drift eliminators. Canal water salt concentration is in the range of 0.4 - 1.2% and has a pH range of 8.0 to 8.7.

2. EXPERIMENTAL

A total of eight test runs plus a limited near tower test were carried out during the June drift study at Pittsburg, CA. Downwind deposition measurements were coordinated with ESC's source measurements on seven different tests. An eighth test was conducted with no concurrent source measurements. Limited droplet measurements were made on the fan deck of a single tower to examine near field deposition during a ninth and final test. The tests were divided into two-tower operation (three tests), Tower 7-2 alone (two tests), and Tower 7-1 alone (three tests).

Meteorological conditions were not nearly as ideal as previous June climatology would indicate. The winds, though persistently from SW to W to NW, were more intense during the morning hours than usual. Only two or

three runs were made where the wind speed could be classified as 5m/s or less. The other tests were carried out under wind speeds ranging from 5 - 10m/s.

It was desirable to have as much information as possible about the operating conditions in the tower at the time the emissions data were recorded in order to assist in applying these results to other towers at other locations.

As mentioned above, the towers at this site are located along the center of an elongated U-shaped canal which was previously used as spray canal for Unit 7 cooling. The cooling water for the Unit 7 condenser is withdrawn from one end of the canal and discharged to the other. The two cooling towers withdraw from the hot leg of the canal and discharge to the cold leg. Hence, there is no direct connection between the condenser cooling water and the tower flow. Furthermore, the inlet water temperature for the two towers may be slightly different if their withdrawal points are not located at the same point on the hot water leg.

Consequently, a complete description of the plant/tower cooling system required:

- Unit 7 generating load
- Unit 7 condenser water flow rate
- Unit 7 condenser inlet and outlet water temperature
- Canal inlet and outlet temperature
- Cooling Tower 1 water flow rate
- Cooling Tower 1 inlet and discharge water temperature
- Cooling Tower 2 water flow rate
- Cooling Tower 2 inlet and discharge water temperature
- Cooling Tower 1 total fan power (air flow)
- Cooling Tower 2 total fan power (air flow)
- Flow rate, inlet/outlet water temperatures, and fan power for individual cell being monitored (if possible).

Source characteristics included measurements of those variables required to describe the air/vapor and drift emissions from the fan stack. Cells to

be monitored were selected in accordance with the measurement strategy developed in a pre-test phase. Measurements were taken at or near the exit plane. Data were acquired at 12 equal area points along two perpendicular diametral traverses. Variables measured included:

- Updraft air velocity profiles
- Air dry- and wet-bulb temperature profiles
- Drift (water) flux profiles
- Mineral mass flux profiles
- Drift droplet size distribution
- Droplet salinity vs. droplet diameter

Intensive measurements of a single cell during a specific test run were made along with limited measurements of reference cells on each tower. Droplet size distributions and drift flux profiles were determined using sensitive papers (SP) and a light scattering, droplet counting system (PILLS). Additional droplet size distribution data were acquired using a special photographic technique. Mineral mass fluxes were determined with an isokinetic (IK) sampler. Updraft velocity profiles were measured with a gill anemometer while the air temperatures were obtained with standard precision thermistors.

Meteorological data were collected at two levels from an instrumented 10 m tower upwind of the cooling towers during the period June 16-25, 1978. Temperature (dry- and wet-bulb), u, v, and w components of the wind were recorded continuously onto a seven track magnetic tape at five minute intervals over the experimental period.

A tethered balloon system provided vertical profiles of temperature, moisture and horizontal wind speed and direction within the vicinity of the cooling towers as well as in the upwind direction. Profiling was performed from the surface up to as high as 400 m on one occasion. The bulk of the profiles extended up to only 100 m. During the experimental period, the tethered balloon system was flown on only seven days (June 15, 16, 17, 21, 23, 24 and 25). Its operation was limited by high winds (>10 m s^{-1}). The system was interfaced with an HP-97 calculator and provided print-out onto paper tape of time, pressure, height, temperature,

relative humidity, mixing ratio, wind speed and direction and potential temperature.

During the last three days of the experiment a Doppler acoustic sounder was employed to determine the wind profile in the boundary layer. A monostatic acoustic sounder also operated continuously during the period June 16-25; data from this device were recorded on a strip chart recorder. Plume photography was also conducted during the experiment using automatic time lapse camera systems. Visible plume lengths were in general very short during the test period; no further reference is made to this phase of the study.

Downwind drift deposition patterns were determined using sensitive papers (SP) and deposition pans distributed in arcs about the cooling towers. In addition, untreated filter papers were also exposed. These latter papers can be examined either as additional deposition receptors for further chemical analysis, or developed for Cl^- ion using Ag NO_3 (the papers treated in this manner should produce stains similar to those found on the SP's). At selected locations a rotating arm sampler with sensitive papers attached was used to determine near surface air concentrations of drift. Canal and basin water samples were collected regularly during test runs.

3. DATA ANALYSES AND REDUCTIONS

Of the eight test runs, five to six were of sufficient quality to warrant intensive analyses. For the purposes of this paper, only deposition data for the 6-16 (two tower operation) and the 6-17 (Tower 7-1 operation only) tests are presented. The source measurements for all seven test days were reduced and analyzed by ESC, from which a composite emissions inventory with a range of daily deviations was established; these emissions are assumed to be representative for any given day.

The analyses of the deposition samples were of two types:

- Chemical analysis of bulk deposition samples
- Droplet size distribution analysis of sensitive papers.

Mineral ion species, including Na^+, K^+, NH_4^+, Cl^-, NO_3^-, and SO_4^{--}, were obtained with the positive and negative ion chromatographs (IC) respectively, while Ca^{++} and Mg^{++} were determined by atomic absorption spectroscopy. Deposition pan samples and canal and basin water samples were analyzed using these techniques. Samples were recovered from the deposition pans using 10 ml of double-distilled, deionized rinse water. Canal and basin water samples were usually diluted by a factor of 100-1000 before analysis on the IC's.

Drift droplet size distributions were obtained from the sensitive papers with an automated scanning and sizing device, the Quantimet 720 system. The system was interfaced with a mini-computer which allowed the measured stain sizes to be converted to droplet sizes, binned according to size category and number and volume size distributions stored on cassette tape for later hard copy retrieval.

The results of the chemical and droplet analyses were then converted to deposition rates. The downwind deposition patterns were obtained by combining data from all of the sampling stations in each arc. It became apparent from preliminary analysis of the 6-16 test that because of the wind and dust conditions at the site during the experiment, larger background values of mineral deposition were present in the data than originally anticipated. Fortunately the sampling procedure allowed for enough outside-the-plume stations such that, with suitable statistical procedures, it was possible to eliminate most of the influence of this variable background component.

Ratios of mineral ion mass deposition provided a convenient method to distinguish drift from non-soil, background aerosol since these ratios for drift droplets should be similar to those of the basin and/or canal water. The problem of soil contamination in the deposition pans was not so straightforward. This is because the soil had been exposed to drift deposition, and more importantly, canal water from water trucks as a part of PG&E's dust abatement efforts. The upwind stations in most cases provided a useful indicator for estimating the non-soil background. Soil samples, collected near many of the sampling stations, were examined to see if any useful method for qualitative estimates of soil/dust contamination could be found. These

samples however were too inhomogeneous to help in the evaluation of the soil background.

The meteorological data from the PNL 10m meteorology tower, the tethered balloon system and the PG&E meteorology station were averaged, where practical, over intervals compatible with actual downwind sampling periods. The most important parameters affecting the drift deposition pattern were the wind speed and direction and the ambient relative humidity. At a few stations close to the tower(s) and directly beneath the plume, it was possible to obtain several sequential SP exposures. For these stations the effect of rising temperature and decreasing relative humidity was clearly evident.

4. RESULTS

In presenting the results for the two test days, 6-16 and 6-17, it is useful to summarize the plant operational data, cooling tower drift emission data, meteorological data and deposition data separately.

Average plant loads for the two days were 682 MWe and 492 MWe, respectively. Condenser water temperatures averaged 25.6°C and 24.6°C at the inlet and 36.5°C and 32.6°C at the outlet, respectively, for the two days. Average canal water temperatures were 35.7°C and 32.0°C at the inlet and 25.5°C and 24.6°C at the outlet, respectively. Cooling tower operational conditions are summarized in Table 1.

Table 1. Cooling Tower Operational Data

Date	Tower #	Cells Operating	Avg Fan HP/Cell	Water Flow (m^3/min)	Avg T_{hot} (°C)	Avg T_{cold} (°C)
7-16	7-1	12	208	570	35.6	24.5
	7-2	10	206	625	34.6	27.6
7-17	7-1	12	205	570	32.0	23.9
	7-2	0	---	---	---	---

Drift emission characteristics are based upon data derived from updraft air speed, temperature, mineral and liquid drift mass emission measurements from four cells of Tower 7-1 and three cells of Tower 7-2. The velocity

profile for each cell exhibits the double-lobed structure common to fan driven flows. The highest observed average air speed was 12.7 m/s in one of the lobe regions and the lowest speed was -4.6 m/s in the center region over the hub of the fan (see Figure 1 for a typical example). The air speed profiles were not bilaterally symmetric, due in part to the influence of external crosswinds. Calculated volumetric air flow rates were 557 ± 17 m^3/s which corresponds to an average updraft air velocity of 7.1 ± 0.2 m/s for a cell exit area of 77.8 m^2.

Typical cell temperature profiles are also shown in Figure 1; these profiles were not bilaterally symmetric either, with higher temperatures

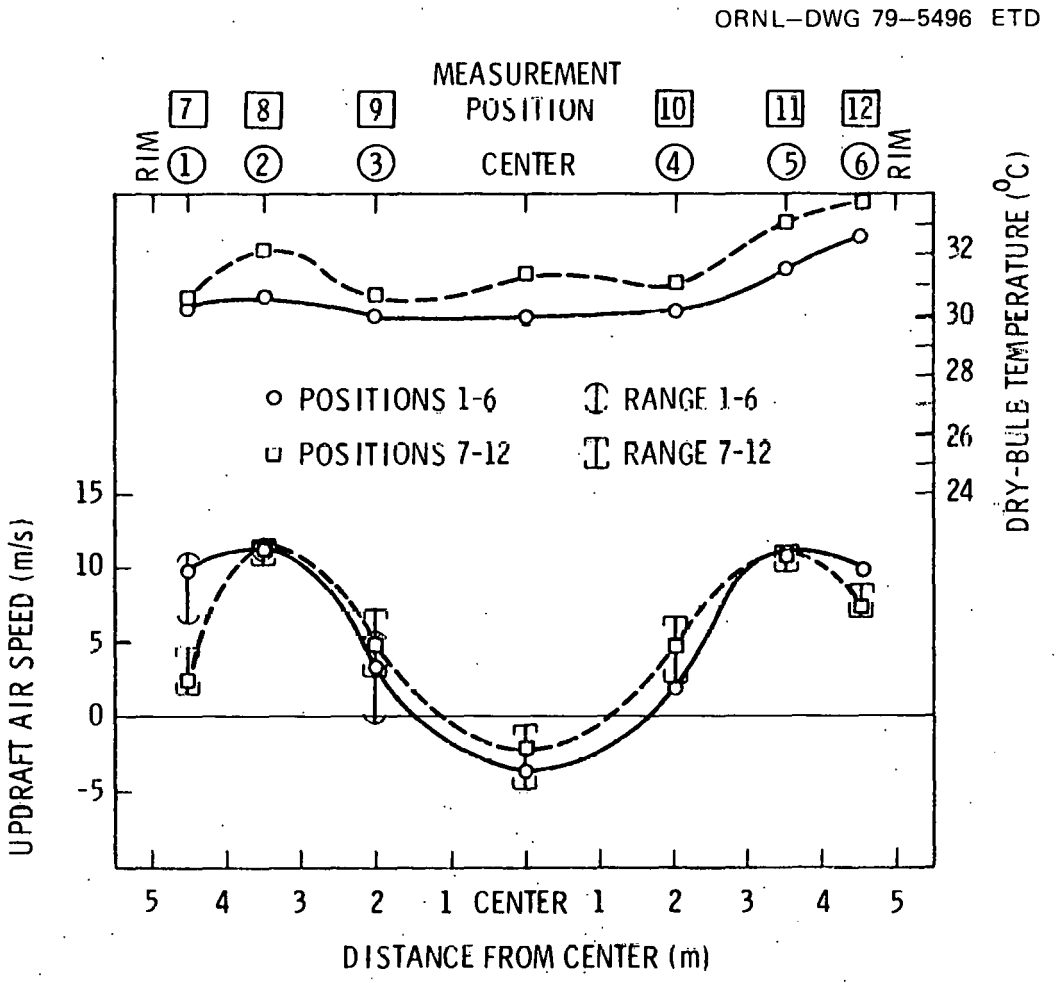

Figure 1. Updraft Air Speed and Dry-Bulb Temperature Profiles PG&E Pittsburg Unit #7, Tower #1, Cell #12. June 16, 1978. 7:30 - 12:00 PDT.

toward the rim on the downwind side of the cell. As expected for saturated air, wet- and dry-bulb temperatures were the same within sensor accuracy (±0.2°C); dry-bulb temperatures varied by as much as 6°C during a given day's characterization.

Cooling tower circulating water samples and the isokinetic (IK) tube drift mineral sample washes were analyzed for sodium and magnesium ion. Sodium mass emission rates of the seven characterized cells varied in the range 1380 to 3890 μg/s with Mg^{++} emission rate averaging ∿11% of the Na^{+} value. If no evaporation of droplets occurs in the fill region, then the mineral mass emission rates coupled with the basin water mineral concentration yield a liquid mass emission rate in the range 6.8 to 18.2 g/s. The corresponding range of values of liquid mass emission from analysis of SP drift droplet spectra were 2.6 - 8.2 g/s. The ratio of IK to SP liquid mass emission values varied from 1.3 to 6.2 with an average value of 2.8, indicating that evaporation effects within the fill are significant.

Because of the variability of drift mass emission from cell to cell, a representative emission rate per cell was calculated using a weighted average of those cells judged during a pre-test survey to have high, medium or low emissions. The result was found to be 4.8 g/s per cell or 124 g/s total emission rate if all 26 cells are operating. This corresponds to a drift fraction of 0.0006% for a total circulating water flow rate of 20 m^3/s. A representative drift mass emission spectrum is shown in Figure 2, where the mass peak near 30 μm represents droplets from the fill which have passed through the drift eliminators while the mass peak at 300 μm (and perhaps beyond) is due to large droplets formed by leakage of water into the tower plenum. Half hourly averaged values of dry-bulb temperature, relative humidity, wind speed and direction were computed and synthesized from data obtained from the 10 m meteorological tower, tethered balloon system and PG&E Station.

On June 16 the wind was relatively strong and steady from the west. The average direction was 267° with a standard deviation of 4°. During the test period (0730 - 1300 PDT), the greatest half hourly change in wind direction was only 7°. Mean wind speed and standard deviation were 4.7 ms^{-1} and 0.4 ms^{-1}, respectively. The maximum half hourly wind speed was 9.0 ms^{-1}.

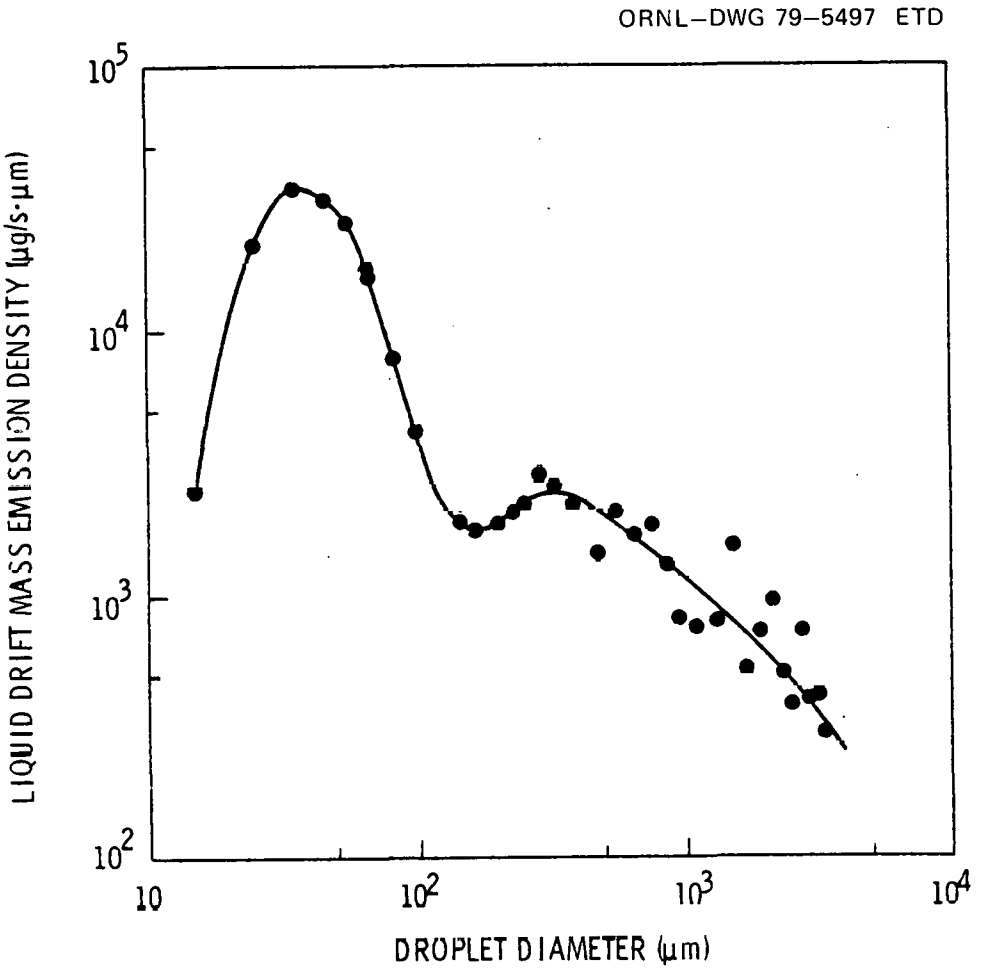

Figure 2. Composite Drift Droplet Emission Spectrum

The temperature reflected the normal heating trend on a clear day. During the measurement period, the low and high temperatures were 15.1°C and 25°C respectively. The average temperature was 20.2°C with a standard deviation of 5.6°C. The maximum half hourly relative humidity was 73% at the beginning of the test decreasing to a minimum of 35%. The average relative humidity was 46% with a standard deviation of 14%.

Meteorological conditions on June 17 were quite similar to that of the previous day except during the beginning of the measurement period when the average winds were out of the south at approximately 1.8 ms^{-1}. The average wind direction was 273° with a standard deviation of approximately 42°. Wind speed increased steadily during the morning reaching a half hourly

maximum of 6.5 ms^{-1} near noon. Mean wind speed and standard deviation were 4.1 ms^{-1} and 2.7 ms^{-1}, respectively. The average temperature was 22.0°C with a standard deviation of 4.3°C. The maximum and minimum half hourly relative humidities were 66% and 38% respectively. The average relative humidity was 52% with a standard deviation of 9%.

Figure 3 shows the sampling network with respect to the two cooling towers. The intent was to establish arcs at radii of 1/4, 1/2 and 3/4 km from Tower 7-1 with sampling stations located about every 10° along a given arc. An additional arc was set up during the test which was to be mid-way between the 1/4 and 1/2 km arcs. A separate arc at ∿1/4 km was set up for Tower 7-2. The two upwind arcs were located 1/4 and 1/2 km west of Tower 7-2, assuming persistent westerly winds. Spacings of individual stations, both radially and azimuthally, were irregular due to physical constraints of obstructions, roadways, etc. on the plant site. This irregularity, of course, made interpretations of the downwind deposition patterns somewhat more difficult than for an ideal layout; uncertainties in the measured mineral and water mass deposition rates were found to be sufficiently large such that high precision in the actual station locations was not necessary.

The drift deposition pattern was determined by first establishing a background pattern from stations outside the plume and subtracting this background component from the uncorrected pattern. An example of the pattern for Na^+ for the 6-16 test is shown in Figure 4. The error bars represent the uncertainty in the mineral mass deposition when the two deposition pans per station were analyzed separately rather than the two pans added together before analysis. The data points should also show the uncertainties in determining the background component. Along the plume center line the ratio of drift to background depositions varied from about 1 to 6, depending on the distance from the towers. Outside the plume these ratios were generally less than 1.

Peak or plume centerline deposition rates as a function of distance are shown in Figure 5 for Na^+. Also shown are predictions made by ESC with the ESC/Schrecker drift deposition model for two values of the droplet salinity and the measured drift flux from the cooling towers. The salinity value of

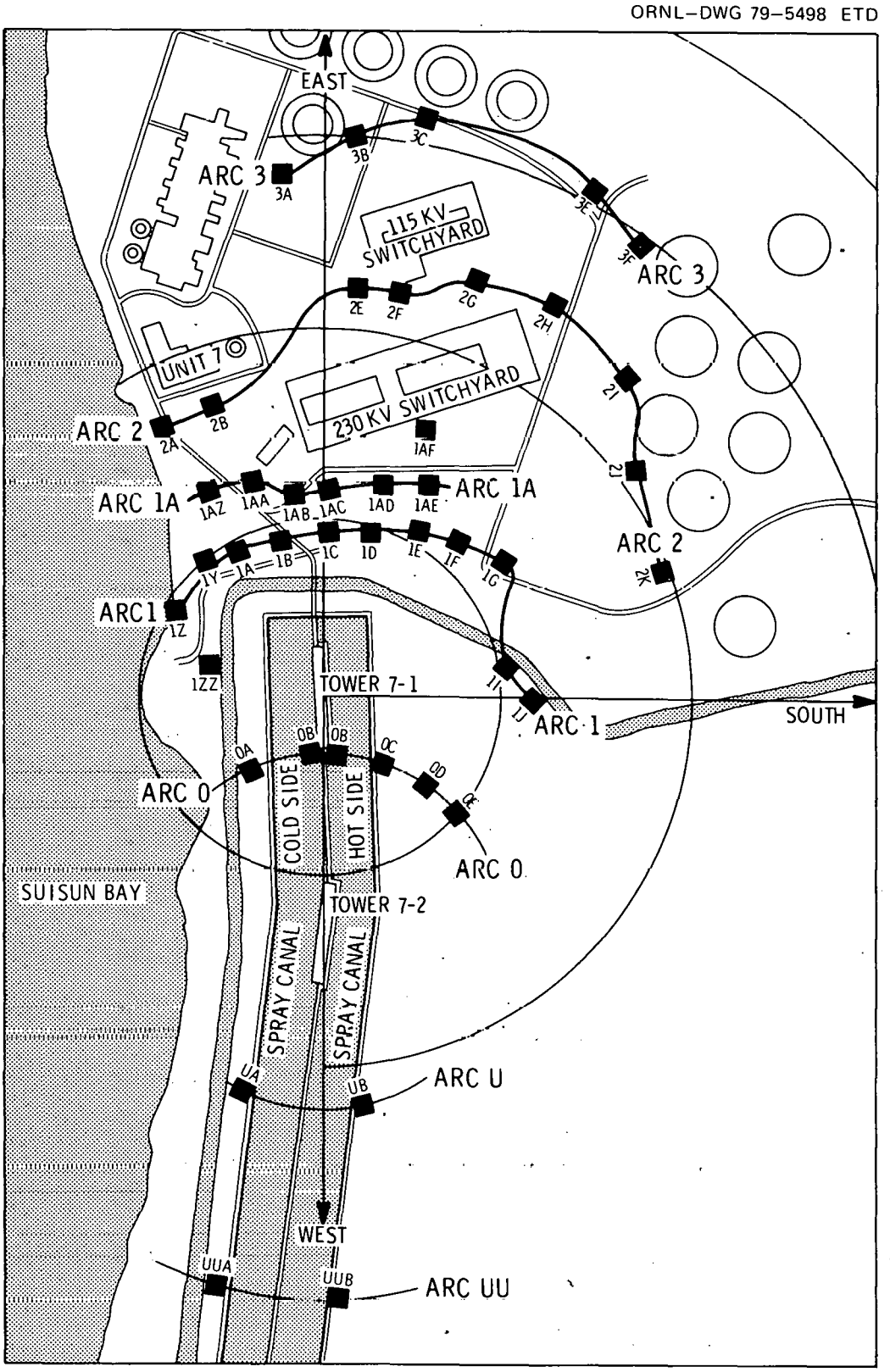

Figure 3. Sampling Station and Plant Layout for the PG&E Pittsburg Power Plant Cooling Tower Drift Study

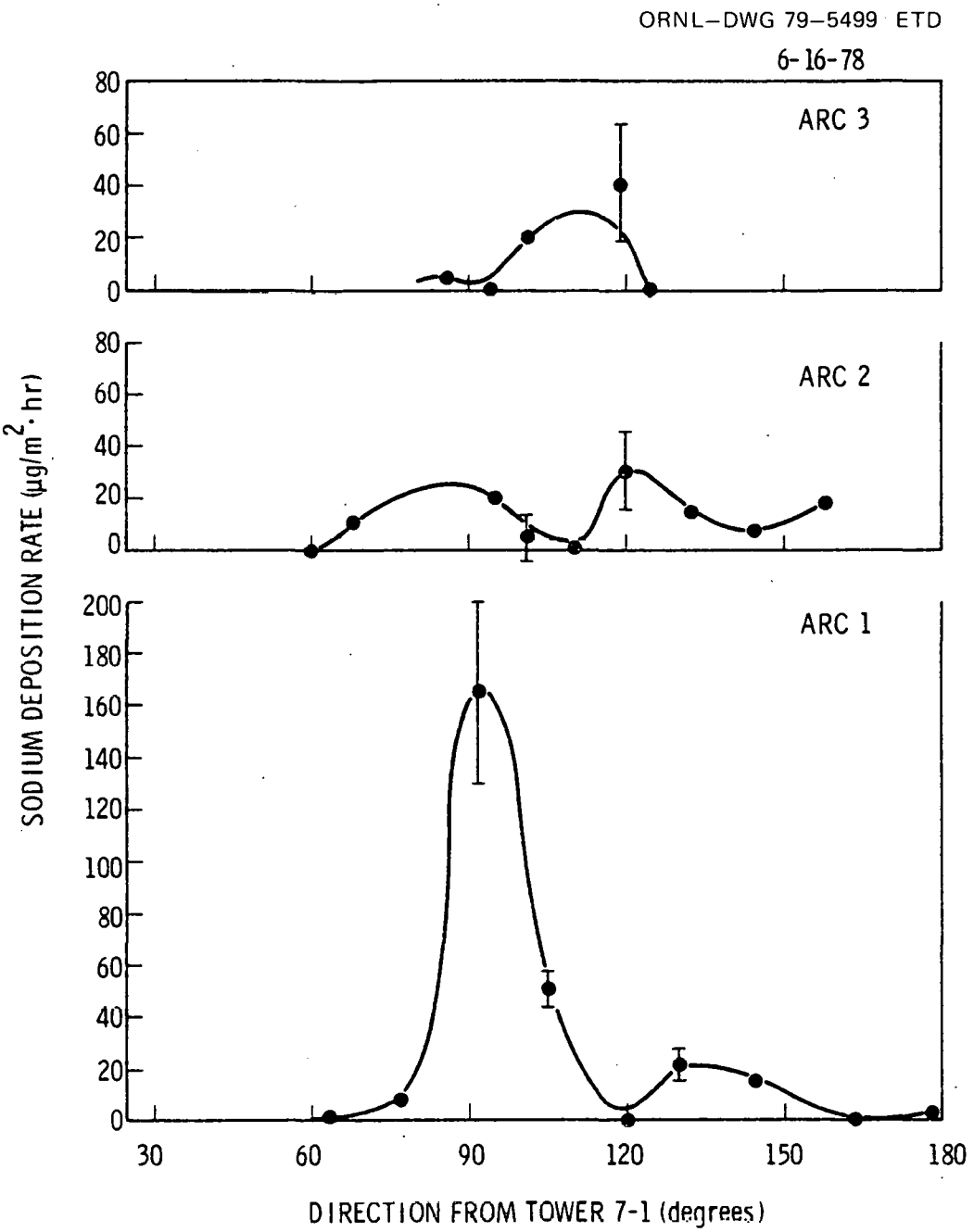

Figure 4. Downwind Surface Drift Deposition Pattern for Na^+ Ion

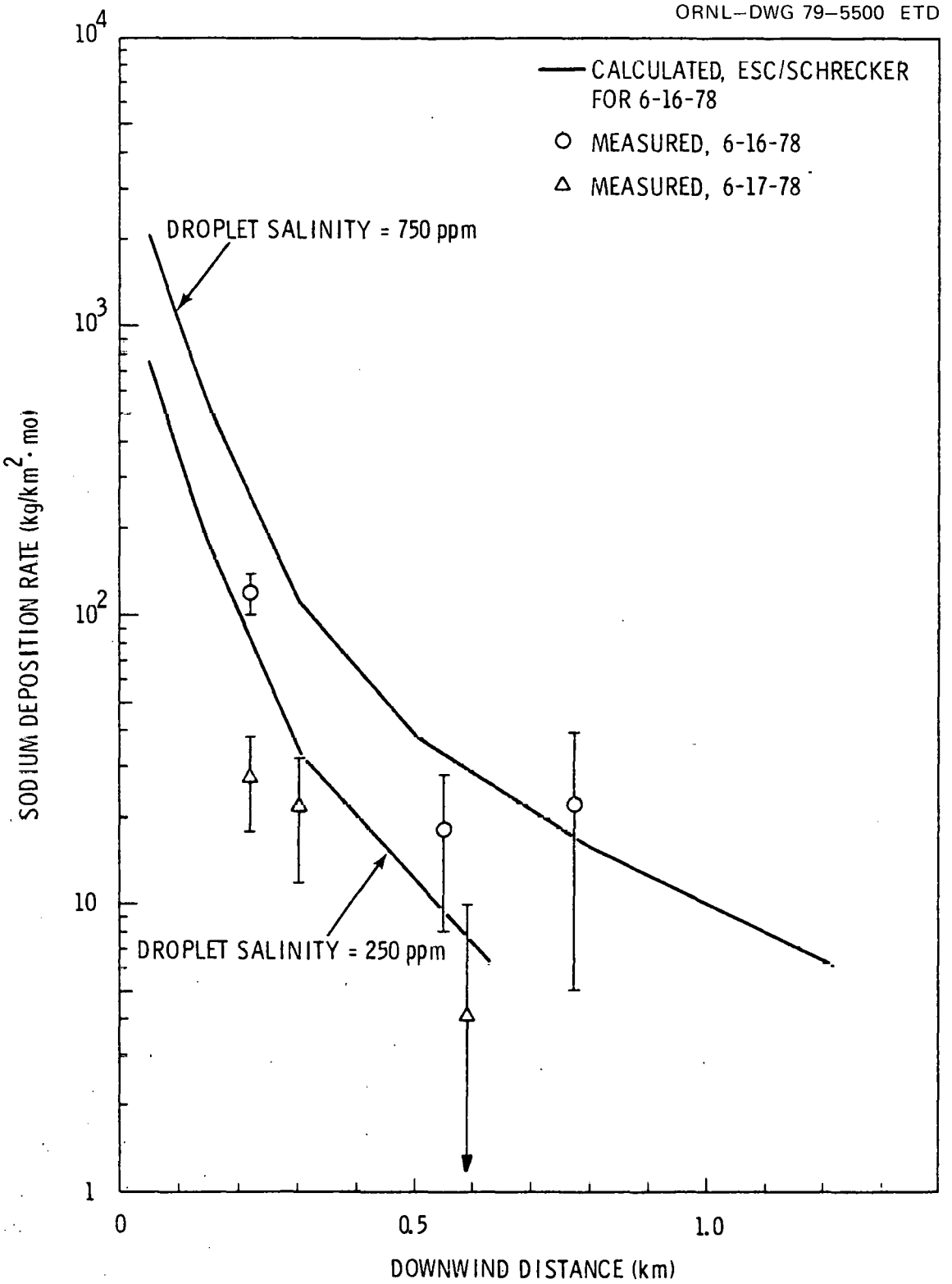

Figure 5. Peak Drift Deposition Rate as a Function of Downwind Distance

250 ppm is an average basin water value found by ESC while the 750 ppm value is one determined by ESC using the IK and SP methods for the droplets leaving the tower.

Similar deposition patterns were found for the other mineral ions, including Cl^-, SO_4^{--}, and Ca^{++}. Peak deposition rates had a distance dependence similar to the Na^+. Water droplet mass deposition rate had a much steeper falloff with distance than the mineral mass; this is a reasonable expectation because of evaporation of the droplets as they travel downwind. Deposition droplets were found to have salinities of 0.26%, 2.9%, and 2.5% at 1/4, 1/2 and 3/4 km from Tower 7-1, respectively. These salinity values are based upon the measured peak sodium mass and water mass deposition rates for each arc.

Several other observations are also apparent from an examination of Figures 4 and 5 (as well as the other data not shown). The effect of a shift in wind direction from 270° to around 300-310° during the last hour of the test is seen in Figure 4. It is not clear from these data what effect the switchyard structures had on the interception of drift material before its deposition onto the receptors.

From a comparison of the experimental values at 1/2 and 3/4 km alone it would appear that the switchyards could have reduced the drift deposition by as much as a factor of two. Referenced to the ESC/Schrecker model the value at 3/4 km would appear to be too high. The deposition values (Figure 5) for the 6-17 test are lower than the 6-16 test values primarily because of a reduced power load; otherwise wind conditions were similar for both days. Consequently, additional test days where the wind did not blow the drift plume through the switchyard, will be required to examine the effect of these structures on the drift.

The effect of decreasing relative humidity during the course of a test run was also observed on the sensitive papers. The peak droplet mass deposition rate for the 6-16 test changed from a value of 1070 mg/m^2 hr during the first 1 1/4 hr of the test to a value of 310 mg/m^2 hr during the next 1 3/4 hr, although a value of 280 mg/m^2 hr was also measured at an adjacent station corresponding to the wind shift which had occurred during the final

hour of the test. Similarly for the 6-17 test, the droplet mass deposition rate changed from 530 mg/m^2 hr during the first 1 1/4 hr to 145 mg/m^2 hr during the final 2 1/2 hrs.

5. CONCLUSIONS

A comprehensive experiment to study drift from mechanical draft cooling towers was conducted during June 1978 at the PG&E Pittsburg Power Plant to establish a data base for use in drift deposition model validation. Results from two test runs have been discussed. It was found that using the source measurements obtained by ESC and the ESC-Schrecker drift model that the predicted downwind depositions are in reasonable agreement with the observed values. Background mineral depositions arising mainly from blowing dust produced substantial interference with the downwind deposition patterns, especially at the larger downwind distances where drift deposition rates were small.

The effects of wind direction changes and relative humidity changes during the course of an experiment were easily seen in the results. The effect of structures such as the electrical switchyards, in sweeping out drift material before it arrives at the surface was examined. With the limited data which has been presently analyzed, no definite conclusion can be established.

6. ACKNOWLEDGMENTS

The author acknowledges with gratitude the efforts of John Maulbetsch of EPRI in providing funds for the source characterization part of the study, and the efforts of Ron Webb and Karl Wilber of ESC in conducting the source measurements and reporting the results in a timely fashion. The following people contributed to the success of the PNL field effort: Owen Abbey, Don Glover, Roger Schreck, John Thorp and Stan Ulanski. Jane Rothert and Steve Harris carried out the chemical analysis of the drift mineral samples while Lee Daniel was in charge of the droplet sizing analysis from the SP samples. Stan Ulanski was responsible for meteorological data reductions.

III. STUDIES OF THE ENVIRONMENTAL IMPACT OF EVAPORATIVE COOLING TOWER PLUMES

D. W. Thomson* and A. C. Dittenhoeffer*

1. INTRODUCTION

This ongoing research program of the environmental impact of cooling tower plumes included during the past year three principal areas of study. These were:

1. Airborne observations of turbulence in cooling tower plumes including detailed measurements of temperature, velocity and moisture fluctuations in a wide variety of meteorological and plume conditions.

2. Measurements and modeling of the conversion of SO_2 to sulfate particles in coal-fired power plant plumes in both "dry" and merged (with the cooling tower) plumes.

3. Assessment of remote probing sodar (sound detection and ranging) techniques for indirect sensing of turbulent temperature and velocity fluctuations in plumes.

Progress in each of the above areas is summarized below.

2. AIRBORNE TURBULENCE MEASUREMENTS

The onset of airborne field work in FY-78 was nearly disastrously delayed by late arrival of the funding for and the long delivery time of the required Lyman-α humidiometer. Fortunately, it was possible to arrange for the loan of a unit from the Argonne National Laboratory so that many installation, calibration and evaluation procedures were completed before the airborne unit was delivered. Flight testing was completed in July before the research aircraft was committed to another field program in August. During the months of September and October, research measurements for either the turbulence or SO_2 studies were then made

*Department of Meteorology, The Pennsylvania State University, University Park, Pa.

on essentially every possible day. In the two month period a total of 29 research flights were completed; 13 for in plume turbulence analyses; 16 for SO_2 studies. Analyses of the water vapor fluctuation measurements are now in progress.

T.N. Chin completed the difficult analysis of the airborne vertical velocity measurements in the Keystone Power Plant cooling tower plumes. The summary and conclusions of his M.S. Thesis "Characteristics of Vertical Velocities and Vertical Sensible Heat Fluxes in Cooling Tower Plumes" follows:

As part of the Cooling Tower Plumes Project in the Department of Meteorology of The Pennsylvania State University, airborne measurements of plume turbulence parameters have been conducted at the Keystone Power Plant near Indiana, Pennsylvania. A technique for calculating vertical velocities and vertical sensible heat fluxes has been developed. As an indication of the relative turbulence level in the plumes, the standard deviations for vertical velocity, excess temperature and vertical sensible heat flux in three spatial intervals, pre-plume, plume and post-plume values of vertical velocity, excess temperature and vertical sensible heat flux were also constructed. Penetration averaged, width normalized profiles were constructed to yield the average shape of plume profiles. The results of the calculations of the vertical sensible heat flux were compared to a model which predicts the total heat energy dissipated by a cooling tower. The agreement between the two methods is good.

From the individual plots of vertical velocity and excess temperature it can be seen that the definition of plume boundaries decreases as the plume moved downwind. It might be concluded that the scale, on which most entrainment occurs, grows from a scale which is small compared to that of the plume to a scale which is on the order of the size of the plume as a function of downwind distance. A boundary layer between the upward moving part of the plume and the relatively calm ambient air can be seen in a large number of the individual vertical velocity penetrations. This boundary layer appears as a layer of sinking air which is not necessarily, in general, symmetrically located around the plume.

Roughly two-thirds of the plumes considered in this thesis have vertical velocities which are mainly positive. The remaining third exhibits velocities of both signs, even adjacent to one another. These latter plots suggest that some of the parcels making up the plume have complex internal circulation as well as a mean positive vertical velocity. Plots were constructed of means and standard deviations of vertical velocity, excess temperature and vertical sensible heat flux as a function of downwind range. Also constructed were the same plots in which the penetrations were grouped according to range and averaged. In the plots of individual penetrations a large amount of variability in the values of these parameters is evident, even for values obtained repeatedly at the same range. This, along with other documented observations, lends support to the idea that the cooling tower plume is made up of "puffs". Also, from these plots it can be concluded that beyond 300 to 400 meters downrange the mean values and standard deviations of these parameters closely approaches ambient values.

Widths of the vertical velocity or momentum plumes and the excess temperature plumes were measured and plotted as a scatter diagram. On the average, the widths are the same.

Penetration averaged, width normalized profiles were constructed for vertical velocity, excess temperature and vertical sensible heat flux. Near the cooling tower, the profiles have a "top-hat" shape and the interior is chaotic. Further downrange (300-400m) the edges of these profiles are more diffuse; the interior remains chaotic.

Figure 1, a reproduction of Figure 4.16 in his thesis, clearly illustrates one of his important findings. That is the high degree of correlation between the "widths" of the velocity and temperature plumes. In the past models of plume behavior have frequently assumed these widths not to be equal, an assumption which we feel can no longer be justified as a consequence of these observational results.

Some of the thesis study results, used to analyze drift breakaway, were presented in a paper by J. A. Pena and T. N. Chin, "Vertical Velocities in Cooling Tower Plumes" which was given at the Symposium on Environmental Effects of Cooling Tower Emissions at the University of Maryland on 2-4 May 1978.

3. CONVERSION OF SO_2 TO SULFATE PARTICLES

A. C. Dittenhoeffer, as a Ph.D. dissertation study, and R. G. de Pena have been evaluating the effects of meteorological parameters such as solar radiation flux and relative humidity on the sulfate particles. Aerosol sampling equipment on-board the research aircraft includes a condensation nucleus counter, an optical particle counter, and an electrical aerosol analyzer. Plume particles within the size range 0.10 - 1.30 μm diameter are collected with a cascade impactor, onto which carbon-coated electron microscope grids were placed. A quantitative method developed at Penn State (Mamane and de Pena, 1978) for the analysis of individual sulfate particles using a transmission electron microscope allows for the identification and sizing of the sulfate aerosol collected. A rapid-response pulsed fluorescent analyzer provides measurements of SO_2. Sampling is performed upwind of the power plant at plume elevation to determine background SO_2 and sulfate particle concentrations, and these are subtracted from concentrations measured downwind of the plant and are not only dependent upon plume dynamics and chemistry, but also upon the position in the plume where the sampling takes

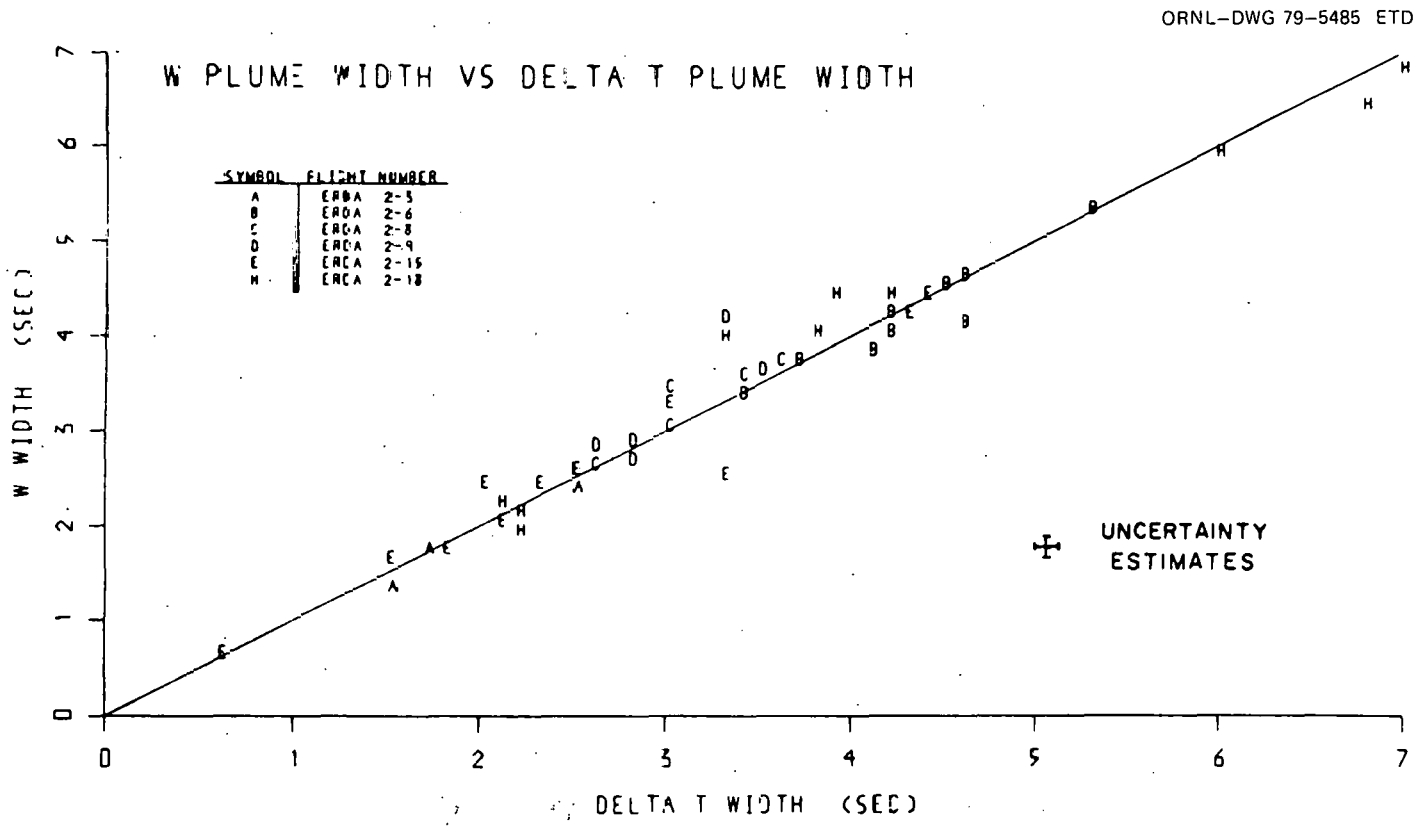

Figure 1. Plot of vertical velocity plume width vs delta T plume width.

place. It is therefore common to find irregular variations of gas and particle concentrations within power plant plumes. To eliminate the effects of plume inhomogeneity and thus isolate the effects attributable to plume chemistry, all particle number and volume concentrations are normalized by simultaneous concentrations of SO_2.

Pertinent meteorological conditions that prevailed during the flights conducted for this study are listed in Table 1. Plumes were classified as merging or non-merging. In only one case, flight 4, did significant interaction between the power plant stack plume and cooling tower plume occur, and measurements were made within this visible, merged plume out to 50 km downwind of the plant, the point at which the liquid plume had dissipated. For the other flights, sampling proceeded out to distances where SO_2 approached background levels.

Comparisons are made between the flights at thirty minutes plume travel time. In Figure 2, normalized sulfate particle concentrations are plotted against the cosine of the solar zenith angle, which is proportional to the flux of solar radiation received at the top of the atmosphere. For cases in which cloud cover existed during the sampling period, cos Z was multiplied by a factor (1-A), where A is an estimate of the cloud albedo according to Sellers (1965). For small sulfate particles, diameter ranging from 0.15 and 0.30 μm, there appears to be a direct relationship between cos Z and number concentration. For larger

Table 1. Summary of Flights

Flight	Date	Time of Day	Plume Type	Sky Condition	Relative Humidity	Cos Z
3	12/14/76	07:04 - 09:59	non-merging	clear - sunny	55	.369
4	2/08/77	06:51 - 08:57	merging	clear - ground fog	>95	.157
6	4/18/77	05:39 - 07:10	non-merging	cirrus, 2/10	59	.173
9	5/04/78	05:53 - 07:33	non-merging	cirrostratus, 9/10	44	.046
11	7/07/78	13:56 - 14:56	non-merging	cumulus, 3/10	83	.663

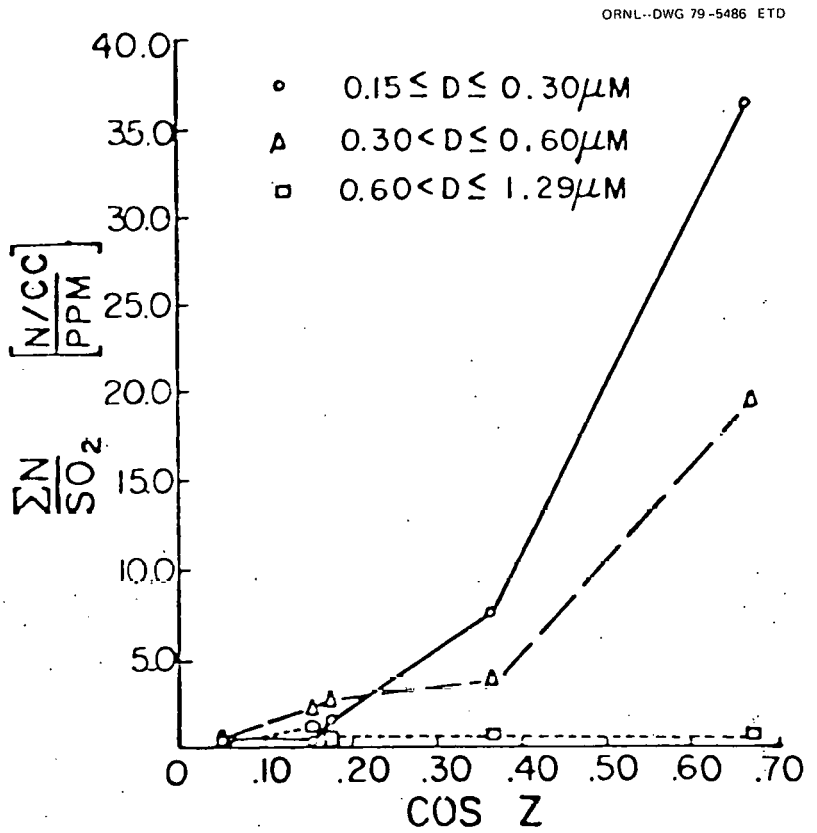

Figure 2. SO_2-normalized sulfate particle number concentration vs. the cosine of the solar zenith angle for various particle sizes.

particle sizes this relationship gets progressively less distinct. No apparent relationship exists between particle concentration and cos Z for the largest particles (0.60 - 1.29 μm dia.). The SO_2-normalized condensation nuclei (total Aitken particles) as measured by the CNC for each of these flights are displayed in Figure 3 as a function of the cosine of the solar zenith angle, and a relationship similar to that for small sulfate particles is observed. These results suggest that photochemical reactions involving the gas phase homogeneous oxidation of SO_2 are at work. At 30 minutes plume travel time, the largest of the sulfate particles resulting from these reactions have grown to sizes of the order of 0.6 μm diameter.

Sulfate particle concentrations within the 0.15 - 0.60 μm size range display erratic behavior with respect to relative humidity (Figure 4), while the largest

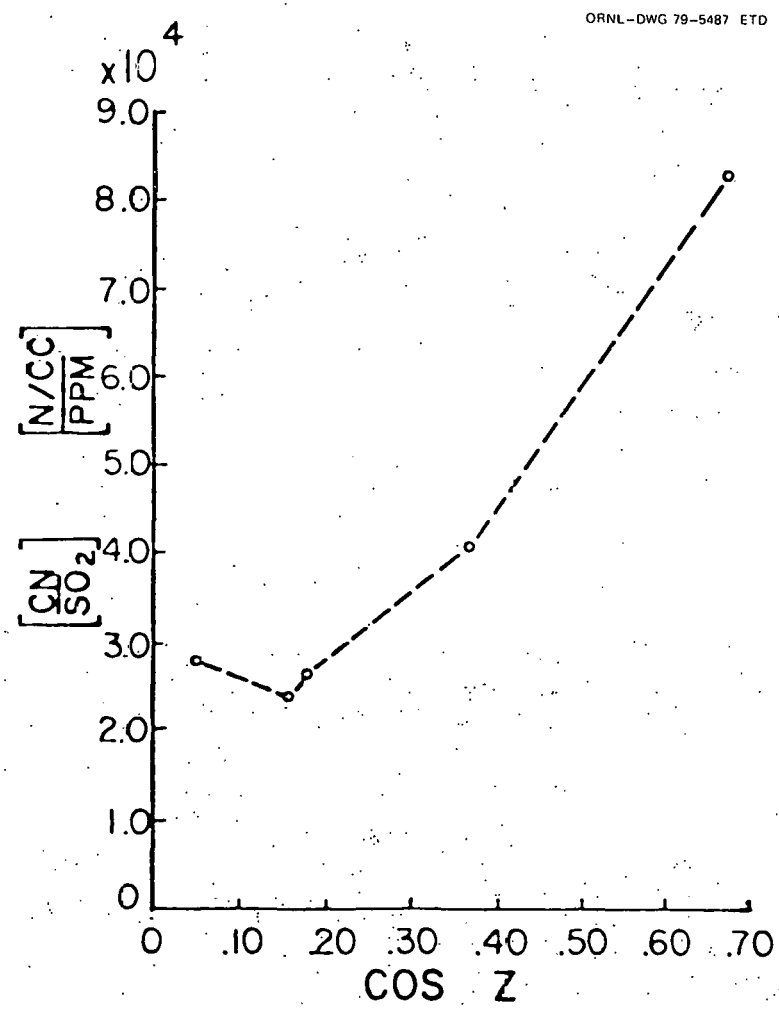

Figure 3. SO_2-normalized condensation nuclei (total Aitken particles) vs. the cosine of solar zenith angle.

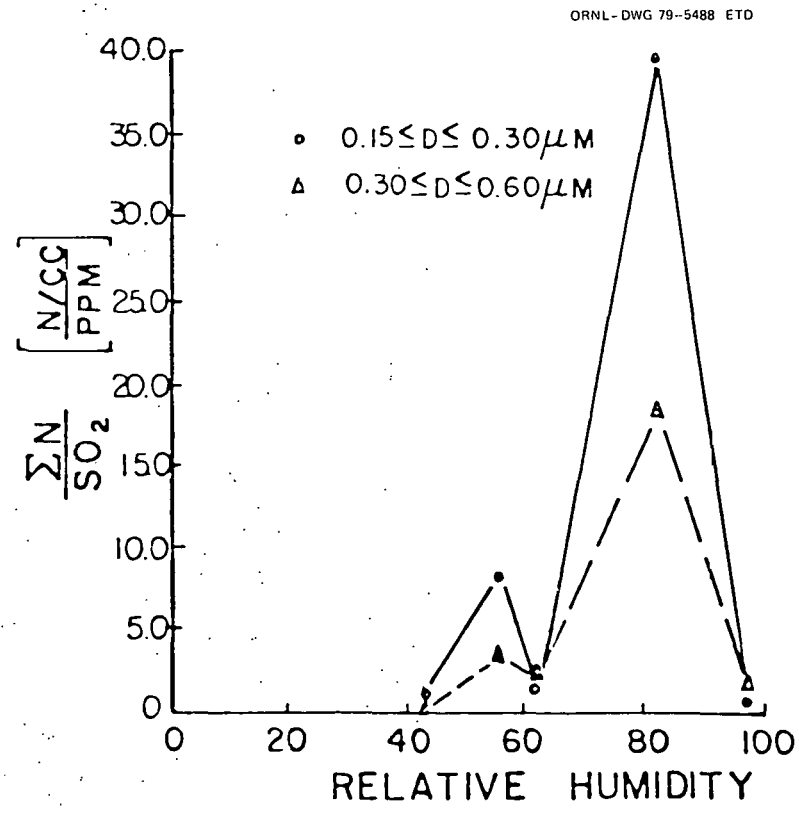

Figure 4. SO_2-normalized sulfate particle number concentrations vs. relative humidity for two particle size ranges.

particles exhibit a direct relationship (Figure 5). This relationship is more obvious for particle volume, as shown in Figure 6. The volume of sulfate contained in the particle size range 0.60 to 1.29 μm is significantly highest for flight 4, the case in which the plume of the cooling towers merged with that of the stacks. For the smaller sulfate particles (0.15 to 0.60 μm), the aforementioned effects of solar radiation have obscured any possible relationship relative humidity might have with particle number and volume.

The particle size distributions appear in Figures 7 and 8. In Figure 7, for the case of moderately intense solar radiation and low relative humidity, flight 3, sulfate particles are far more numerous than for flights 4 and 6, especially for sizes less than 0.5 μm. The background-corrected plume of flight 9 only contained sulfate particles within the size range 0.10 - 0.28 μm and was omitted from the diagram. During conditions of very intense solar radiation and high relative humidity (flight 11, Figure 8), nuclei production within the plume is most prolific, resulting in extremely high particle concentrations at the lower end of the size spectrum. These particles have grown from embryo-size, of the order of tens of angstroms, to several tenths of a micron in the span of less than thirty minutes. Significant concentrations of sulfate particles larger than 0.7 μm diameter were found only during flight 4, the case of plume merger. Particles as large as 1.30 μm were collected on the fourth stage of the impactor during this flight. The oxidation of SO_2 in the droplets maintained by the high relative humidity of the cooling tower plume most likely accounted for this particle growth.

In Figures 9 and 10 the normalized particle number and volume concentrations are displayed as a function of plume travel time for particles ranging from 0.15 to 1.29 μm. The sharp increase in sulfate particle number and volume with plume age for flight 11 clearly exhibits the vital role solar radiation plays in plume chemistry. The rate of change of particle volume, i.e., the SO_2 conversion rate, during the latter portion of flight 4 approximates that of flight 11,

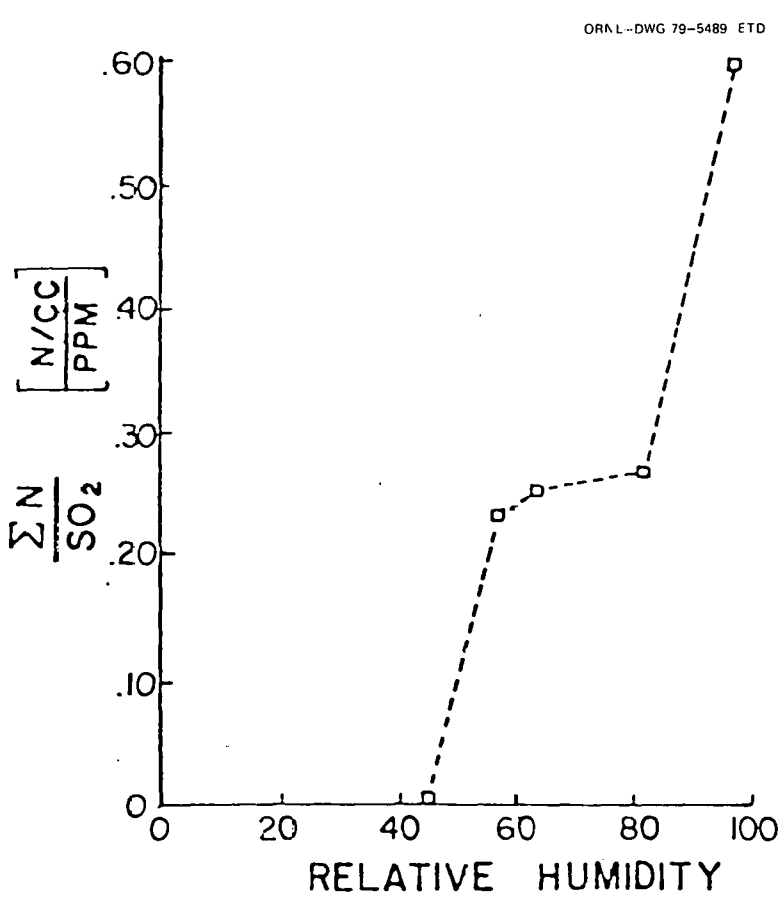

Figure 5. SO_2-normalized sulfate particle number concentrations vs. relative humidity for particles $0.60 < D \leq 1.29$ μm.

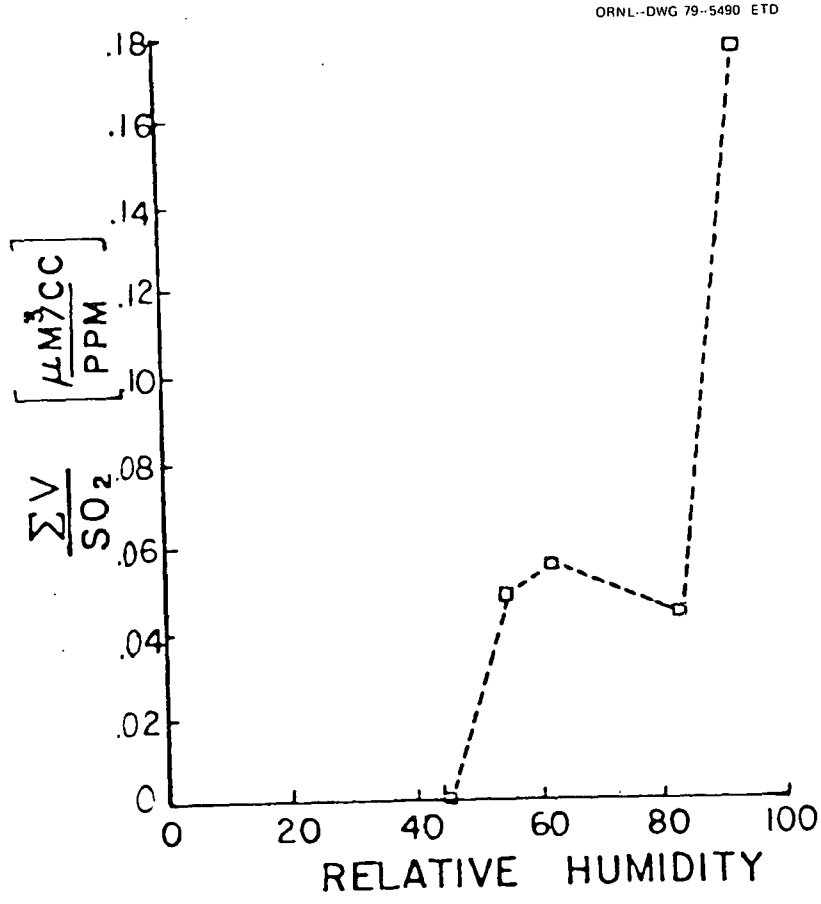

Figure 6. SO_2-normalized sulfate particle volume concentrations vs. relative humidity for particles $0.60 < D \leq 1.29$ μm.

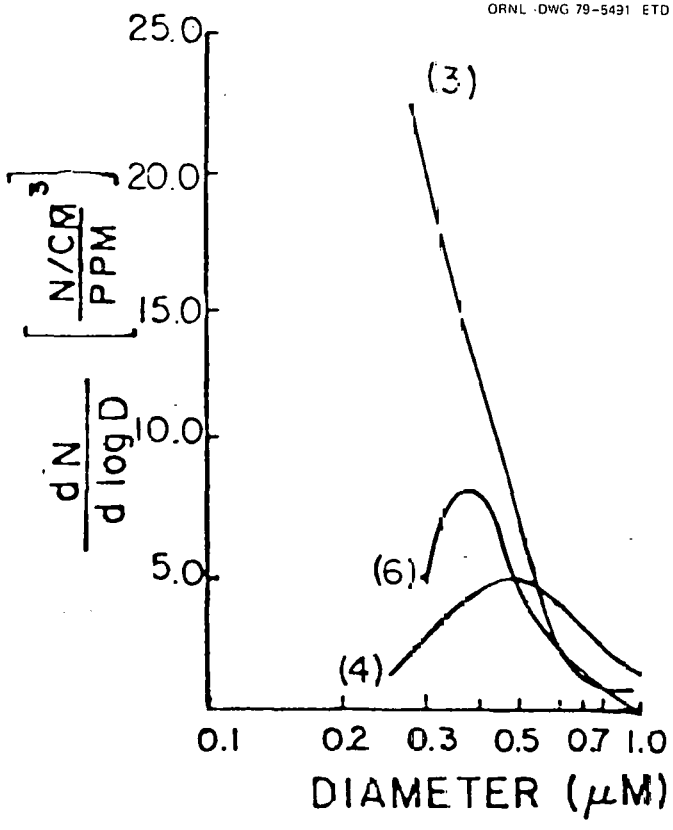

Figure 7. SO_2-normalized sulfate particle size distributions for flights 3, 4, and 6.

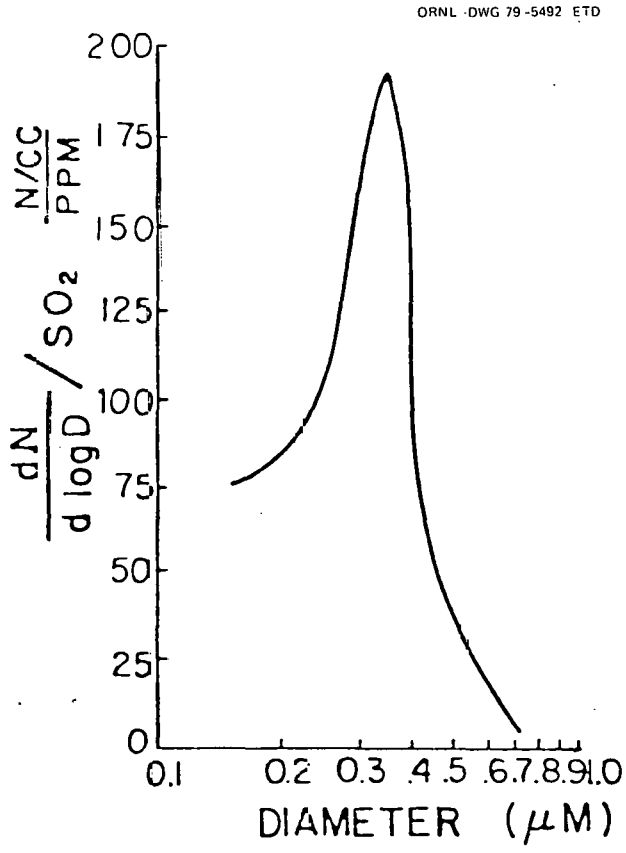

Figure 8. SO_2-normalized sulfate particle size distribution for flight 11.

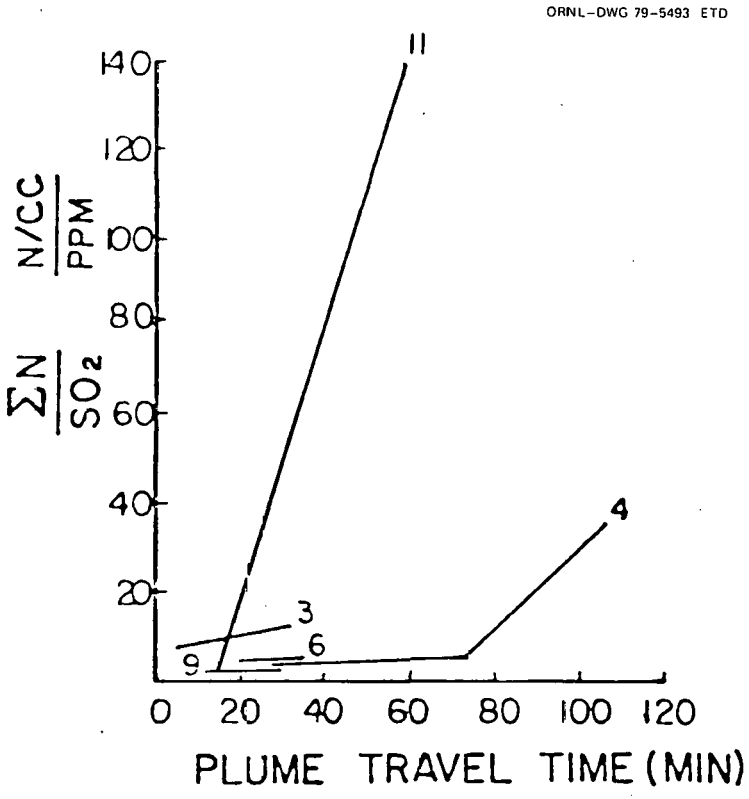

Figure 9. SO_2-normalized sulfate particle number concentrations vs. plume travel for all the flights.

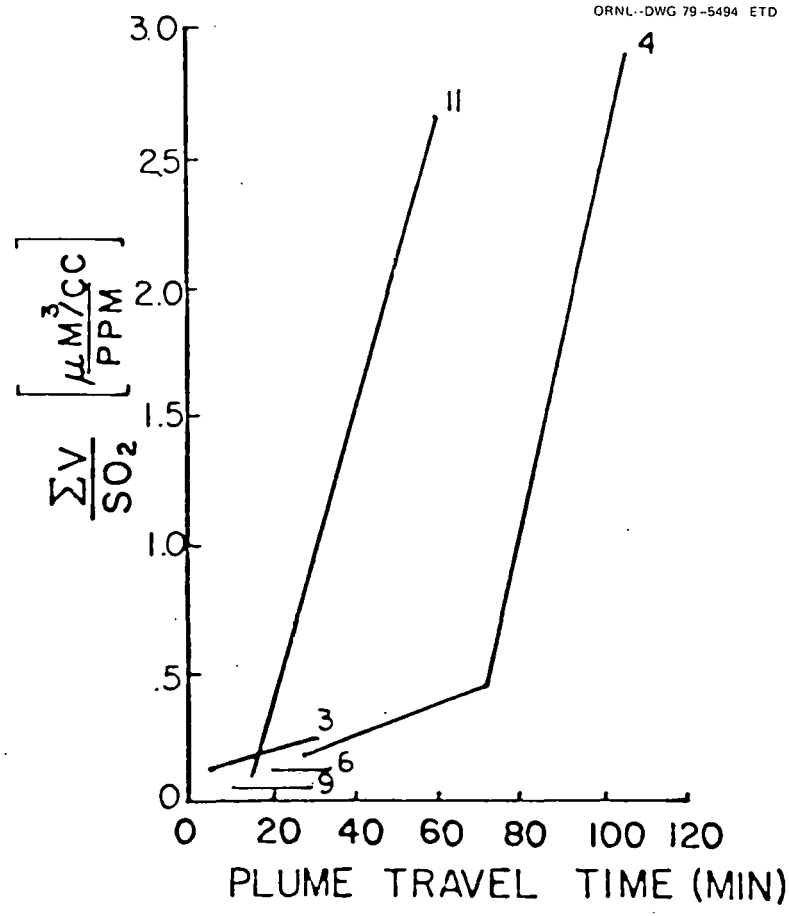

Figure 10. SO_2-normalized sulfate particle volume concentrations vs. plume travel time for all the flights.

indicating that the predominant chemical mechanisms existing during each of the flights were of comparable importance. The conversion rates during flights 6 and 9, situations of low intensity radiation and low relative humidity were negligibly small compared with the aforementioned flights.

Comparisons made between flights at equal plume travel times reveal a direct dependence of SO_2-normalized sulfate particle concentration on solar radiation flux for particle sizes 0.10 - 0.30 μm. This relationship gets progressively less distinct for larger sulfate particles. Total SO_2-normalized Aitken particle concentrations display a similar direct relationship with solar radiation, suggesting that photochemical reactions involving the gas phase oxidation of SO_2 are at work. It is observed that the largest of the sulfate particles resulting under these conditions grows to roughly 0.7 μm diameter after 30 mintues of plume travel.

Under conditions of high plume relative humidity in which the stack and cooling tower plumes merge, the sulfate particle size spectrum shifts toward much larger sizes. These particles are found to have grown to sizes greater than 1.30 μm after 30 minutes. The oxidation of SO_2 in the droplets maintained by the high relative humidity of the cooling tower plume most likely accounted for this particle growth.

Finally, when the rates of change of SO_2-normalized sulfate particle volume are compared for flights conducted under highly varying meteorological conditions, it is found that the predominant chemical mechanisms responsible for SO_2 conversion are of comparable importance. When both relative humidity and solar radiation flux are low, the sulfate production rate within the plume during the initial 40 minutes of plume travel is negligibly small.

4. ASSESSMENT OF SODAR TECHNIQUES

In D. W. Thomson's absence (sabbatical leave at Risø National Laboratory, Denmark), K. Underwood and L. Kristensen continued analysis of the Autumn 1976

Keystone measurements. This phase of the work was essentially completed with publication of the following thesis and reports:

Underwood, K. H. (1978), A Quantitative Study of Cooling Tower Plumes using a Monostatic Sodar, M.S. Thesis, The Penn State University, University Park, PA, March, 1978.

Kristensen, L. and K. H. Underwood (1978), Sodar Geometry, Fourth Symp. Meteo. Obs. and Instru., Amer. Meteo. Soc., 10-14 April 1978.

Coulter, R. L. and K. H. Underwood (1978), Sodar and Aircraft Measurements of Turbulence Parameters within Cooling Tower Plumes, loc. cit.

Conclusions and recommendations of the Underwood thesis follow. Figure 11, extracted from Underwood, clearly shows the viability of the sodar technique for "close-in" continuous measurements where aircraft work is both difficult and dangerous.

This thesis has analyzed the effects of cooling tower plumes on the local atmosphere in terms of parameters directly measurable by a monostatic sodar. To support the analysis of the backscattered power, it was first necessary to show that a lognormal distribution of power is obtained within the plume. Evidence of a distinctly non-lognormal distribution would have placed the assumption of sensing within the inertial wavenumber range in doubt. Once it was established that the backscattered power followed a lognormal distribution, C_T^2 values could be estimated with some confidence.

The main focus of the study centered on the usual measurement of monostatic sodar, i.e. C_T^2. Modification of C_T^2 by 2 to 3 orders of magnitude over normally obtained atmospheric values was noted. This confirms the existence of the intense turbulent activity necessary to homogenize the large temperature fluctuations produced by the plumes. The decrease of C_T^2 by 2 orders of magnitude within the nearest 55 m to the cooling tower is best explained as a function of both distance from the source stack and the sensible heat flux from the stack. This allowed as much as 85% of the variation of C_T^2 to be explained when a power law dependence on both distance and heat flux was assumed.

To support the measurements of C_T^2 by the acoustic sounder, aircraft-derived C_T^2 values were computed by applying Taylor's hypothesis. These derived C_T^2 values supported both the magnitude and variation of C_T^2 values observed with the sodar. The derived C_T^2 values were tested to ensure that they followed a lognormal distribution. Thus, they enabled an independent test to be made for both the existence of an inertial range and the magnitude of C_T^2.

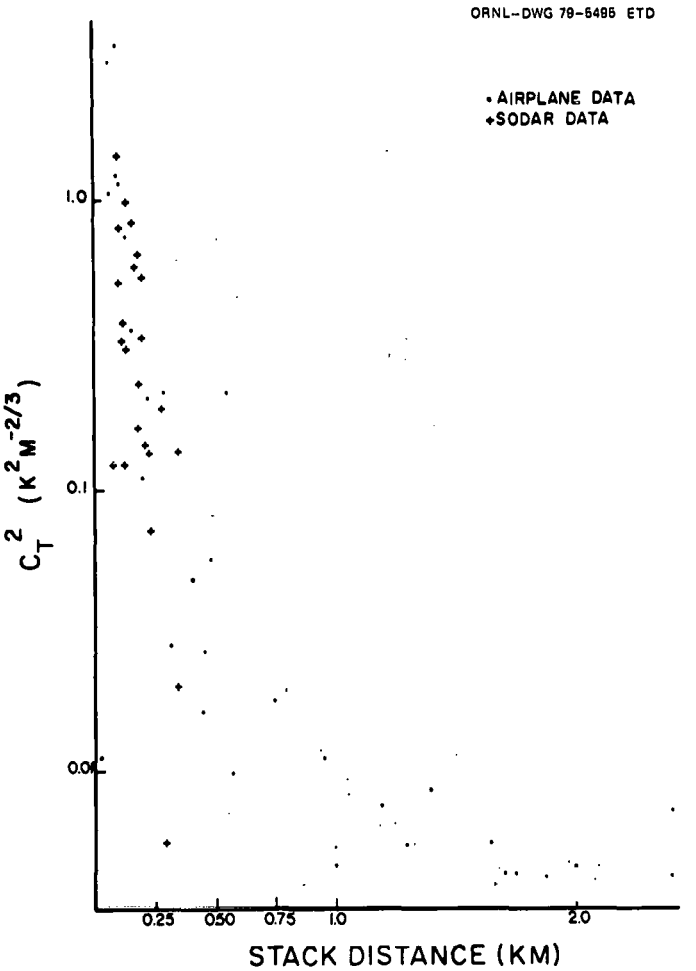

Figure 11. Observed Variation of Sodar and Aircraft C_T Magnitudes Versus Distance from Cooling Tower Stack 2A.

Finally, a method of utilizing a phase-coherent monostatic sodar to compute C_V^2 was attempted. The C_V^2 computed from this method was compared to that obtained from a bistatic power measurement simultaneously performed. The results showed agreement to within one order of magnitude.

Although the analysis presented here is not exhaustive, it does provide a first step toward utilization of the sodar for the study of modification of a local environment by cooling tower plumes. Many further areas need to be examined to increase the utility of the sodar in the study of environmental modification. Some of these areas are: 1. the effects of the volume averaging inherent to a sodar of finite beamwidth, 2. the effect of partial beamfilling and how reasonable corrections can be made, 3. the interpretation of Doppler-derived monostatic C_V^2 values in terms of volume averaging and pulse to pulse averaging, and 4. utilization of multifrequency sodar data to provide estimates on scattering from the hydrometeors which constitute the visible plume.

Through further study of these areas it should be possible to provide a nearly continuous estimate of the fundamental turbulence parameters ε and ε_o within a plume from a monostatic sounder. Realization of this objective would greatly improve the phase-coherent monostatic sounder as an environmental modification monitoring instrument.

REFERENCES

Chin, T. N. (1978), Characteristics of Vertical Velocities and Vertical Sensible Heat Fluxes in Cooling Tower Plumes, M.S. Thesis, The Penn State University, University Park, PA 16802.

Gillani, N., Husar, R., Husar, J., Patterson, D., and Wilson, W., 1978: Project MISTT: Kinetics of Particulate Sulfur Formation in a Power Plant Plume out to 300 km. Atmos. Env., 12, 589-598.

Mamane, Y., R. G. de Pena, 1978: A Quantitative Method for the Detection of Individual Submicrometer Size Sulfate Particles. Atmos. Env., 12, 69.

Sellers, W. D., 1965: Physical Climatology. University of Chicago Press, 272 pp.

Underwood, K. H. (1978), A Quantitative Study of Cooling Tower Plumes Using a Monostatic Sodar, M.S. Thesis, The Penn State University, University Park, PA 16802.

PHYSICAL MODELING

PAGES 77 to 78

WERE INTENTIONALLY

LEFT BLANK

IV. PLUMES FROM THREE AND FOUR COOLING TOWERS

L. D. Kannberg*

1. INTRODUCTION

Use of mechanical- and natural-draft cooling towers is expanding in the United States in response to pressures for better resource allocation and preservation. Specifically, increasing public and regulatory concern over the effects of the intake and discharge of large volumes of cooling water has encouraged electric utilities to accept cooling towers as the primary method of removing condenser waste heat even though once-through cooling is considerably less expensive. Other factors encouraging the use of cooling towers include small water supply and consumption rates, reduction in land requirements (compared to cooling ponds or lakes), and operational flexibility. The growing demand for electric energy should also add to the increase of cooling tower use.

For economic and technical reasons, future electric generating stations will be larger than those currently in use. Because there is roughly 2 MW of waste heat produced for every megawatt of electricity generated, waste heat disposal becomes a significant factor in the design of these large generating facilities. This is particularly true for siting of the station and the towers at the station. Economics usually dictate that the cooling towers be located as close to the generating unit as possible, whereas environmental and cooling tower operational considerations encourage widely spaced towers. This opposition of interests requires that station designers be capable of assessing the relative impacts of various siting and operational configurations. It is therefore important to understand both the environmental and operational characteristics of cooling towers, especially multiple towers. This paper presents experimental data concerning the temperatures of downwind plumes for stations having three or four mechanical-draft cooling towers in flat terrain. The work presented here is an extension of work summarized in references 1 and 2.

* Battelle Pacific Northwest Laboratories, Richland, WA.

Parameters investigated include the effects on plume mixing and trajectory by various wind speeds, Froude numbers (discharge density and velocity), orientation of multiple towers (relative to wind direction), and number of towers. Mechanical-draft cooling towers similar to those now in operation at the Centralia Power Plant in southwestern Washington were used as prototypes for physical models. Simulations employing the physical models were made in a glass-walled hydraulic flume. The data obtained from these physical model simulations are presented first for three towers and then for four towers.

2. EXPERIMENTAL DESIGN AND EQUIPMENT

The simulation of cooling towers in a hydraulic flume is desirable because of the special scaling characteristics of water. Since water has a kinematic viscosity nearly 20 times lower than air at standard temperature and pressure, the length scaling for Reynolds number and, more importantly, for turbulence simulation is improved by an order of magnitude in water. This is not particularly important if high air speeds can be used; however, when Froude number similarity is also required, such high velocities are not permissible.

The glass-walled hydraulic flume used for the experiments is 4 ft wide, 4 ft deep, and 40 ft long. The flow system can circulate up to 10 cfs at water depths as low as 1.5 ft. The facilities are also equipped with separate pumps for heated discharge and suction from test structures within the flume. Water for the plumes is heated by a power-controlled 255-kW heater.

The cooling towers were constructed at a length scale of 250:1. Prototype and model tower characteristics are given in Table 1. Warm water was discharged from the tower stacks to simulate the warm moist plume from the prototypic cooling tower At the same time water was being sucked from the tower through the tower cell faces at the same flow rate as the discharge in order to simulate the induced flow into the tower and out of the stacks that occurs in the prototype towers. Flow rates to and from the towers were controlled at the tower and at flowmeters outside the

Table 1. Prototype and Model Parameters

Parameter/Tower	Prototype	Model
No. of cells	6	6
Tower length	241 ft	11.5 in.
Cell width top/bottom	75 ft/55.5 ft	3.6 in./2.66 in.
Packing height	47 ft 4 in.	2.25 in.
Total tower height	65 ft 4 in.	3.15 in.
Air flow	9,444,000 cfm	9.5 gpm (water)
Stack diameter	26 ft	1.25 in.
Average stack velocity	32.6 fps	0.410 fps

flume. The maximum deviation observed was 9%, and flows generally were within 3% of the desired values as measured by volume-per-time-interval methods.

Thermistors were installed in the tower discharges to monitor temperatures. Measurements of the plume temperatures were made in vertical cross sections of the plume at as many as 19 downwind distances varying from 1.45 to 80 stack diameters. At each downwind cross section an array of 105 thermistors positioned in 7 columns and 15 rows was used for measurement. The maximum variation of thermistors in the array was 0.3°C as determined in the flume for cases where there were no tower discharges. In all cases, downstream temperatures were correlated to measurements by the same thermistors at an unaffected upwind station. All measurements were made with an analog-to-digital converter with a multiplexer controlled by a PDP 11/10 computer system. This enabled rapid data acquisition and analysis with analytic and graphic computer techniques.

The matrix of measurement parameters is shown in Table 2. The bulk of the tests were conducted to investigate trends in plume temperatures for variations in Froude number, wind speed, and multiple tower orientation. Froude numbers were varied by changing tower discharge temperature. The tower configuration and position of vertical thermister columns are shown in Figure 1 (A, B, C) for these tests.

Table 2. Experimental Parameter Matrix

Number of Towers	Configuration (See Figure 1)	Froude Number FD	Wind Speed 3.3 10	1.67 20	0 94 35	0.62 50	K[a] fps[b]
3	A	2.5		X			
		3.1		X			
		3.6	X	X	X	X	
		5.7		X			
		9.0		X			
3	B	2.5		X			
		3.1		X			
		3.6	X	X	X	X	
		5.8		X			
		12.2		X			
4	C	2.5		X			
		3.1	X	X	X		
		3.7		X			
		6.6		X			
		10.3		X			

a K = Wind speed/stack discharge velocity (nominal values).
b Prototype wind speeds (nominal values).

3. EXPERIMENTAL RESULTS

Cooling tower stack discharges into moderate winds display complex three-dimensional characteristics as evidence of the complex interplay of dynamic forces on the plume. Because this study was basically concerned with the gross features of the plume and primarily with determining the basic trends of behavior, the detailed structure of the plume was not closely examined. Instead, the analysis was confined to a comparison of the maximum plume temperature and trajectory as functions of downwind distance for three and four cooling towers. Comparisons are also provided for data obtained earlier for one and two[1, 2] cooling towers.

Results will be provided for the three configurations presented in Figure 1. Discussion will be directed at the downwind decay of plume maximum excess temperatures and the trajectory of the plumes. The plume excess temperature ratio is a dimensionless value which provides the plume temperature excess above ambient as compared to the discharge temperature

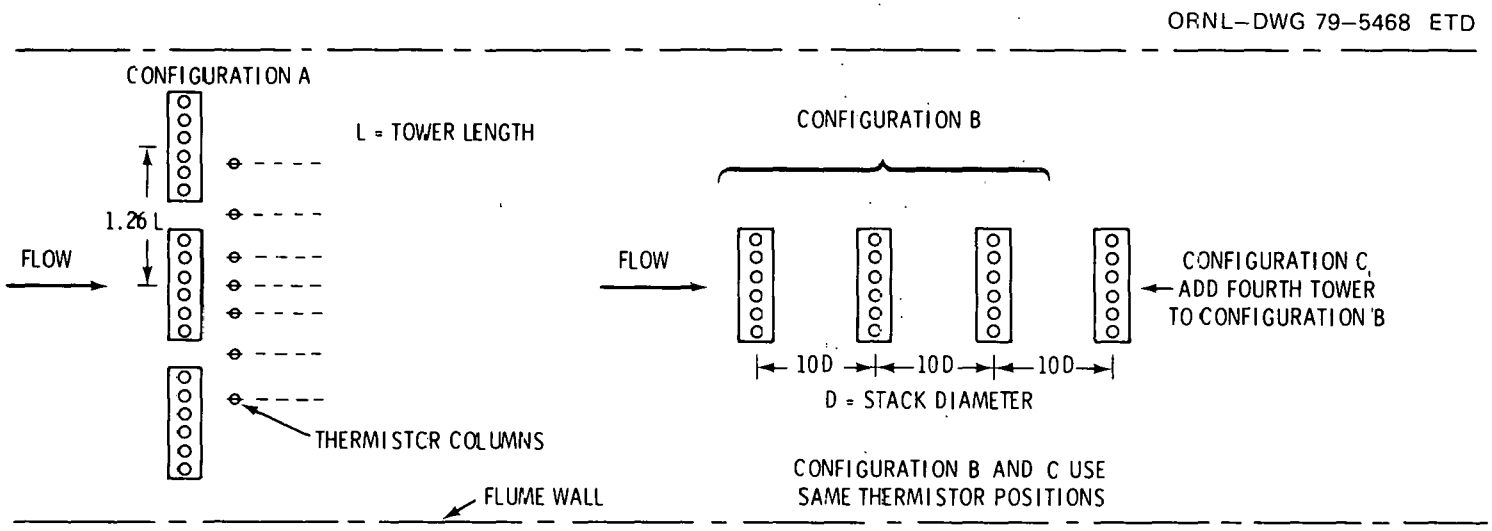

FIGURE 1. Experimental tower configurations.

excess over ambient. It is computed as $T-T_a$ divided by T_o-T_a. During the experimental program the maximum value of this ratio is computed as the largest ratio for the cross sectional thermistor array. Trajectories are generally taken to be the elevation above the tower stacks of maximum plume temperatures. This is not a strictly appropriate trajectory definition for multiple plume systems since only the closest plume will be represented. However, since most plume analyses are directed at determining the locations of the greatest plume concentrations, this definition is employed as the most serviceable.

The use of a single phase medium in simulation of cooling tower plumes is not strictly accurate. Phase change dynamics affect the buoyancy of the plume by a complex interchange of latent and sensible energy. The importance of this interchange is not available from field data. Inherent in the quantitative use of the data offered here is the assumption that phase change dynamics are unimportant in the near field. The dilution and trajectory trends provided here should be qualitatively representative of moist plumes. Until a better understanding is gained of moisture effects on near field plume dynamics, the reader must make his own decision as to the quantitative acceptability of these results for moist plumes. It is the author's opinion that the error incurred by use of these experimental results for moist plumes will be small. Especially in light of the diversity and significance of other factors affecting plume behavior.

Configuration A

In this configuration there were three towers on a single line perpendicular to the flow with a major axis of each tower also perpendicular to the flow (cross flow). The spacing between the centers of the towers was 1.26 times the length of the tower (L). Thus, there is only 0.26 L between the towers.[a]

Conditions were varied for this configuration to simulate a range of Froude numbers and wind speeds. The variation of plume maximum excess

(a) This is approximately equivalent to the tower's height.

temperature ratio with downwind distance is shown in Figure 2 for several wind speeds. Downwind distance is measured from the centerline of the towers. The figure illustrates that the rate of decay in excess temperatures increases with higher wind speeds. This is what would be expected from simple Gaussian mixing formulas although direct comparison is not feasible. Plume temperature ratios near the tower are not very different except for the highest wind speed case.

Figure 3 illustrates the effect of wind speed on trajectory for Configuration A. The trajectories shown are from measurements taken at

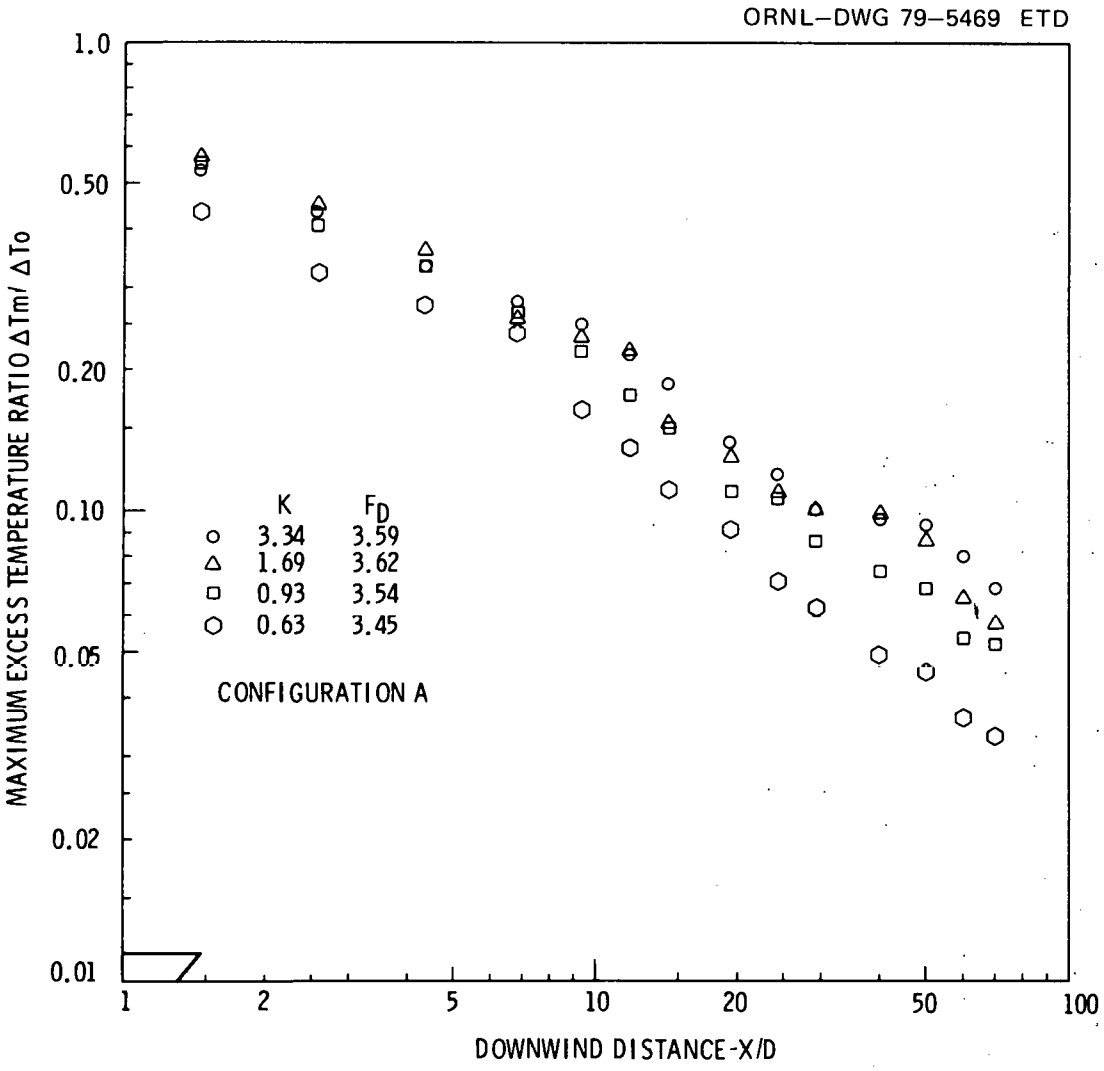

FIGURE 2. Wind speed effects on plume excess temperature ratio as a function of downwind distance; Configuration A.

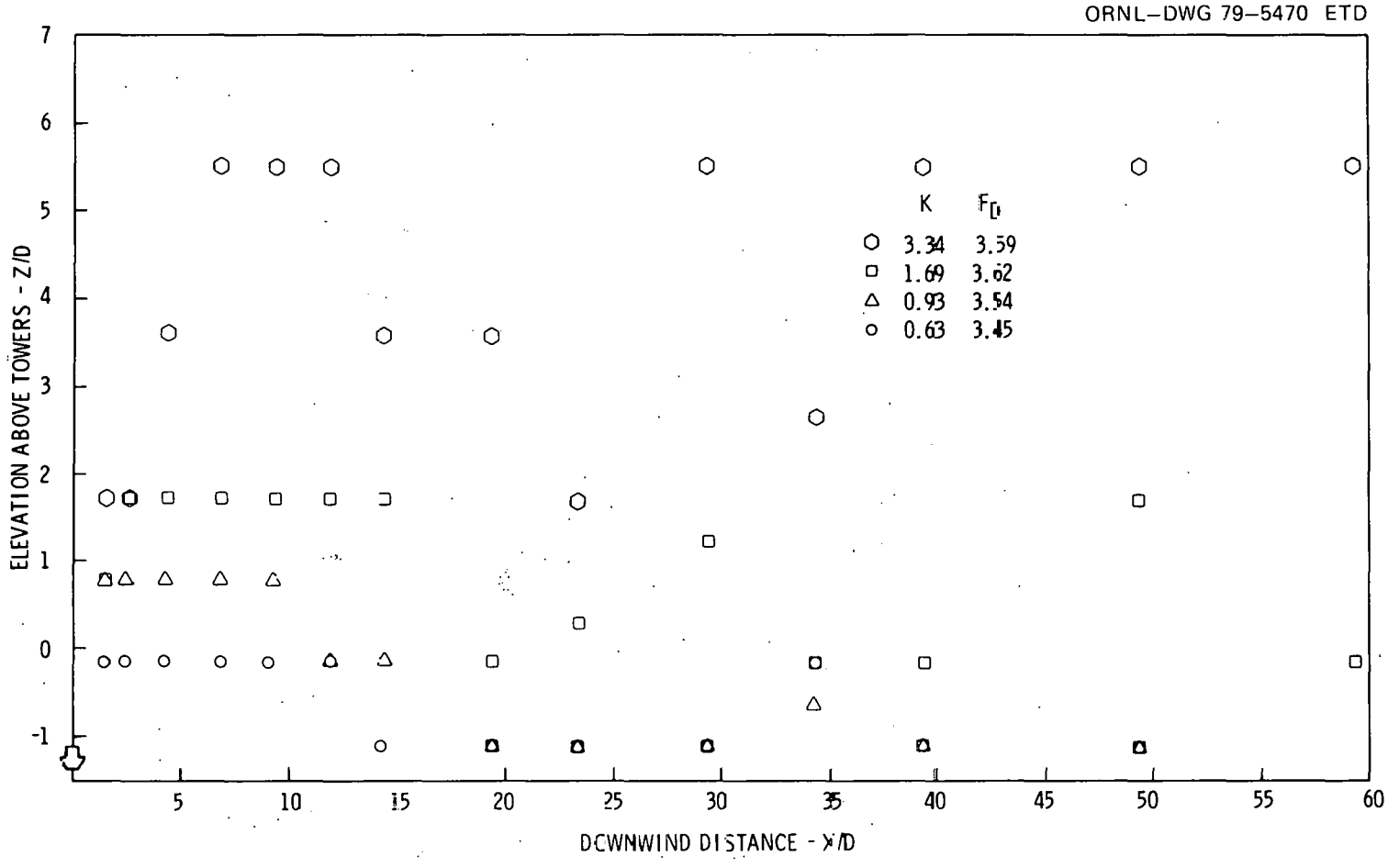

FIGURE 3. Wind speed effects and plume trajectory; Configuration A.

discrete elevations. The plume elevations therefore appear as discrete values. Care should therefore be exercised when interpreting the data. It should also be noted that the lowest thermistor was located 1.1D below the tower height (1.4D above the simulated ground surface; D is the stack diameter). The trajectories for the high wind speed cases are significantly lower than those for lower wind speeds.

One rather interesting feature is that all of the trajectories appear to drop beyond about 12D downwind. At moderate wind speeds (less than 35 fps) the trajectories appear to rise again although the elevation of maximum plume temperatures are highly variable. This is probably due to severe mixing in the wake of the towers.

The varieties of plume temperature and trajectories with Froude number is illustrated in Figures 4 and 5. Figure 4 illustrates that maximum plume temperature ratios decay faster with downwind distance as Froude number decreases. This is likely due to the fact that lower Froude number discharges have greater buoyancy than higher Froude number discharges when stack velocity and diameter are held constant. The greater buoyancy probably causes greater entrainment, thereby increasing dilution.

This hypothesis would result in lower trajectories for higher Froude number (lower buoyancy) cases. Figure 5 illustrates that this is indeed the trend. Data scatter is, however, quite severe (as might be expected in the tower wake at a wind speed of 20 fps). At this wind speed, 20 fps, all of the plumes rise initially above the tower and then fall to lower elevations further downwind. This indicates the importance of the tower wake on the behavior of the plume.

The effects of wind speed and discharge Froude number on plume temperature decay and trajectory observed here are similar to those observed for one and two cooling towers.[1,2]

Configuration B

This configuration is three towers in sequence with respect to the wind; each tower oriented with its major axis perpendicular to the wind (cross flow; see Figure 1). The towers are a distance of 10D apart,

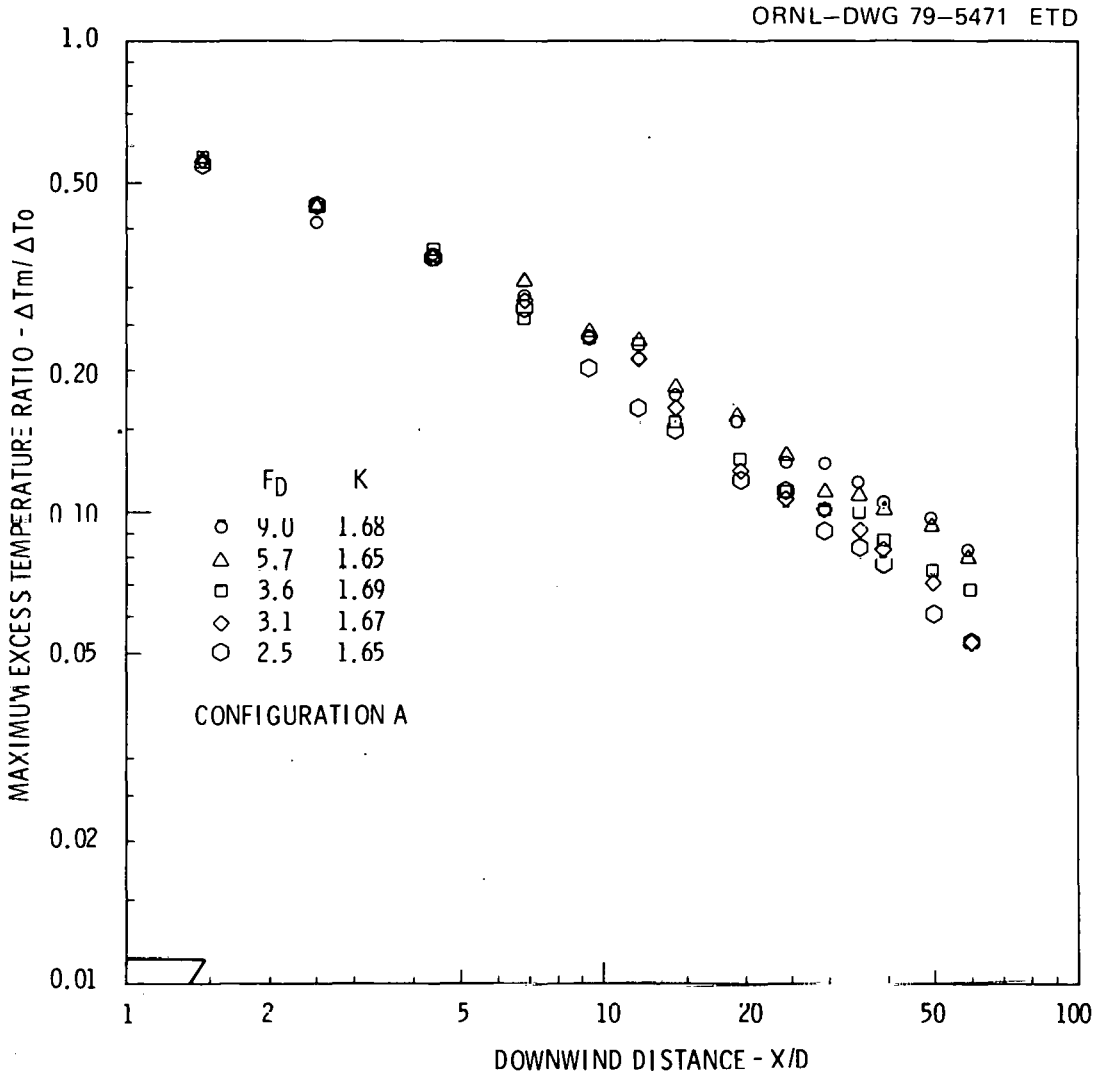

FIGURE 4. Froude number effects on plume excess temperature ratio as a function of downwind distance; Configuration A.

center to center. The data are compared as before for wind speed and Froude number effects.

Figure 6 illustrates the maximum excess plume temperatures as a function of downwind distance for several wind speeds. No clear trend emerges from the data obtained. Near the second and third towers the temperature ratios for the low wind speed case are less than for the other cases, but this does not hold for the next higher wind speed. Farther downwind of the last tower this observation changes and the slower wind

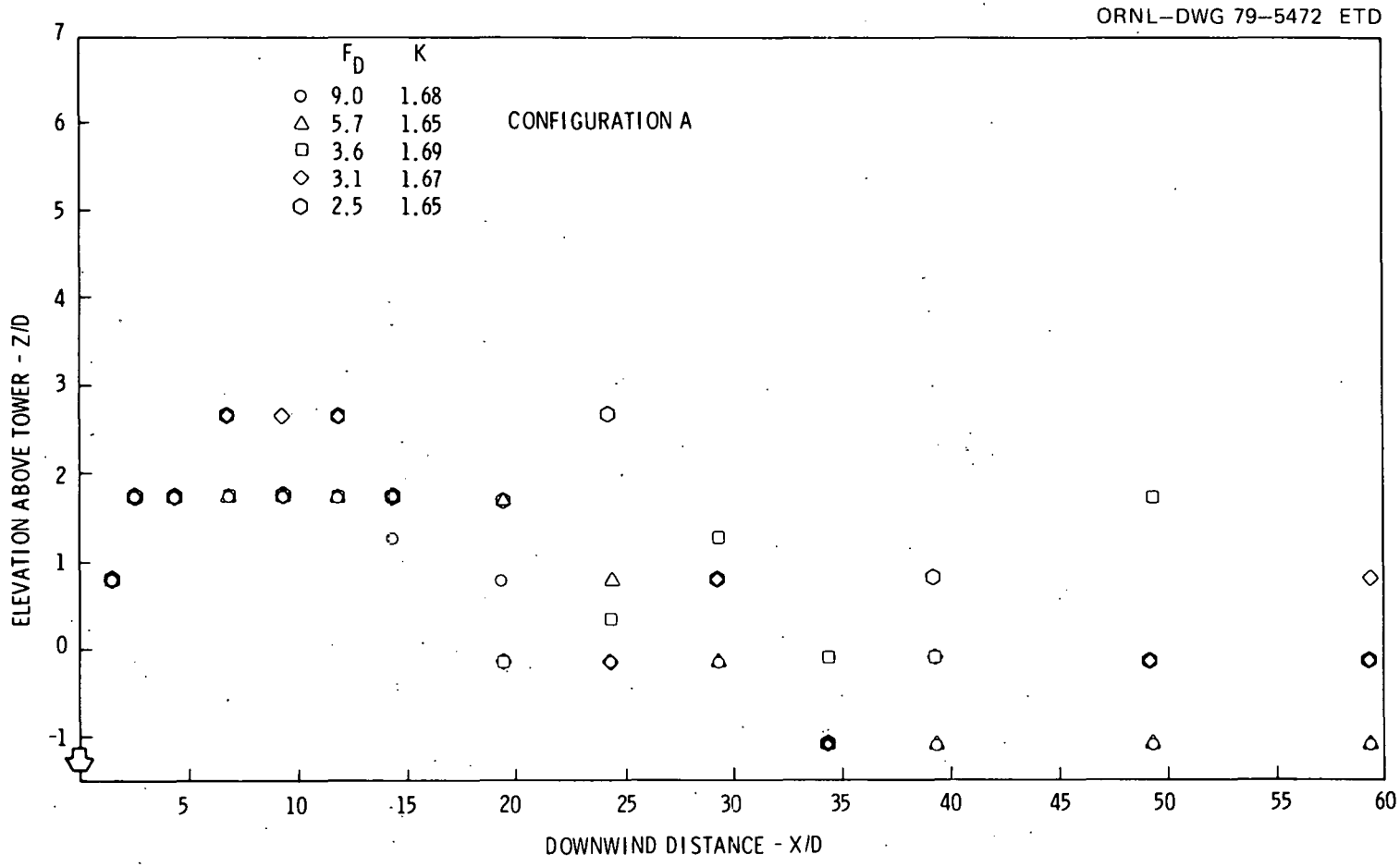

FIGURE 5. Froude number effects on plume trajectory; Configuration A.

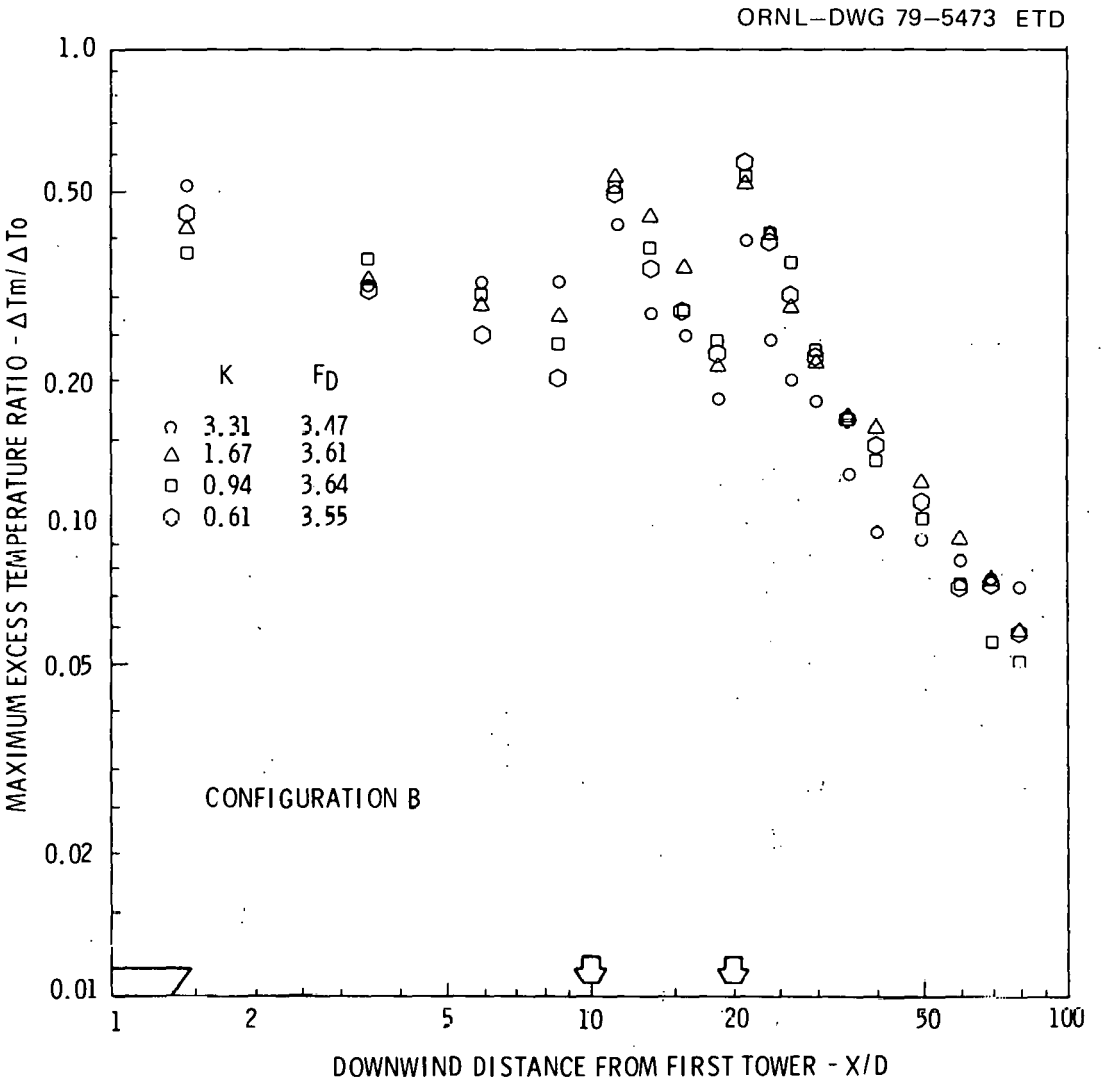

FIGURE 6. Wind speed effects on plume excess temperature ratio as a function of downwind distance; Configuration B.

speed plume shows less dilution than other cases. This may be due to conflicting influences of wake and buoyancy induced entrainment. Again, no trend is obvious.

Figure 7 illustrates the effect of wind speed on plume trajectories for this tower configuration. As noted earlier, increasing wind speed lowers trajectories.

The effects of Froude number on plume temperature ratios and trajectories for this configuration are illustrated in Figures 8 and 9,

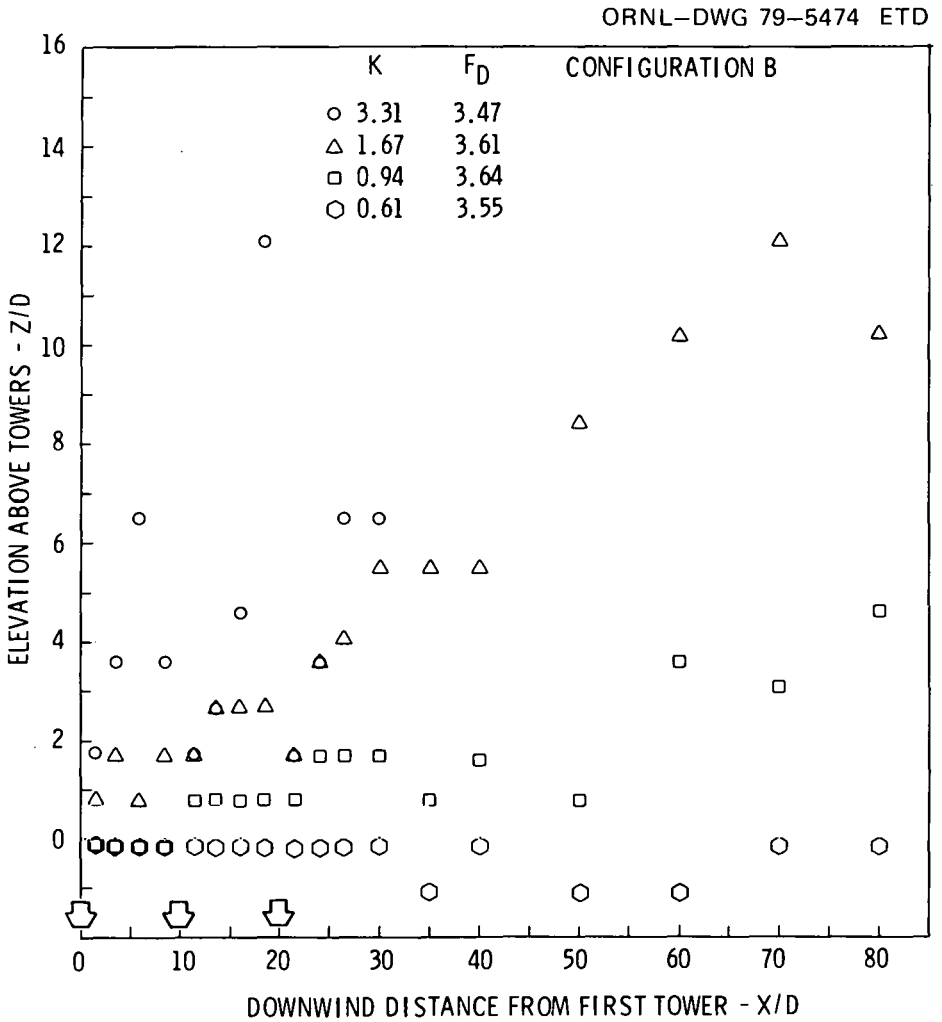

FIGURE 7. Wind speed effect on plume trajectory; Configuration B.

respectively. The variation of downwind plume temperature ratios with Froude number (Figure 8) is quite dramatic. As Froude number decreases, so do the excess temperature ratios relative to higher Froude number discharge. This is particularly true after the third tower. At farther downwind distances a factor of two decrease in excess temperature ratios is observed for a factor of about six decrease in the Froude number. This same trend was observed for both a single tower and two towers[1,2]. Earlier speculation on the hypothesis that greater buoyancy causes greater entrainment is certainly supported by these data.

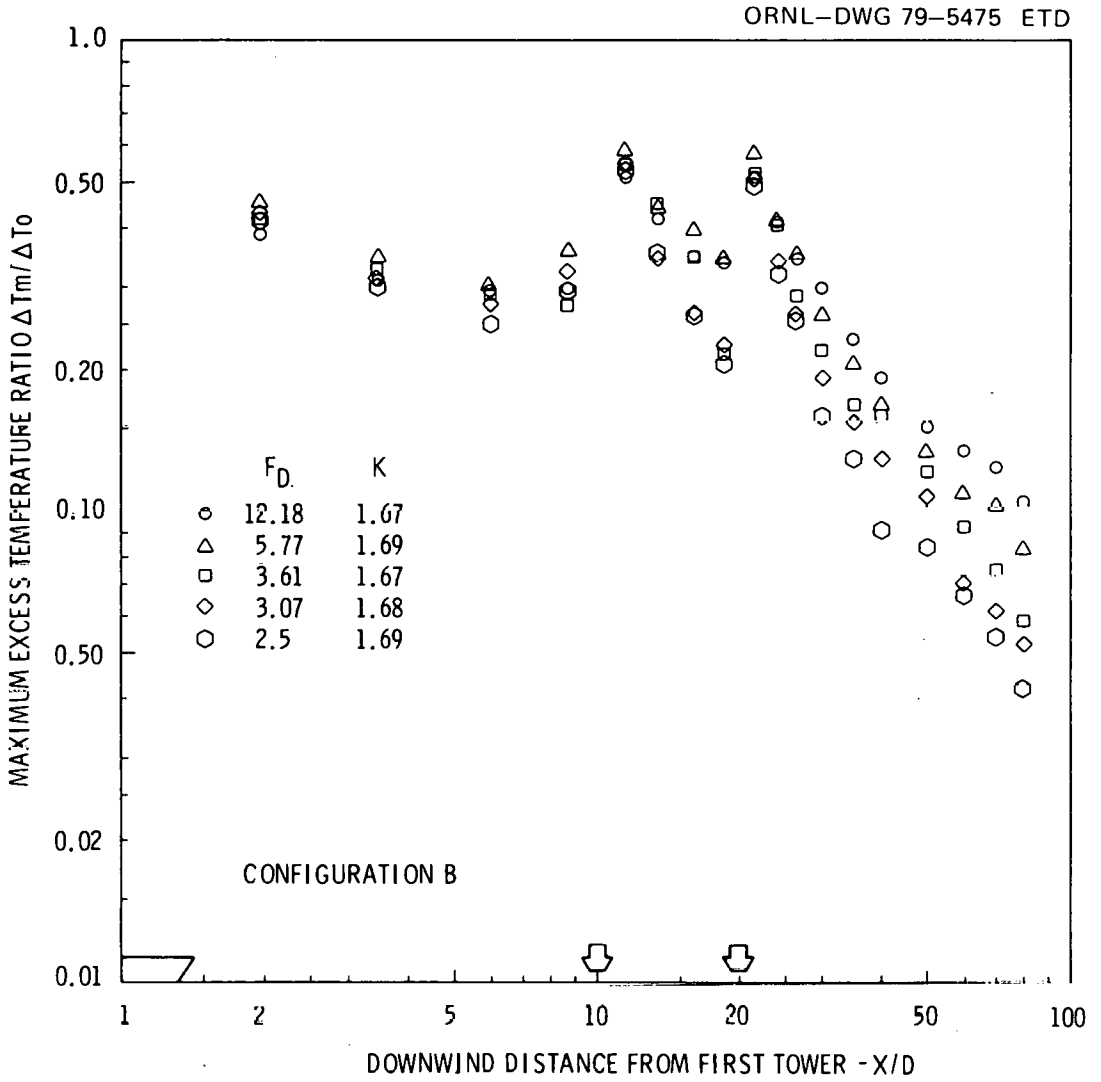

FIGURE 8. Froude number effects on plume excess temperature ratio as a function of downwind distance; Configuration B.

The trajectories also display a significant Froude number effect (Figure 9). Lower Froude number discharges display much higher trajectories than larger Froude number cases. This ties in well with the buoyancy induced entrainment hypothesis as well.

Configuration C

This configuration is an extension of configuration B. A single tower has been added downwind of the previous three, with major axis

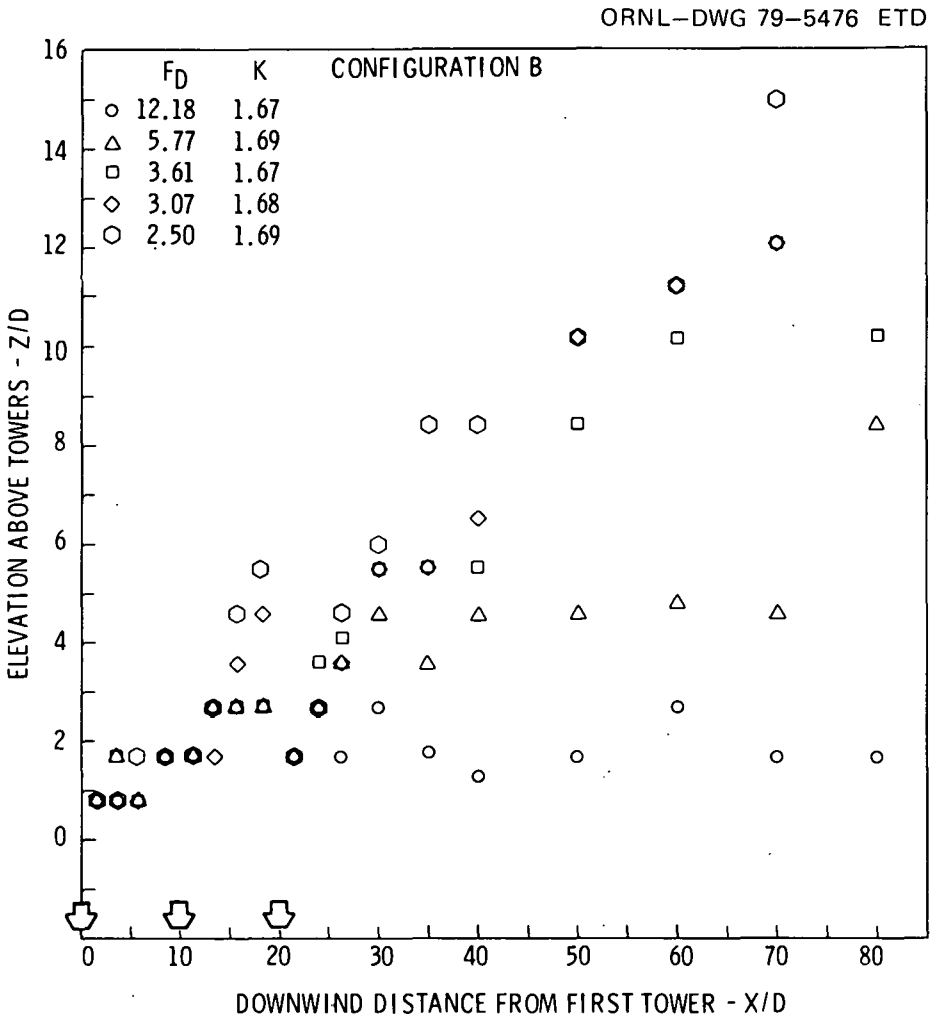

FIGURE 9. Froude number effects on plume trajectory; Configuration B.

perpendicular to the wind direction (see Figure 1). Plume temperature ratio and trajectory data were gathered for a variety of wind speeds and Froude numbers.

The plume maximum excess temperature ratios are plotted as a function of downwind distance for several wind speeds in Figure 10. This figure is very similar to that offered for three towers (Figure 6). Only three wind speeds are offered because of pump failure at the highest wind speed. There are no distinct trends evident in the data, although one feature that was observed for Configuration B is also displayed in Figure 10.

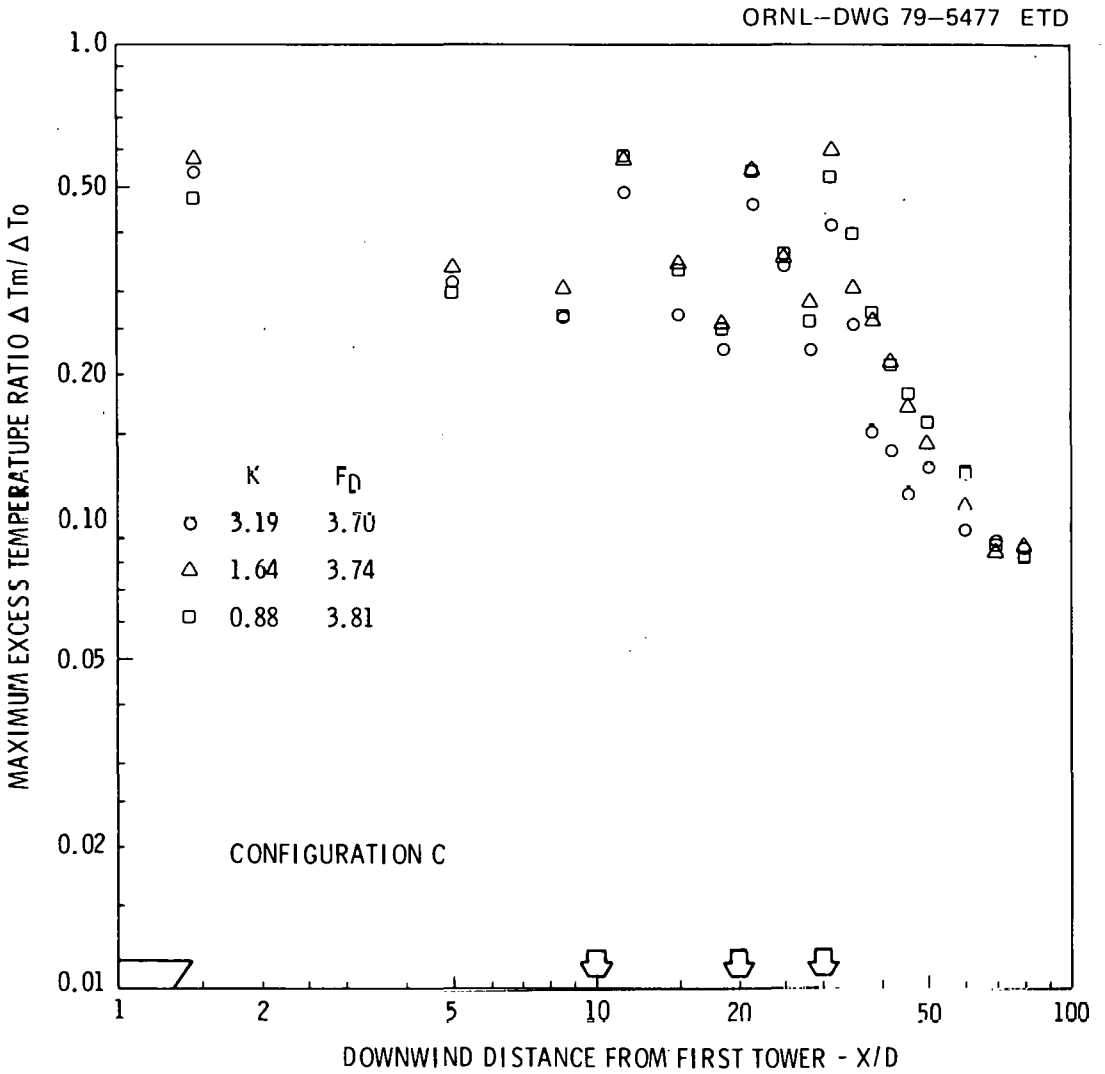

FIGURE 10. Wind speed effects on plume excess temperature ratio as a function of downwind distance; Configuration C.

The plume temperature ratios at the slowest wind speed is more dilute than other cases near the downwind towers. Farther downstream of the last tower the data are indistinguishable for all wind speeds. This may be indicative of shielding by upwind towers. This would have the relative effect of reducing effective wind speed allowing the plume to rise more quickly and entrain more fluid before reaching downwind measurement stations. This would result in slightly lower maximum excess temperature ratios near the towers.

The trajectories for various winds speeds are shown in Figure 11. Trajectories are shown to be affected greatly by the wind speed. Much higher trajectories are observed for slower wind speeds, particularly near the towers. The trajectory for the highest wind speed is virtually the same at all locations downwind of the towers.

Low Froude number discharges have been cited earlier as experiencing greater dilution and having higher trajectories than discharges with higher Froude numbers. These observations are supported by the data for Configuration C shown in Figures 12 and 13. Plume maximum temperature ratios are observed to decay much more rapidly for lower Froude numbers.

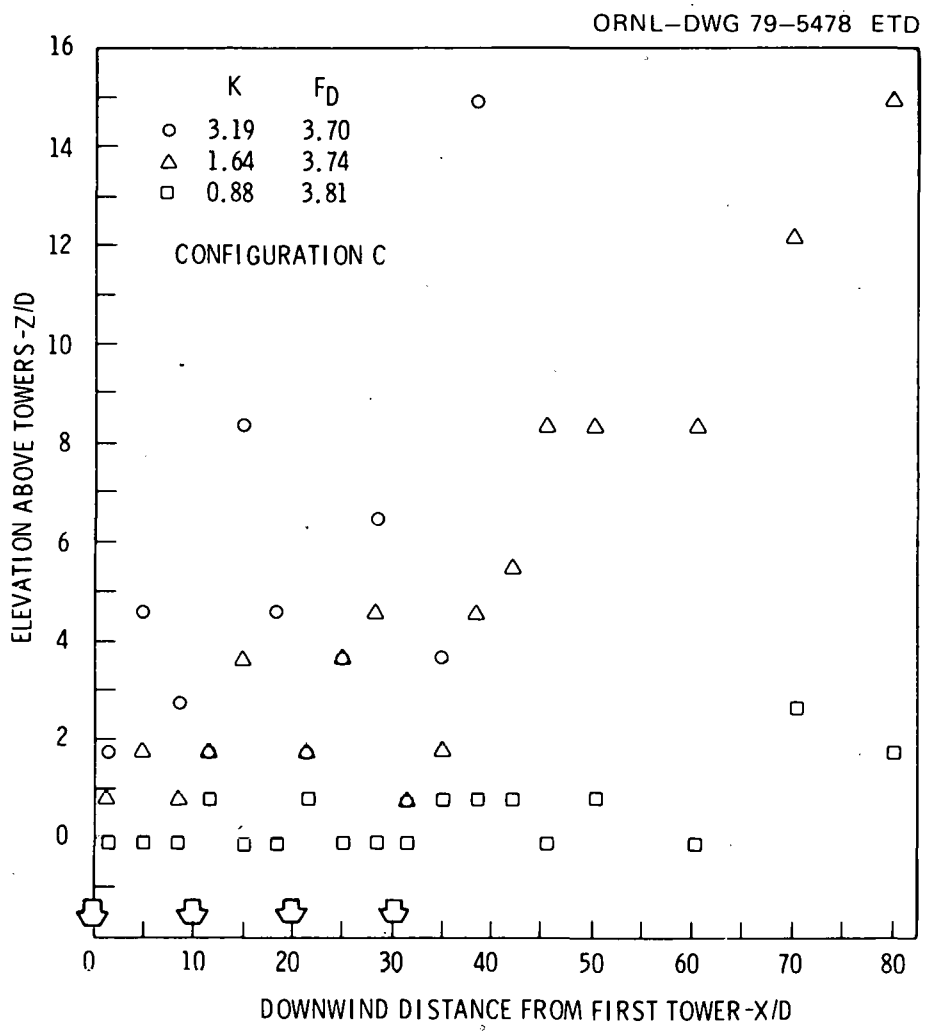

FIGURE 11. Wind-speed effects on plume trajectory; Configuration C.

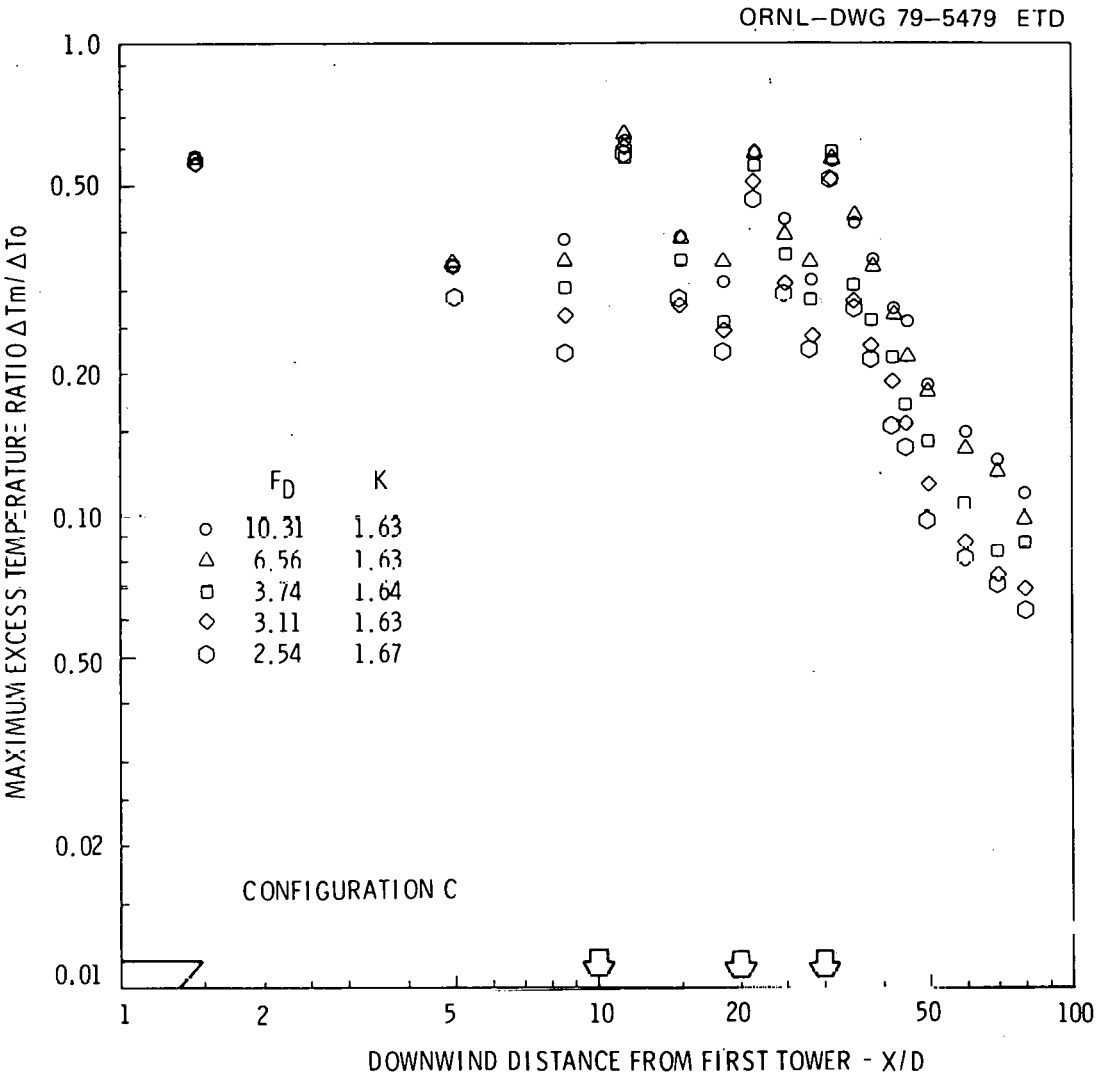

FIGURE 12. Froude number effects on plume excess temperature ratio as a function of downwind distance; Configuration C.

After 10 D beyond the fourth downwind tower, there is nearly a factor of two difference in excess temperature ratios for the five-fold difference in Froude number.

One interesting feature of the variation of plume temperature ratios with multiple towers is that the flow field and plume dilution are affected to a large degree by the presence of a downwind tower, even at a spacing of ten stack diameters between towers. This effect is probably most obvious for the high Froude number cases but it is observable in

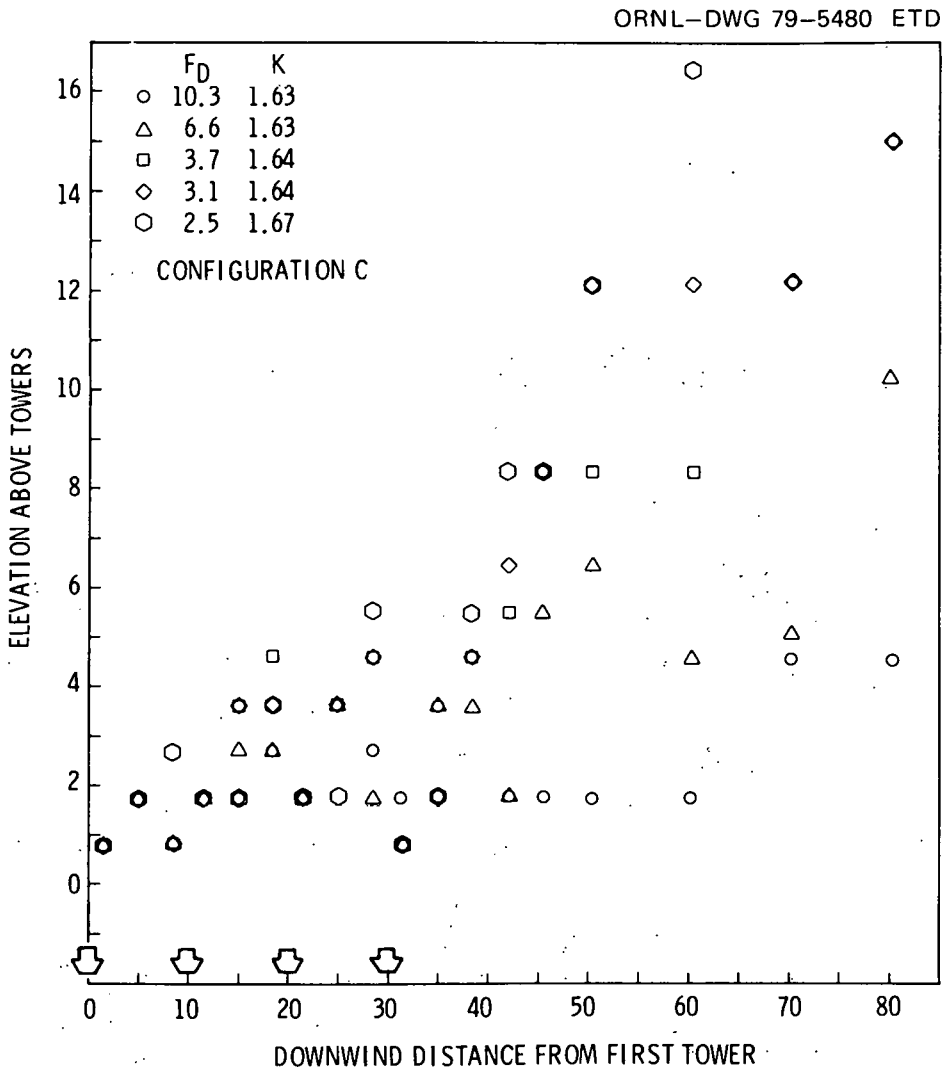

FIGURE 13. Froude number effects on plume trajectory; Configuration C.

nearly all cases. The effect is most clearly observed for data between the first and second tower.

Other Comparisons

The completion of physical model simulations for three and four cooling towers permits the comparison of data for these simulations with data from earlier one and two tower simulations. Of particular interest are answers to questions 1) how does spacing between towers affect plume characteristics, and 2) how are plume characteristics affected by upwind

towers? The comparison offered here are based on a 20 ft/s wind speed and a Froude number of about 3.6.

The first question is considered by plotting data obtained for a single tower[1,2], two towers[1,2], and three towers in cross flow in a configuration like A. The lateral spacings between towers are infinity (single tower), 1.5 L (two towers), and 1.26 L (three towers). The maximum excess plume temperature ratios for these cases are plotted in Figure 14. Very near the towers there is little difference in the temperature ratios. Beyond about four diameters the temperature ratios

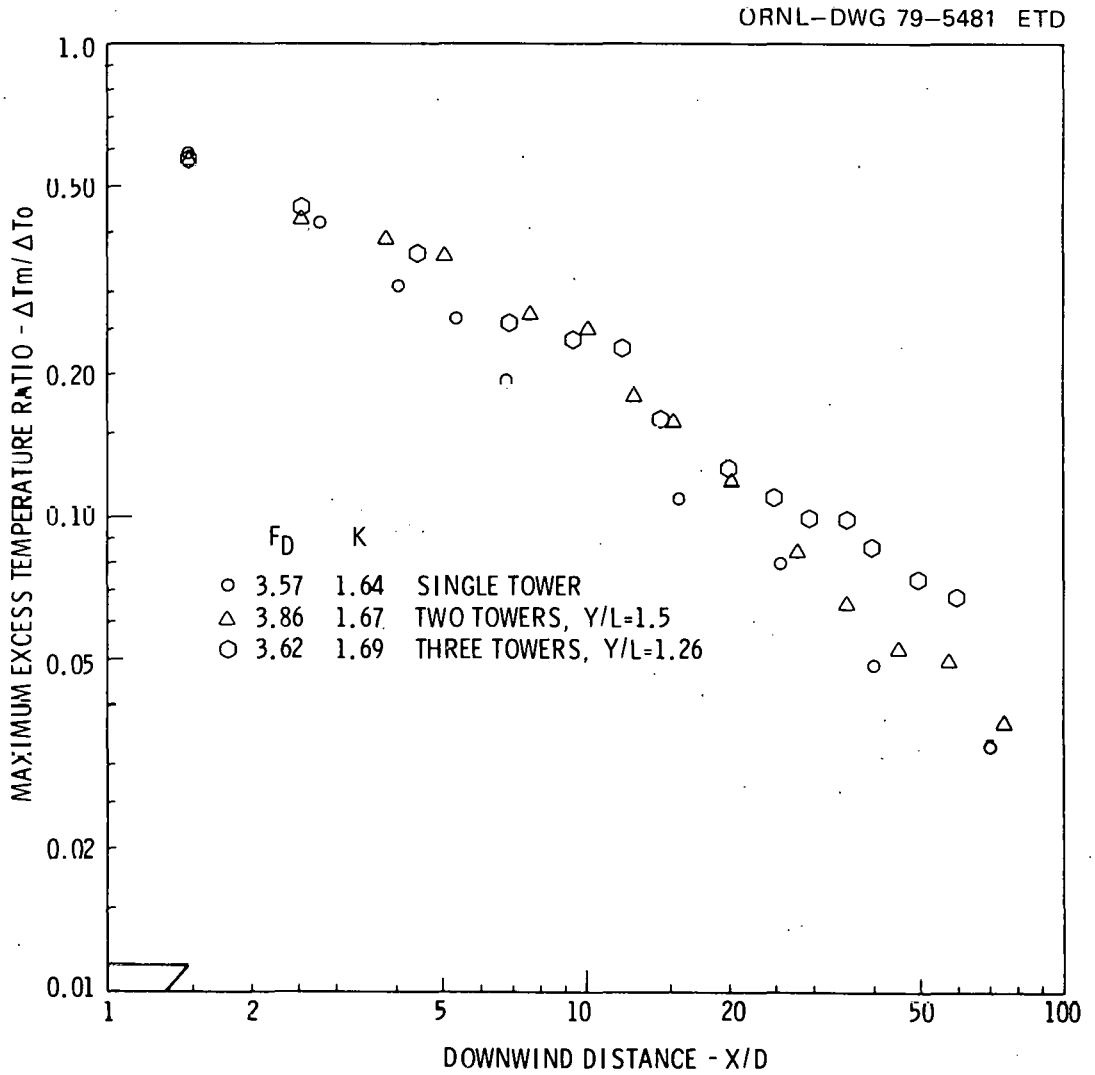

FIGURE 14. Effect of lateral spacing of towers on plume excess temperature ratio as a function of downwind distance.

for the single tower drop below those of multiple towers. The temperature ratios of the multiple towers are nearly equal until about 25D downwind. From this point on the temperature ratio data for the closest spacing exceeds that of either of the other cases. This clearly shows the effect of increased competition for entrainment fluid and the effect of a more extensive wake structure for closely spaced towers. The trajectory data for these cases are plotted in Figure 15. This shows the trajectories for the plumes dropping as the spacing between the towers is decreased. The

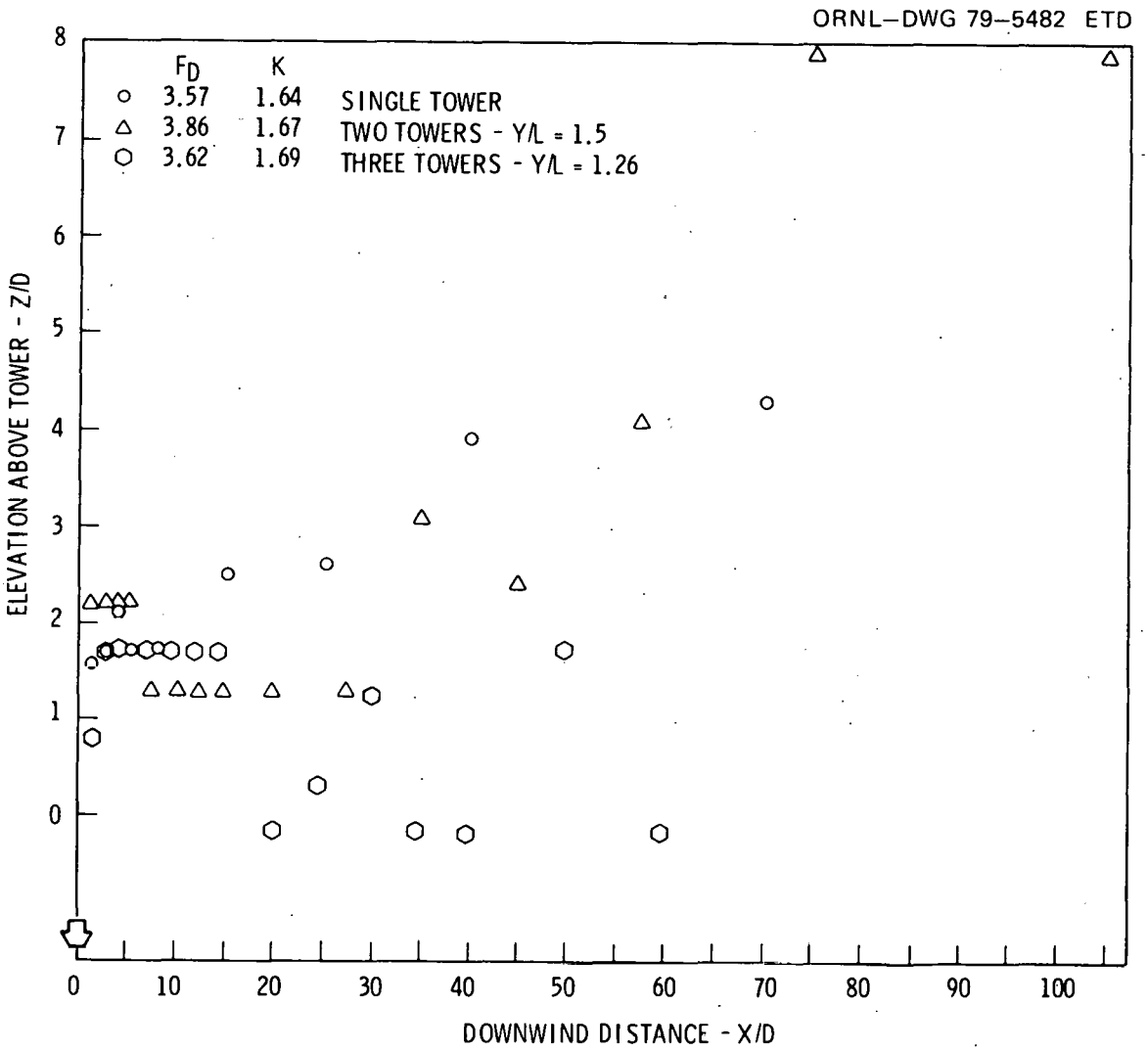

FIGURE 15. Effect of upwind towers on plume excess temperature ratio as a function of downwind distance.

trajectory of the closest spacing indicates the capture of the plume in the extensive wake for that case. Wake effects appear to be very significant for close spacings.

The second question is considered by plotting temperature and trajectory data obtained downwind of the farthest downwind tower for one, two, three, and four towers in a configuration like B or C (see Figure 1). The comparison is done for a spacing between towers of 10D. The maximum excess temperature ratio data are plotted in Figure 16 for each of these

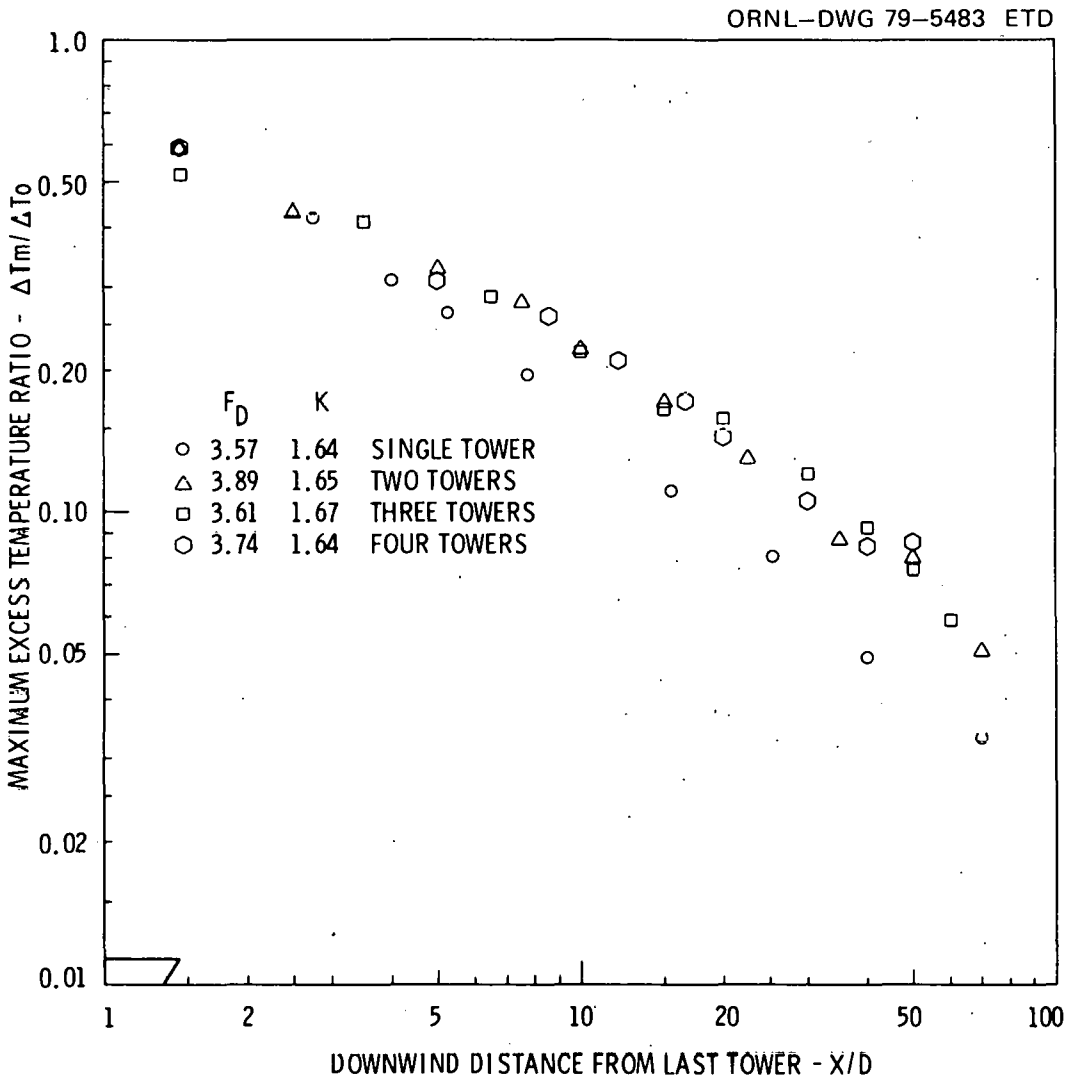

FIGURE 16. Effect of upwind towers on plume excess temperature ratio as a function of downwind distance.

cases.[1,2] The single tower excess temperatures are significantly less than those of the multiple towers. However, the data for the multiple towers indicate only a minor effect, if any, of increasing the number of upwind towers from one to three. This is a rather important observation since it means that siting a moderate concentration of plume sources will have little effect on downwind plume concentrations in the near field. There must certainly be an effect at some distance but not very near the site.

The trajectories for the comparison of upwind tower effects is provided in Figure 17. The trajectories show a very definite demarcation

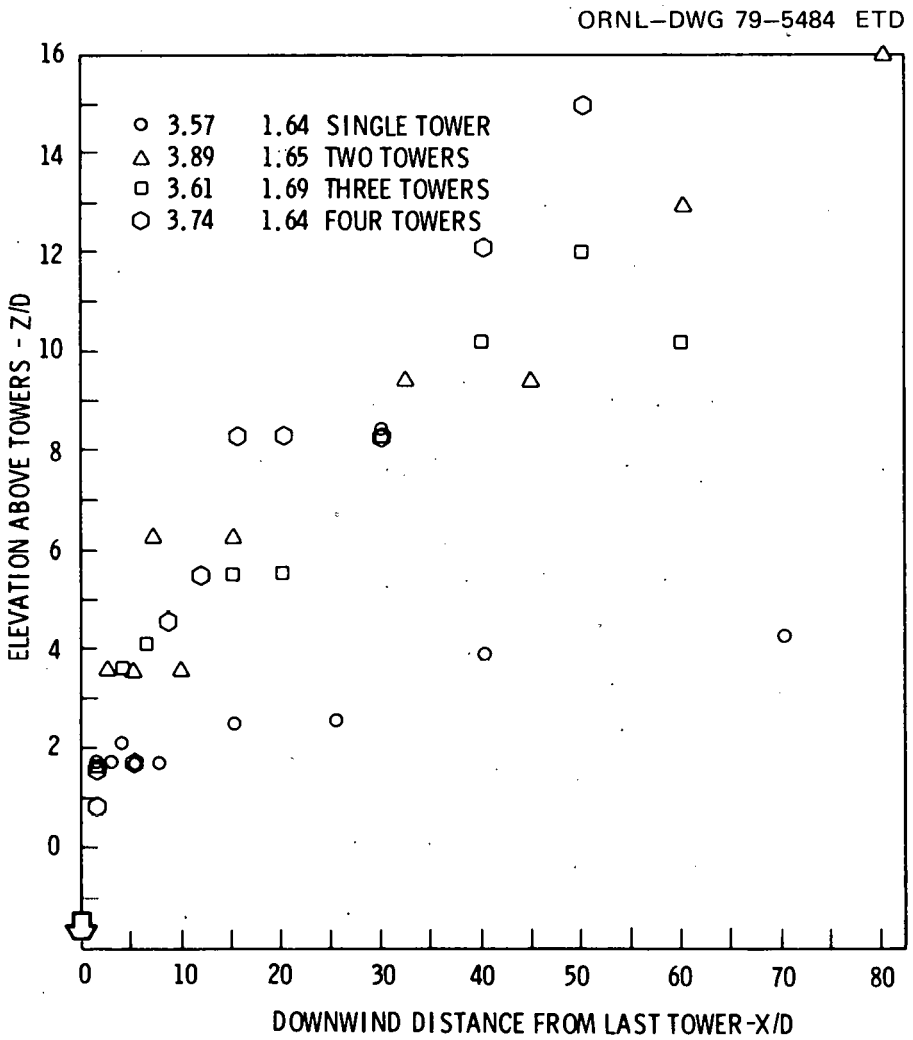

FIGURE 17. Effect of upwind towers on plume trajectory.

between the single tower trajectory and the higher multiple tower trajectories. However, there is only a slight increase in elevation for the trajectory of a tower having three upwind towers over cases having one or two upwind towers. Again it should be noted that there is almost certainly a major difference in trajectory for multiple tower at some larger distance downwind.

4. CONCLUSIONS

A physical modeling study has been completed investigating the plume temperature and trajectory characteristics for three and four mechanical draft cooling towers in three configurations. In general the following can be concluded for each configuration.

Configuration A - Cross flow towers in a line perpendicular to the wind.

1. Increasing wind speed affects plume excess temperature ratios only slightly and decreases trajectories greatly.
2. Increasing Froude number increases plume excess temperature ratios and decreases trajectories.
3. Decreasing the spacing between the towers increases plume excess temperature ratios and decreases trajectories.

Configurations B and C - Cross flow towers in a line parallel to the wind.

1. Low wind speeds result in plume excess temperature ratios only near the towers. Increasing wind speed results in lower trajectories.
2. Increasing Froude number increases plume excess temperature ratios dramatically and decreases trajectories.
3. Single tower plume excess temperatures ratios will be considerably less than those of multiple towers.
4. The number of upwind towers has only a slight effect, if any, on plume excess temperature ratios. A minor increase in plume trajectories is noted with increasing numbers of upwind towers.

The experimental results suggests that optimal siting of cooling towers, particularly multiple towers, is a task requiring knowledge of

ambient wind history, plume dynamics, and tower operating conditions. Based on the tower wake effects and on the results for interaction of plumes from multiple cooling towers, site terrain may be a very significant factor in plume dynamics and interactions.

These conclusions are founded on the ranges of conditions examined in this study. Extension to other conditions may not necessarily follow the trends noted above.

5. NOMENCLATURE

D	Port or stack diameter
F_D	Densimetric Froude number, $F_D = V_j/\left\{\left[(\rho_j - \rho_a)/\rho_a\right]gD\right\}^{1/2}$
g	Gravitational acceleration, 32.2 fps^2
K	V_j/V_a discharge to ambient velocity ratio
L	Length of tower
T	Plume temperature
T_m	Maximum plume temperature
T_a	Ambient temperature
T_0	Discharge temperature
ΔT_m	$T_m - T_a$
ΔT_0	$T_0 - T_a$
$\Delta T_m/\Delta T_0$	Maximum plume excess temperature ratio
V_a	Ambient velocity
V_j	Discharge velocity
X	Downwind horizontal distance
Y	Crosswind (lateral) horizontal distance
Z	Vertical Elevation
ρ_j	Discharge density
ρ_a	Ambient density

6. ACKNOWLEDGMENTS

The author is indebted to the Department of Energy for the financial support of this project under the Meteorological Effects of Thermal Energy Releases (METER) Program.

REFERENCES

1. Meteorological Effects of Thermal Energy Releases (METER) Program Annual Report, October 1976 to September 1977, Rept No. ORNL/TM-6248, compiled by A. A. Patrinos and H. W. Hoffman, prepared by Oak Ridge National Laboratory, operated by Union Carbide Corporation for the Department of Energy.

2. L. D. Kannberg and Y. Onishi, "Plumes from One and Two Cooling Towers," Environmental Effects of Atmospheric Heat/Moisture Releases, Cooling Towers, Cooling Ponds, and Area Sources. The Second Annual AIAA/ASME Thermophysics and Heat Transfer Conference, Palo Alto, CA, May 24-26, 1978 Edited by K. E. Torrance and R. G. Watts.

PREDICTIVE METHODS

THIS PAGE

WAS INTENTIONALLY

LEFT BLANK

V. ON THE PREDICTION OF LOCAL EFFECTS OF PROPOSED COOLING POND

B. B. Hicks*

ABSTRACT

A Fog Excess Water (FEW) Index has been shown to provide a good measure of the likelihood for steam fog to occur at specific cooling pond installations. The FEW Index is derived from the assumption that the surface boundary layer over a cooling pond will be strongly convective, and that highly efficient vertical transport mechanisms will result in a thorough mixing of air saturated at surface temperature with ambient air aloft. Available data support this assumption. An extension of this approach can be used to derive a simple indicator for use in predicting the formation of rime ice in the immediate downwind environs of a cooling pond. In this case, it is supposed that rime ice will be deposited whenever steam fog and subfreezing surface temperatures are predicted. This provides a convenient method for interpreting pre-existing meteorological information in order to assess possible icing effects while in the early design stages of the planning process. However, it remains necessary to derive accurate predictions of the cooling pond water surface temperature. Once a suitable and proven procedure for this purpose has been demonstrated, it is then a simple matter to employ the FEW Index in evaluations of the relative merits of alternative cooling pond designs, with the purpose of minimizing overall environmental impact.

1. INTRODUCTION

Industrial cooling ponds often give rise to localized environmental effects, particularly in winter when steam fog and rime ice can become problems downwind of the hottest areas. Fog generation above artificially heated water surfaces has been the subject of a number of studies[1,2,3], but similar studies of rime ice have not been found. A preliminary study of the matter demonstrated the practical difficulties likely to confront experimental investigations of riming[4,5]. This study, performed at the Commonwealth Edison Dresden plant (near Morris, Illinois) during the winter of 1976/7, provides a four-month record of the occurrence and intensity of fog and rime associated with the operation of a fairly typical industrial cooling lake.

Earlier studies at Dresden succeeded in obtaining direct measurements of turbulent fluxes of sensible and latent heat from the heated water[6]. The resulting improved formulations of these convective and evaporative heat losses can be used in much the same way as the familiar wind speed functions that are used in most contemporary cooling pond design studies. In this

* Atmospheric Physics Section, Radiological and Environmental Research Division, Argonne National Laboratory, Argonne, Ill.

regard the earlier Dresden experiments, which were conducted over the three-year period 1973/1976, addressed the question of how to predict the water temperature characteristics of cooling pond installations. Subsequent studies have refined these techniques by parameterizing the subsurface thermal boundary layer[7], which effectively limits heat exchange between deep water and the air. The premise of the present study is, therefore, that we can predict the temperature characteristics of a proposed cooling pond, but need to assess the potential environmental impact.

2. STEAM FOG

Hicks introduced a Fog Excess Water Index, e_{xs}, based on the supposition that air saturated at surface temperature rises and mixes with equal quantities of ambient, background air. The excess vapor pressure e_{xs} of the mixture can be written as

$$e_{xs} = (e_s(T_s) + e_a)/2 - e_s((T_s + T_a)/2)$$

where $e_s(T)$ is the saturated vapor pressure at temperature T, T_a is the ambient air temperature and e_a is the air vapor pressure. When tested against the data of Currier et al.[1], the FEW Index was found to provide a good indication of the occurrence of steam fog, as well as some measure of its intensity. The FEW Index was further verified by use of observations of fog generated by cooling-pond simulators at Argonne National Laboratory and by data from Dresden.

Figure 1 is a further test of the FEW Index, again largely based on observations made at Dresden but supplemented by a series of measurements made at the Cal-Sag shipping canal, a major inland waterway which passes conveniently near Argonne. Canal water temperatures in winter are typically more than 20°C higher than in nearby lakes and streams, due to heavy industrial usage. The data illustrated in the diagram give further support for the validity of the FEW Index method.

3. RIME ICE DEPOSITION

A few obvious (and perhaps trivial) considerations should be set down at the outset. Firstly, it is clear that rime ice deposition is a cold-weather phenomenon which is constrained, by definition, to occasions when the surface temperature is below freezing. This constraint does not apply to the generation of steam fog, and hence rime deposition might well be considered as a sub-set of steam fog cases. Secondly, it follows that riming will be mainly a wintertime phenomenon, most often at night. In the nocturnal case, it seems

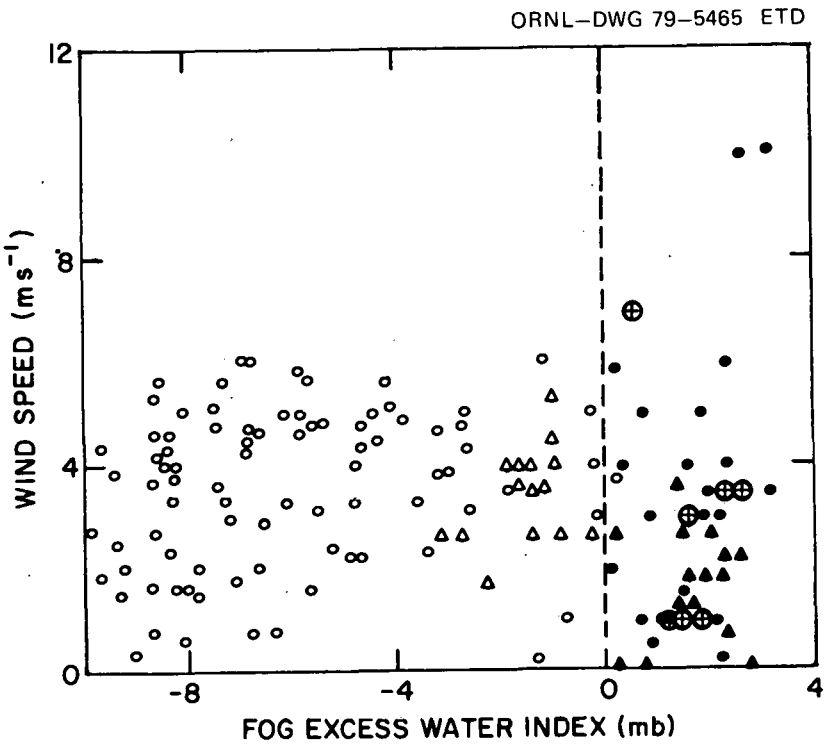

Fig. 1. Observations of the Fog Excess Water Index made at the Dresden cooling lake (circles), over cooling pond simulators at Argonne[8] (triangles), and above a shipping canal near Argonne (circles and crosses). Except in the last case, solid symbols indicate that fog was observed; fog was always observed over the canal.

likely that accurate prediction of riming will prove extremely demanding, since nocturnal surface temperatures are highly variable both in space and in time and thus great care must be taken in selecting an appropriate data base.

Figure 2(a) illustrates the first point; the Dresden 1976/7 winter data do indeed show riming to be a subset of the fog occurrences. Observations were made on a total of 84 mornings. On no occasion was the observation of overnight rime deposition not accompanied by steam fog from the pond. Furthermore, the amount of rime deposited is well correlated with a measure of steam fog intensity. To show this, rime deposits have been quantified according to the visual observations; none = 0, slight rime = 1, moderate rime = 2, heavy rime = 3. The fog intensity is conveniently quantified by the reported depth of the fog layer over the hottest part of the cooling pond, estimated from a comparison with the known heights of surrounding obstacles. Figure 3 demonstrates the correlation. Thus, it appears reasonable to expect the FEW Index to be an appropriate measure of the intensity of rime deposit, since it

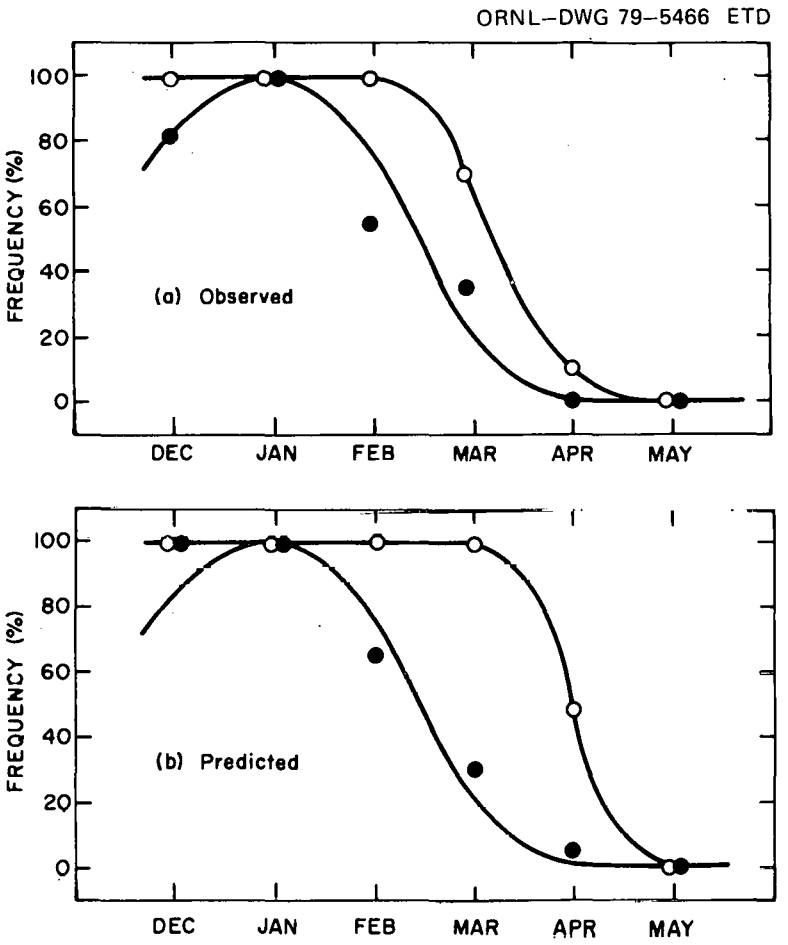

Fig. 2. Observed (a) and predicted (b) frequencies of occurrence of overnight steam fog (open circles) and local rime ice deposition (solid circles) at the Dresden cooling lake.

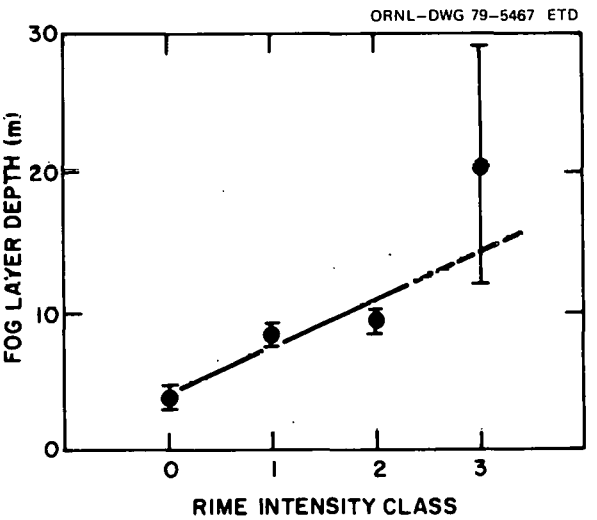

Fig. 3. The relationship between the intensity of overnight rime deposition and the reported depth of the fog layer at Dresden.

has already been shown to be an indicator of steam fog intensity. The present limited set of data do not allow direct investigation of the interrelation between rime intensity and e_{xs}, since reliable nocturnal evaluations of e_{xs} at the Dresden site are not available[8].

Figure 2(b) shows the frequency of occurrence of fog and rime that would have been expected on the basis of the arguments presented above. It is assumed that steam fog will occur when $e_{xs} > 0$, based on the observed Dresden water temperatures and overnight air temperatures and humidities measured some 40 km away at Argonne National Laboratory. Rime is then predicted on each of those occasions for which sub-freezing overnight temperatures were reported. Comparison between Figures 2(a) and 2(b) shows fairly good agreement: the rime curves are drawn to be identical.

4. DISCUSSION AND CONCLUSIONS

Although it is clear that the depth of steam fog and the amount of rime deposited are well correlated, there is no strong dependence of riming upon meteorological quantities such as wind speed, nocturnal net radiation, etc. To a considerable extent, this is as must be expected as a consequence of the lack of correlation between e_{xs} and wind speed (see Figure 1). The 1976/7 results are not suitable for investigating this matter with confidence. Nor is it clear that the physics involved will permit a clear-cut conclusion to be obtained. Nevertheless, it is intended to proceed with investigations of the thermal and moisture plumes arising from heated water surfaces, in part to derive better methods for predicting the frequency of events in the design stage but also to investigate the role of steam fog as an interference with the natural infrared radiation regime of a water surface.

5. ACKNOWLEDGMENTS

The work performed at Dresden was made possible by the complete cooperation of the Commonwealth Edison Company. The Dresden data reported here were obtained during a field program directed by Dr. J. D. Shannon. Dr. P. Frenzen obtained the canal data. This study was supported by the U. S. Department of Energy, as part of an investigation of the Meteorological Effects of Thermal Energy Release.

REFERENCES

1. E. L. Currier, J. B. Knox, and T. V. Crawford, "Cooling Pond Steam Fog," J. Air Pollut. Control Assoc. 24, 860-864 (1974).

2. B. B. Hicks, "The Prediction of Fog over Cooling Ponds," J. Air Pollut. Control Assoc. 27, 140-142 (1977).

3. D. M. Leahey, M. J. E. Davies, and L. A. Panek, "A Study of Cooling Pond Fog Generation," Paper #78-40.2 presented at the 71st. Annual Meeting of the Air Pollution Control Association, Houston, Texas, June 25-30, 1978.

4. R. G. Everett and G. A. Zerbe, "Winter Field Program at the Dresden Cooling Ponds," Argonne National Laboratory Radiological and Environmental Research Division Annual Report, January-December 1976, ANL-76-88 Part IV, 108-113 (1976).

5. J. D. Shannon and R. G. Everett, "Effect of a Severe Winter Upon a Cooling Pond Fog Study," Bull. Amer. Meteorol. Soc. 59, 60-61 (1978).

6. B. B. Hicks, M. L. Wesely, and C. M. Sheih, "A Study of Heat Transfer Processes above a Cooling Pond," Water Resources Res. 13, 901-908 (1977).

7. M. L. Wesely, "Behavior of the Thermal Skin of Cooling Pond Water Subjected to Moderate Wind Speeds," Proceedings, Second Conference on Waste Heat Management and Utilization, Miami Beach, FL, XI-A-40 (1-8), Dec. 4-6, 1978.

8. B. B. Hicks, "The Generation of Steam Fog Over Cooling Ponds," Environmental Effects of Atmospheric Heat/Moisture Releases, Proceedings of the Second AIAA/ASME Thermophysics and Heat Transfer Conference, Palo Alto, California, 24-26 May 1978 (Library of Congress Catalog Card Number 78-52527).

VI. SELF-PRECIPITATION OF SNOW FROM COOLING TOWERS

L. R. Koenig*

1. INTRODUCTION

The use of large evaporative cooling towers to dissipate heat from industrial processes causes a variety of atmospheric effects. Cases of snowfall from cooling tower plumes have been well documented, over 13 cm (5 inches) of snow being measured in one instance. Snowfall produces hazardous driving conditions, and the sudden encounter of snow or ice-covered roadways when roads are otherwise clear causes unexpected conditions for which drivers may be ill-prepared. This and other consequences of snow on the ground convert the condensate plume from a benign annoyance to an agent of potentially serious consequences.

This paper defines the conditions under which significant snowfall from cooling tower plumes should be expected. The analysis does not address conditions for snowfall from supercooled fogs infested by industrial effluents.

2. OBSERVATIONS AND THEIR INTERPRETATION

2.1 Source of Observations

Kramer and his colleagues at Smith-Singer Meteorologists (undated reports), under contract from the American Electric Power Service Corporation, made a series of aerial surveys of cooling towers located in WV, OH, and KY. Observations were made on 63 days in the winters of 1974-75 and 1975-76. Kramer et al. (1976) provides additional information.

On two occasions during the winter of 1975-76, Otts (1976) of the National Weather Forecast Office at the Charleston, WV, Airport observed abnormal snowfall associated with the John E. Amos facilities

* The Rand Corporation, Santa Monica, California.

of the AEP, one of the sites regularly surveyed by the aerial program of Smith-Singer Meteorologists.

2.2 Conditions Favoring Plume Glaciation and Snowout

Within a glaciating plume there exists a continuous competition between the evaporation of the plume due to mixing with the (commonly) subsaturated environment and the growth of ice to substantial size. Glaciation and snowfall are promoted by long plume lifetimes and conditions that favor the production of large quantities of ice particles together with their rapid growth.

The single most important parameter regulating the rapidity of plume evaporation and, hence, its lifetime is the ambient saturation deficit--the water vapor density required for saturation minus that existing. Since ice growth rates and ice-particle concentration are strong functions of temperature, we expect that the probability of a plume glaciating and causing substantial snowfall will be a function of temperature and ambient saturation deficit.

Plots of plume observations against temperature and saturation deficit are shown in Figure 1. *The combination of temperatures below -13°C and ambient saturation deficits below 0.5 g m^{-3} with respect to liquid provides an empirical basis for separating circumstances in which self-precipitation of snow from plumes should and should not be expected.*

Data primarily apply to the Amos plant with its capacity of 2900 MW_e, but since snow occurred at the Muskingum plant (535 MW_e on one cooling tower) on two marginal days, the source strength apparently is not a dominant factor.

Kramer et al. (1976) suggested a possible correlation between stability and snowout. In general, greater stability produces less turbulence and longer plume lifetime and, therefore, increases the opportunity for liquid-to-ice conversion.

Otts (1976) believes glaciation is favored by conditions typically following the passage of a cold front: cold, moist, unstable air capped at about 1.5 km by a strong inversion.

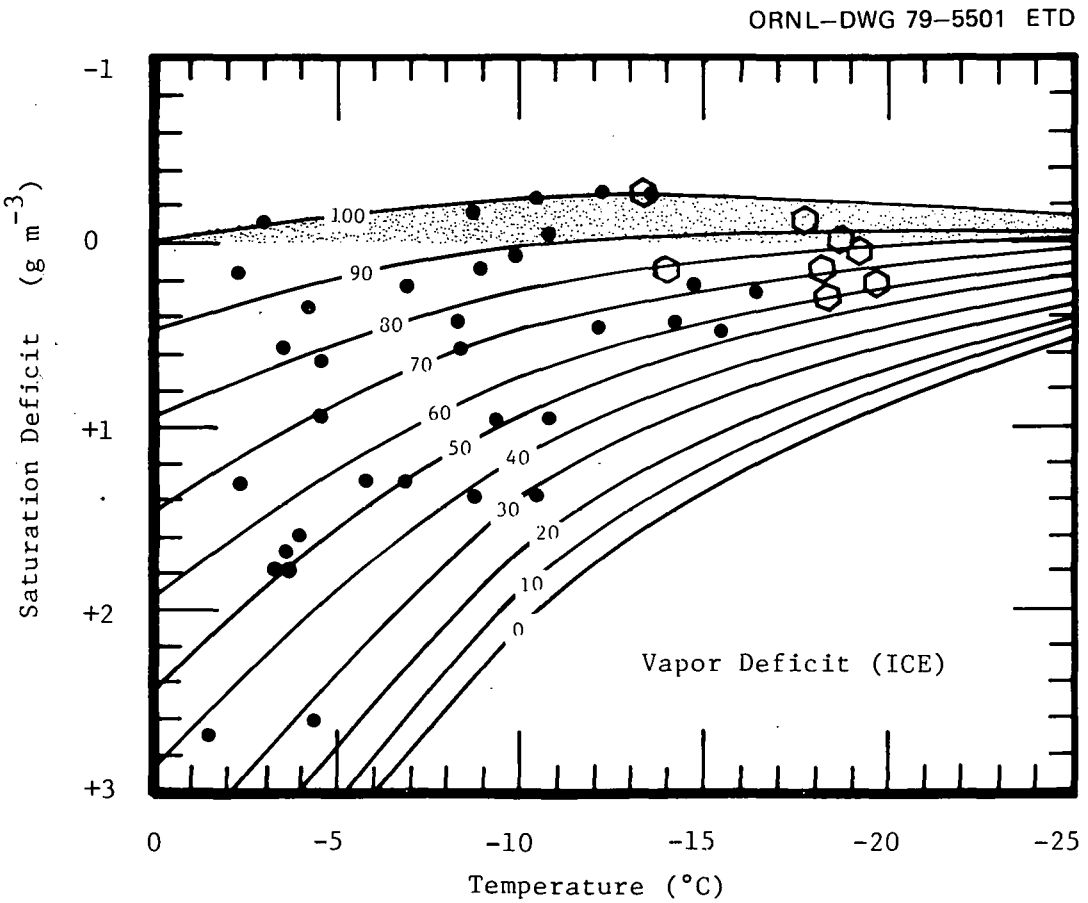

Fig. 1. Plume behavior as a function of temperature and saturation deficit with respect to ice. Black dots indicate absence of snowfall; open hexagons indicate snowfall from plume. Sloping lines are percentage relative humidity with respect to liquid water.

Observations indicate that too much stability may be counterproductive for snowout to the ground, for a long-lasting but thin plume may form. Ice particles within such a plume may fall out and evaporate before achieving sufficiently great size or fallspeed to reach the ground.

2.3 Theoretical Criteria for Snowfall

Whether or not a plume glaciates and forms important snow amounts depends upon the ratio of ice production (particle mass multiplied by concentration) to water lost by evaporation. Time periods on the order of one hour are of interest, since parcels in liquid water plumes

seldom exist beyond this period, although glaciated plumes may persist for several hours.

Ice-particle growth depends strongly upon temperature and the bulk density of accompanying water droplets. Measurements of plume water content are few. None exist for conditions of interest in this work, but it is likely that water contents range downward from about 0.2 g m^{-3} during periods of significant plume glaciation and snowout. For very long-lasting, snowing plumes (measurements show distances of snowout exceeding 70 kilometers) the liquid water content probably approaches zero.

Figure 2 shows the bulk density of ice as a function of temperature and liquid water content using particle concentrations given by:

$$N(m^{-3}) = 0.1 \exp[0.5756(273.16 - T)]$$

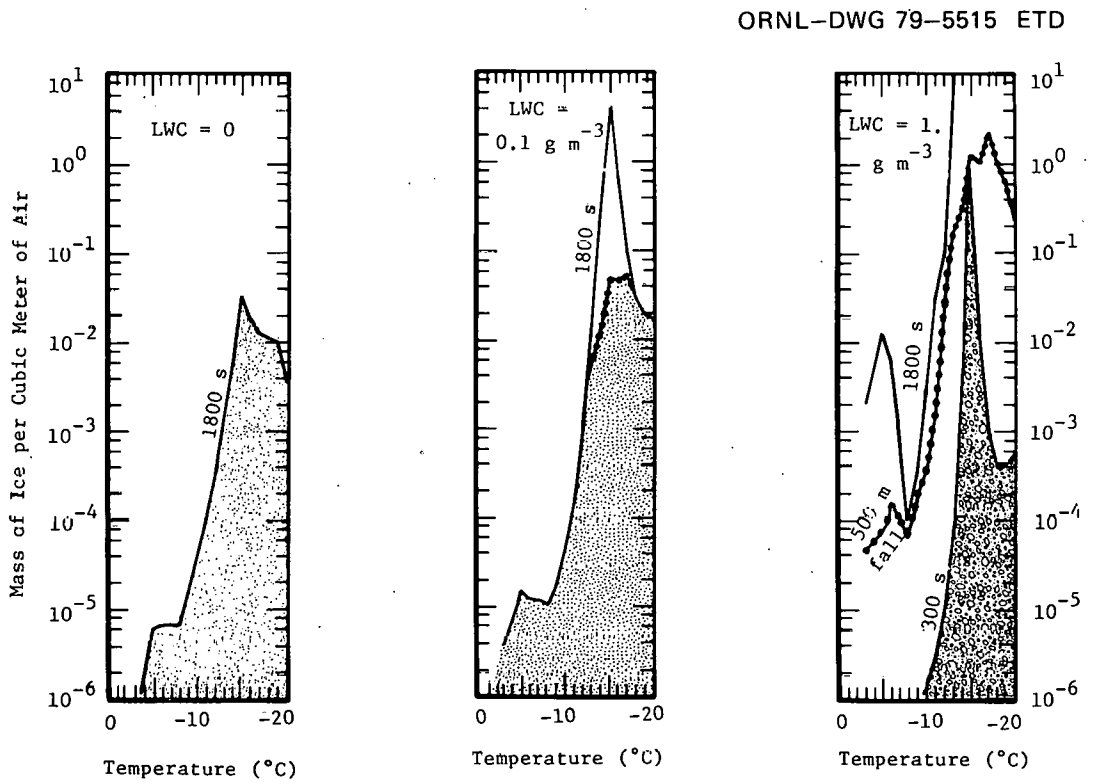

Fig. 2. The mass of ice per cubic meter of air produced as a function of temperature and liquid water content (which remains constant) of the mixture. Solid line indicates mass after growing for 1800 seconds; line with dots indicates growth after 500 m fall if this occurs before 1800 s.

and ice-particle growth rates calculated using a modification of the method of Koenig (1971).

Limits of fall distances of 500 m (a typical plume thickness) and 300 seconds at liquid water content of 1 g m^{-3} (water contents quickly drop due to dilution) are shown in Figure 2. The important result shown is that very little ice is produced until temperatures of about -13°C are reached.

Figure 3 shows fall distances as a function of time and temperature using this model. Again, calculations were limited to 30 minutes because of uncertainties in the model. However, the general trend clearly shows the importance of temperatures being not much warmer than -13°C if ice production is to consume the available water content before complete evaporation occurs and ice particles are to grow to sizes with insufficient fallspeeds to reach the ground within the observed lifetime and distances (snowfall typically reaches the ground within 5 km of the source after falling 500 to 1000 m in winds of 4 to 10 m s^{-1}).

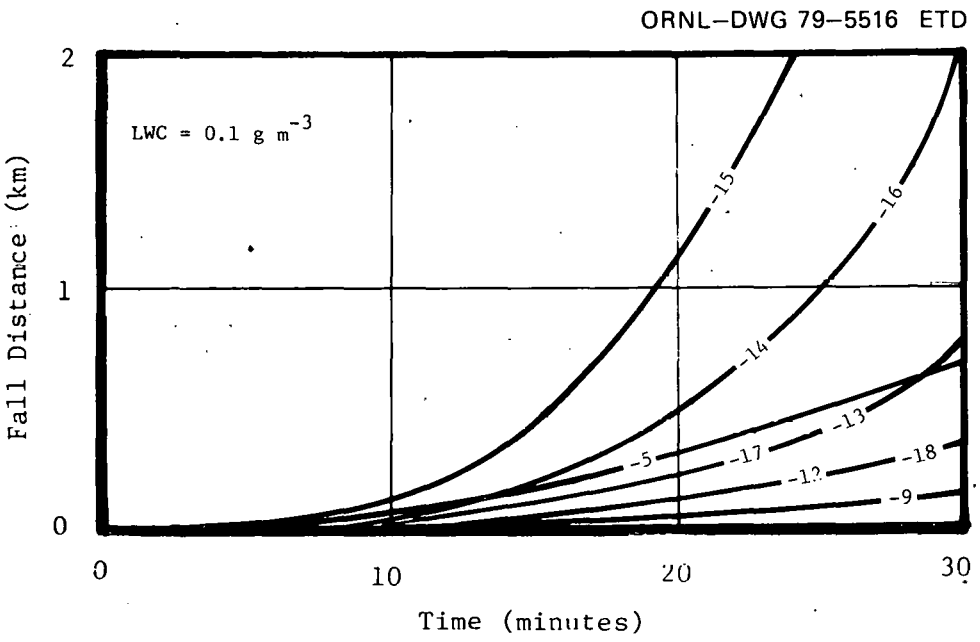

Fig. 3. The distance a growing ice particle will fall as a function of time and temperature in an environment having 0.1 g m^{-3} liquid water content.

2.4 Snow Quantity Compared with Tower Water Output

Figure 4, after Otts, provides a mapping of snowfall accumulation over a five-hour period on 4 January 1976. From this, a conservative estimate of 2×10^{13} cm^3 of snow can be made.

Kramer describes snow at the ground as being very light and fluffy, and Otts (personal communication, 1977) described the snow in similar terms. On the assumption that the density of the snow lay between 0.1 g m^{-3} (a typical value) and 0.01 g cm^{-3} (a very low value), the estimated snowfall rate is between 1×10^8 and 1×10^7 g s^{-1} over the entire area of accumulation--two or one orders of magnitude greater than the evaporation rate of water in the cooling towers.

This shows convincingly that greater snow mass can accumulate than the water vapor mass leaving the tower exit in the same period of time.

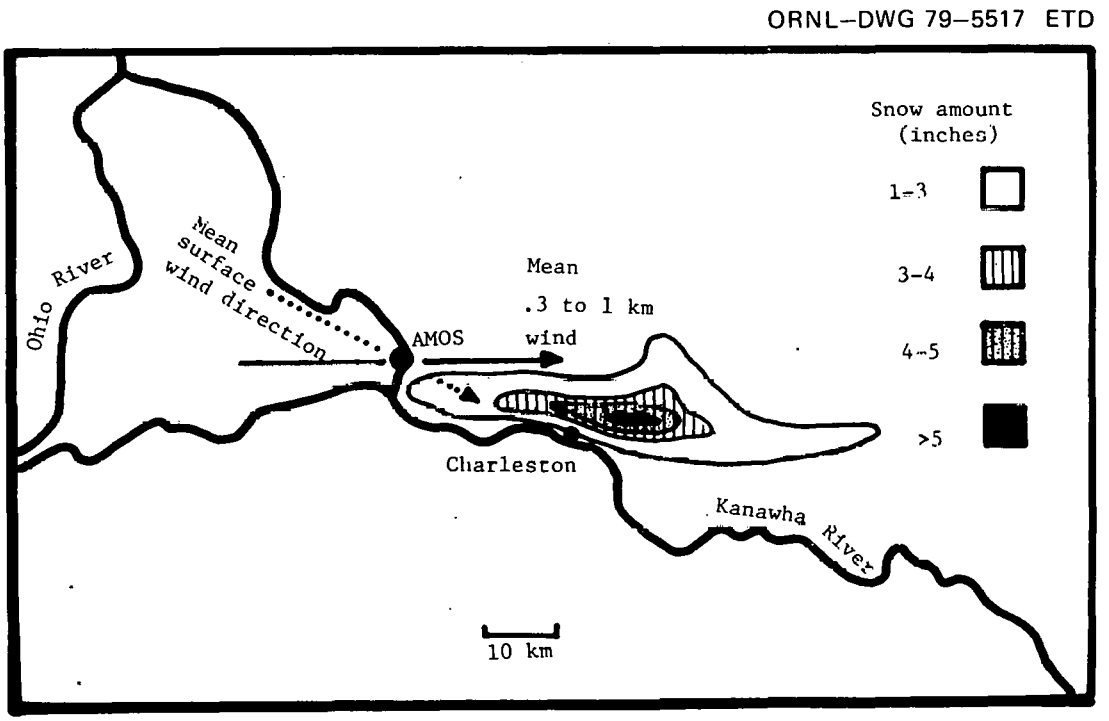

Fig. 4. Map of snowfall that occurred on 4 January 1976 (after Otts, 1976). The emissions of the natural draft cooling towers at the John E. Amos Power Plant are believed to be the source of the snow.

Since natural clouds were in the vicinity on 4 January 1976, the enhanced snow amount probably resulted from the initiation of precipitation in otherwise benign clouds.

Natural clouds indicate regions of low, if not nil, saturation deficit and, therefore, regions conducive to long-lasting plumes. A glaciating plume that mixes with a supercooled, nonglaciated natural cloud deck, in effect, can feed on a much greater quantity of water than that emitted from the cooling tower. The plume acts to "seed" the natural cloud and cause it to snow, but the effect seems limited by the nuclei introduced into the natural cloud and by the dynamics of the interaction. Maximum snowfall occurs on the center line of the plume: the glaciated portion of the natural cloud does not spread unrestrictedly, and snow does not continually spread outward. There is a movement of the natural cloud condensate toward the plume rather than a spread of ice nuclei or small ice particles outward into the natural cloud.

Thin supercooled clouds, on occasion, can be observed to develop a glaciated area that widens, with snow apparently continuing to fall at the center of the glaciated circle. The appearance suggests motions resembling a spherical vortex. The diameter of the circle does not expand without limit, however. As expansion ceases, the hole may fill with supercooled droplets and the layer return to its initial condition.

Excess snowfall may also involve condensation of moisture in entrained air. This may come about through the lifting and cooling of air entrained in a rising plume or, and probably more importantly, the deposition of vapor on ice crystals when the entrained air, while subsaturated with respect to liquid, is supersaturated with respect to ice.

2.5 Modification of Ice-Nucleus Concentration

Effluents from coal-fired power plants contain ice-forming nuclei that can seed supercooled clouds. Parungo et al. (1978) observed the anomalous occurrence of ice crystals and snowfall in a deep supercooled fog having temperatures between -5.5 and -4.8°C. The pattern of snowfall led to the conclusion that ice-forming nuclei in effluents from the Valmont Power Plant in Boulder, CO , caused the snowfall by seeding

the fog. Measurements by Parungo et al. (1978) of ice-nucleus concentrations indicate about two orders of magnitude more active nuclei within the plume (after it had spread to a width of 0.5 km) than in the surrounding air (the measurements were taken at -20°C).

LANDSAT images (Fig. 5) of a broken cloud layer indicate more complete glaciation in clouds lying downwind of power plants than in clouds lying outside of the zone of influence of plant emissions. This

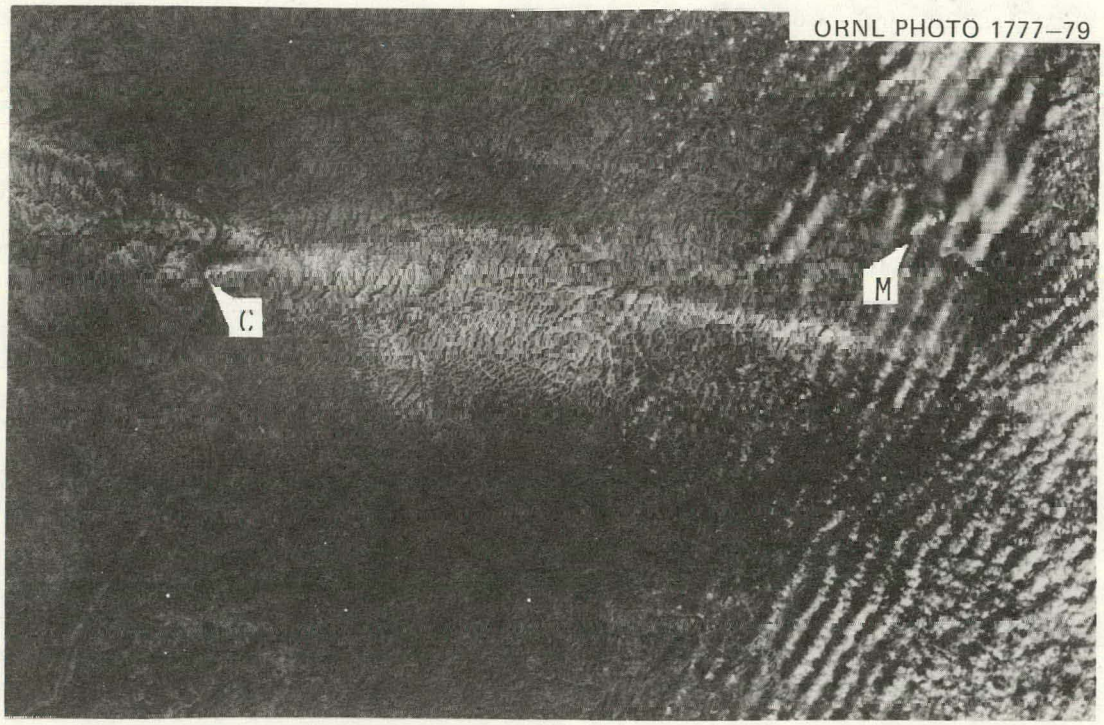

Fig. 5. A portion of LANDSAT image 1173-15362-5 obtained on 12 January 1973 showing parts of OH, PA, and WV. The image depicts an area of about 100 km by 75 km.

"C" points out a power plant plume near Captina, WV

"M" points out a power plant plume near Morgantown, WV

The clouds immediately downwind of the Morgantown plume appear more fuzzy and perhaps taller than those to the north and south. This suggests that the clouds exposed to the plume contain more ice than those not so exposed. There is also indication of cloud glaciation in the clouds to the west of Morgantown. These clouds may have been exposed to effluents in the Captina plume, for it appears to be immediately upwind.

suggests the presence of abnormally large concentrations of ice-forming nuclei in the stack emissions of these coal-fired plants.

In spite of evidence for ice nuclei in coal-fired plant effluents, there is little need for augmentation of natural concentrations of ice-forming nuclei to account for the observed glaciating behavior of cooling tower plumes. Therefore, it is concluded that the conditions under which plumes from nuclei-fueled plants (or others not producing fly ash) will be substantially the same as for coal-fired plants.

3. CONCLUDING REMARKS

Current understanding of ice nucleation and growth provides reasonable explanation for the environmental conditions that separated situations when snowfall from cooling tower plumes did and did not occur.

This agreement between theory and observation encourages a more rigorous treatment of a capability for predicting the snow deposition pattern, including depths.

4. ACKNOWLEDGMENTS

The American Electric Power Service Corporation sponsored the aerial observations, gathered by Mark L. Kramer of Smith-Singer Meteorologists, that led to this work.

The Department of Energy sponsored this work [contract E(04-3)-1191]. It is a part of their Meteorological Effects of Thermal Energy Release (METER) Program.

REFERENCES

Koenig, L. R., 1971: "Numerical Modeling of Ice Deposition," *J. Atmos. Sciences*, Vol. 28, pp. 226-237.

Kramer, M. L., D. E. Seymour, M. E. Smith, R. W. Reeves, and T. T. Frankenburg, 1976: "Snowfall Observations from Natural-Draft Cooling Tower Plumes," *Science*, Vol. 193, pp. 1239-1241.

Otts, R. E., 1976: "Locally Heavy Snow Downwind from Cooling Towers," *NOAA Technical Memo*, NWS ER-62, 8 pp.

Parungo, F. P., P. A. Allee, H. K. Weickmann, 1978: "Snowfall Induced by a Power Plant Plume," *Geophysical Research Letters*, Vol. 5, pp. 515-517.

Smith-Singer Meteorologists, Inc., "John E. Amos Cooling Tower Flight Program Data," December 1974-March 1975, prepared for and available from American Electric Power Service Corporation, Canton, Ohio.

Smith-Singer Meteorologists, Inc., "John E. Amos Cooling Tower Flight Program Data," December 1975-March 1976, prepared for and available from American Electric Power Service Corporation, Canton, Ohio.

ORNL/TM-6867
Dist. Category UC-12

Internal Distribution

1. S. I. Auerbach
2. S. Baron
3. H. F. Bauman
4. T. J. Blasing
5. G. A. Briggs (ATDL)
6. N. C. J. Chen
7. T. E. Cole
8. W. E. Cooper
9. W. B. Cottrell
10. C. C. Coutant
11. D. M. Eissenberg
12. M. H. Fontana
13. W. Fulkerson
14. F. A. Gifford (ATDL)
15. M. J. Goglia
16. S. R. Hanna (ATDL)
17. J. F. Harvey
18. R. P. Hosker (ATDL)
19-21. H. W. Hoffman
22. L. Jung
23. M. Levenson
24. S. Lindberg
25. R. E. MacPherson
26. H. A. McLain
27. R. L. Miller
28. C. J. Nappo (ATDL)
29-48. A. A. N. Patrinos
49. S. Rau (ATDL)
50. J. L. Rich
51. M. W. Rosenthal
52. T. H. Row
53. R. E. Saylor
54. I. Spiewak
55. H. E. Trammell
56. D. B. Trauger
57. R. Turner
58. G. D. Whitman
59. W. J. Wilcox
60. A. J. Witten
61. ORNL Patent Office
62. Nuclear Safety Information Center
63. EISO Library (Bldg. 2028)
64-65. Central Research Library
66. Document Reference Section
67-69. Laboratory Records Department
70. Laboratory Records (RC)

External Distribution

71. R. F. Abbey, Jr., Office of Nuclear Regulatory Research, U.S. Nuclear Regulatory Commission, Washington, DC 20555
72. E. Altooney, Electric Power Research Institute, P.O. Box 10412, Palo Alto, CA 94303
73. D. S. Ballentine, Office of Health and Environmental Research, U.S. Department of Energy, Washington, DC 20545
74. T. G. Brna, U.S. Environmental Protection Agency, IERL-RTP (MD-G1), Research Triangle Park, NC 27711
75. R. Braham, Jr., University of Chicago, Chicago, IL 60601
76. W. Cliff, Battelle Pacific Northwest Laboratories, Battelle Blvd., Richland, WA 99352
77. J. H. Coleman, Air Quality Branch, Tennessee Valley Authority, River Oaks Building, Muscle Shoals, AL 35660
78. W. R. Cotton, Department of Atmospheric Science, Colorado State University, Fort Collins, CO 80523
79. T. Crawford, Environmental Transport Division, Savannah River Laboratory, Aiken, SC 29801
80. T. Dana, Battelle Pacific Northwest Laboratories, Battelle Blvd., Richland, WA 99352

81. J. W. Deardorff, National Center for Atmospheric Research, Boulder, CO 80302
82. N. Dingle, Department of Atmospheric and Oceanic Science, University of Michigan, Ann Arbor, MI 48109
83. R. A. Dirks, National Science Foundation, 1800 G Street, Northwest, Washington, DC 20550
84. W. E. Dunn, Argonne National Laboratory, 9700 South Cass Avenue, Argonne, IL 60439
85. O. Essenwanger, Missile Research Directory, HEL Laboratory, Bldg. 77-70, Redstone Arsenal, AL 35809
86. J. E. Fairobent, Office of Nuclear Reactor Regulation, U.S. Nuclear Regulatory Commission, Washington, DC 20555
87. S. Fellows, Director of Special Programs, Southern States Energy Board, 2300 Peachford Road, Suite 1230, Atlanta, GA 30338
88. P. Frenzen, Argonne National Laboratory, 9700 South Cass Avenue, Argonne, IL 60439
89. A. Gakner, Bureau of Power, Federal Power Commission, Washington, DC 20426
90. N. Goldenberg, Advanced Nuclear Systems and Projects Division, DOE, Washington, DC 20545
91. C. H. Goodman, Southern Company Services, Inc., P.O. Box 2625, Birmingham, AL 35202
92. Ron Hadlock, Battelle Pacific Northwest Laboratories, Battelle Boulevard, Richland, WA 99352
93. C. Hakkarinen, Electric Power Research Institute, P.O. Box 10412, Palo Alto, CA 94303
94. P. Harrison, Meteorology Research, Inc., P.O. Box 637, Altadena, CA 91001
95. B. B. Hicks, Argonne National Laboratory, 9700 South Cass Avenue, Argonne, IL 60439
96. P. Hobbs, Department of Atmospheric Sciences, University of Washington, Seattle, WA 98195
97. J. D. Holmberg, Marley Cooling Tower Company, 5800 Fox Ridge Drive, Mission, KS 66202
98. F. Huff, Illinois State Water Survey, P.O. Box 232, Urbana, IL 61801
99. J. Jansen, Southern Company Services, Inc., P.O. Box 2625, Birmingham, AL 35202
100. Kenneth Juris, New York State Power Pool, 3890 Carmen Road, Schenectady, NY 12303
101. Landis Kannberg, Battelle Pacific Northwest Laboratories, Battelle Boulevard, Richland, WA 99352
102. John Kennedy, Iowa Institute of Hydraulic Research, University of Iowa, Iowa City, IA 52240
103. A. L. Kistler, Department of Mechanical Engineering and Astronautical Sciences, Northwestern University, Evanston, IL 60201
104. L. R. Koenig, Rand Corporation, 1700 Main Street, Santa Monica, CA 90406
105. R. Kornasiewicz, Office of Standards Development, U.S. Nuclear Regulatory Commission, Washington, DC 20555
106. M. L. Kramer, Smith-Singer Meteorologists, Inc., 134 Broadway, Amityville, NY 11701

107. N. Laulainen, Battelle Pacific Northwest Laboratories, Battelle Boulevard, Richland, WA 99352
108. J. Lee, Department of Meteorology, The Pennsylvania State University, University Park, PA 16802
109. D. Lenschow, National Center for Atmospheric Research, Boulder, CO 80302
110. J. Maulbetsch, Electric Power Research Institute, P.O. Box 10412, Palo Alto, CA 94303
111. G. E. McVehil, P.O. Box 4480, Boulder, CO 80302
112. H. Moses, Office of Health and Environmental Research, DOE, Washington, DC 20545
113. J. Motz, Georgia Power Company, P.O. Box 4545, Atlanta, GA 30302
114. F. W. Murray, Rand Corporation, 1700 Main Street, Santa Monica, CA 90406
115. R. S. Nietubicz, Chalk Point Cooling Tower Project, c/o Bureau of Air Quality and Noise Control, O'Conor Building, 201 West Preston Street, Baltimore, MD 21201
116. J. M. Norman, Department of Meteorology, The Pennsylvania State University, University Park, PA 16802
117. J. Norwine, Ecological Sciences, Texas Instruments, Inc., P.O. Box 225621, MS 949, Dallas, TX 75265
118. H. D. Orville, Institute of Atmospheric Sciences, South Dakota School of Mines and Technology, Rapid City, SD 57701
119. T. J. Overcamp, Environmental Systems Engineering, Clemson University, Clemson, SC 29631
120. J. Pell, Director, Office of Environmental Regulations, Office of Energy Conservation and Environment, Federal Energy Administration, Room 7116, 12th Street and Pennsylvania Avenue, NW, Washington, DC 20461
121. J. Pena, Department of Meteorology, The Pennsylvania State University, University Park, PA 16802
122. R. Pena, Department of Meteorology, The Pennsylvania State University, University Park, PA 16802
123. R. Perhac, Electric Power Research Institute, P.O. Box 10412, Palo Alto, CA 94303
124. A. J. Policastro, Argonne National Laboratory, 9700 South Cass Avenue, Argonne, IL 60439
125. G. Reynolds, Air Quality Assessment Section, River Oaks Bldg., Muscle Shoals, AL 35660
126. C. A. Rhodes, College of Engineering, University of South Carolina, Columbia, SC 29208
127–147. Alan Rubin, Advanced Nuclear Systems and Projects Division, DOE, Washington, DC 20545
148. E. Ryzner, Department of Atmospheric and Oceanic Science, University of Michigan, Ann Arbor, MI 48109
149. W. F. Savage, Advanced Nuclear Systems and Projects Division, DOE, Washington, DC 20545
150. H. W. Schmitt, Environmental Systems Corp., P.O. Box 2525, Knoxville, TN 37901
151. G. L. Sherwood, Office of Nuclear Energy Programs, DOE, Washington, DC 20545

152. F. M. Shofner, Singing Hills Point, Knoxville, TN 37922
153. D. H. Slade, Office of Health and Environmental Research, DOE, Washington, DC 20545
154. P. Slawson, Department of Mechanical Engineering, University of Waterloo, Waterloo, Ontario, Canada
155. W. G. N. Slinn, Atmospheric Sciences Department, Oregon State University, Corvallis, OR 97331
156. S. Strauch, Office of Nuclear Energy Programs, DOE, Washington, DC 20545
157. D. W. Thomson, Department of Meteorology, The Pennsylvania State University, University Park, PA 16802
158. J. L. Vogel, Illinois State Water Survey, P.O. Box 232, Urbana, IL 61801
159. J. C. Weil, Martin-Marietta Corporation, Baltimore, MD 21240
160. M. L. Wesely, Argonne National Laboratory, 9700 South Cass Avenue, Argonne, IL 60439
161. L. Winiarski, Environmental Protection Agency, 200 South 35th Street, Corvallis, OR 97330
162. Office of Assistant Manager, Energy Research and Development, DOE, Box E, Oak Ridge, TN 37830
163. Director, Reactor Division, DOE, Box E, Oak Ridge, TN 37830
164–465. Given distribution as shown in TID-4500 under category UC-12

☆U.S. GOVERNMENT PRINTING OFFICE: 1979-640-079/59